Proceedings and workbook of the

Electroporation-based Technologies and Treatments

International SCIENTIFIC WORKSHOP and POSTGRADUATE COURSE

Ljubljana, Slovenia
November 13-18, 2023

9 789612 434571

Proceedings is available in PDF format at ***2023.ebtt.org/proceedings***

Electroporation-based Technologies and Treatments 2023

November 13-18, 2023
Ljubljana, Slovenia

Proceedings and workbook of the

Electroporation-based Technologies and Treatments

International SCIENTIFIC WORKSHOP and POSTGRADUATE COURSE

Edited by:

Saša Haberl Meglič
Damijan Miklavčič

Organised by:

University of Ljubljana
Faculty of Electrical Engineering

Institute of Oncology, Ljubljana

Supported by:

Bioelectrochemical Society (BES)

International Society for Electroporation-Based Technologies and Treatments (ISEBTT)

Bia
DONAU LAB
Elea
Energy Pulse Systems
GFT Uni. Bielefeld
IGEA
Intuitive
Iskra Medical
Iskra PIO
Jafral
Labtim
Medtronic
mPOR
Omega
OnMed
Zeiss

www.ebtt.org

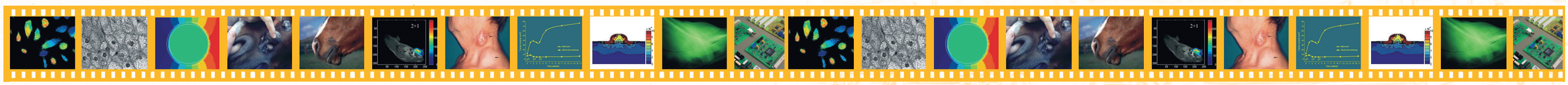

Univerza *v Ljubljani*

bia
TRUSTED LAB PARTNER

DONAU LAB Ljubljana
Member of LPPgroup

elea

ENERGY PULSE SYSTEMS
DESIGNING ENERGY FOR LIFE

GFT
Gesellschaft zur Förderung des Forschungs- und Technologietransfers in der Universität Bielefeld e.V.
Universität Bielefeld

IGEA®
CLINICAL BIOPHYSICS

INTUITIVE

IskraMedical

JAFRAL
passion for biosolutions

Labtim

Medtronic

ELECTROPORATION
MPOR

omega

ONMED®
Oncology Medical Devices AB

p:o
Clean visions.

ZEISS

ISEBTT International Society for Electroporation-Based Technologies and Treatments

B E S
The Bioelectrochemical Society

9 – 13 June 2024
Portorož | Slovenia

embec 2024

9th European Medical and Biological Engineering Conference

Come, share and enjoy!

We could not make it in 2020...so we booked 2024 to make it right!

embec2024.org

IFMBE International Federation for Medical and Biological Engineering

European Alliance for EAMBES Medical and Biological Engineering & Science

SLOVENIAN SOCIETY FOR MEDICAL AND BIOLOGICAL ENGINEERING
Faculty of Electrical Engineering, Tržaška 25, 1000 Ljubljana, Slovenia
tel.: +386 1 4768 783, homepage: www.drmbs.si, e-mail: info@drmbs.si

University *of Ljubljana*
Faculty *of Electrical Engineering*

November 13-18, 2023
Ljubljana, Slovenia

Proceedings and workbook of the

Electroporation-Based Technologies and Treatments

International SCIENTIFIC WORKSHOP and POSTGRADUATE COURSE

Edited by:

Saša Haberl Meglič
Damijan Miklavčič

Organised by:

University of Ljubljana
Faculty of Electrical Engineering

Institute of Oncology, Ljubljana

Supported by:

Bioelectrochemical Society (BES)

International Society for Electroporation-Based Technologies and Treatments (ISEBTT)

Bia
DONAU LAB
Elea
Energy Pulse Systems
GFT Uni. Bielefeld
IGEA
Intuitive

Iskra Medical
Iskra PIO
Jafral
Labtim
Medtronic
mPOR
Omega
OnMed
Zeiss

www.ebtt.org

CIP - Kataložni zapis o publikaciji
Narodna in univerzitetna knjižnica, Ljubljana

602.621(082)
577.352.4(082)

ELECTROPORATION-based Technologies and Treatments (delavnica) (2023 ; Ljubljana)
Proceedings and workbook of the Electroporation-based Technologies and Treatments : international scientific workshop and postgraduate course : [November 13-18, 2023, Ljubljana, Slovenia] / organised by University of Ljubljana, Faculty of Electrical Engineering [and] Institute of Oncology, Ljubljana ; edited by Saša Haberl Meglič, Damijan Miklavčič. - 1. izd. - Ljubljana : Založba FE, 2023

ISBN 978-961-243-457-1
COBISS.SI-ID 168091139

Založnik: Založba FE, Ljubljana
Izdajatelj: UL Fakuleta za elektrotehniko, Ljubljana
Urednik: prof. dr. Sašo Tomažič

Natisnil: Birografika Bori d.o.o.
Naklada: 90 izvodov
1. izdaja

Welcome note

Dear Colleagues, dear Students,

The Workshop and Postgraduate Course on Electroporation-Based Technologies and Treatments (EBTT) at the University of Ljubljana was organized for the first time in 2003. In 2023 the Course is organized for the 17th time! In these twenty years, the school has been attended by more than 1000 participants coming from 45 different countries. And this year again we can say with great pleasure: "with participation of many of the world leading experts in the field". The goals and aims of the school, however, remain unchanged: to provide the participants with sufficient theoretical background and practical knowledge to allow them to use electroporation effectively in their working environments.

It is a great pleasure to welcome you at the EBTT and in particular to the practical lab work taking place at the University of Ljubljana, Faculty of Electrical Engineering organized as an integral part of the Interdisciplinary doctoral program Biomedicine of the University of Ljubljana. From the very beginning we were aiming to prepare lab work for participants, which would complement the lectures. As preparing lab work takes more time than preparing and organizing lectures, we introduced lab work at the second workshop in 2005. Lab work covers different aspects of research: biological experiments taking place in the cell culture labs, microbiological lab, lab for tissue and planar lipid bilayer; numerical and molecular dynamics modelling, e-learning using computer classrooms, pulse generator development and electrical measurements using electronic laboratory workshop and magnetic resonance electrical impedance tomography.

Following the experience gained in 2020 when due to pandemic we organized the school entirely on-line, we decided to continue organizing the course as a hybrid, to enable participation also to those who are still facing difficulties in traveling or suffer from time constraints. The team here in Ljubljana will thus provide on-site hands-on lab works as well as live webinars of the lab works so that you will be able to benefit most even if not actually being in the lab.

The biological experiments were pre-recorded and will be organized in the Infrastructural Centre "Cellular Electrical Engineering", part of the Network of Research and Infrastructural Centers of University of Ljubljana in the Laboratory of Biocybernetics. Lab works would not be possible without extensive involvement and commitment of numerous members of the Laboratory of Biocybernetics and Igor Serša from Jožef Stefan Institute for which I would like to thank them all cordially.

It also needs to be emphasized that all written contributions collected in the proceedings have been reviewed and then thoroughly edited by Saša Haberl Meglič. We thank all authors and reviewers. Also, I would like to express our sincere thanks to the faculty members and invited lecturers for their lectures delivered at the course. Finally, I would like to thank our sponsors who are making our EBTT possible: Bia (Slovenia), DONAU LAB (Slovenia), Elea (Germany), Energy Pulse Systems (Portugal), Technology Transfer office (GFT) of the University of Bielefeld (Germany), IGEA (Italy), Intuitive (USA), Iskra Medical (Slovenia), Iskra PIO (Slovenia), Jafral (Slovenia), Labtim (Slovenia), Medtronic (USA), mPOR (Slovenia), OnMed (Sweden), Omega (Slovenia), Zeiss (Slovenia), the Bioelectrochemical Society and the International Society for Electroporation-Based Technologies and Treatments.

I sincerely hope you will enjoy the experience, benefit from being with us and enlarge your professional network.

Sincerely Yours,

Damijan Miklavčič

INVITED LECTURERS

Human in vitro assay for non-clinical evaluation Pulsed Field Ablation treatments

Maura Casciola, Ksenia Blinova; *Office of Science and Engineering Laboratories, Center for Devices and Radiological Health, United States Food and Drug Administration, Silver Spring, MD, UNITED STATES*

INTRODUCTION

Thermal catheter ablation techniques, such as radiofrequency (RF) and cryoablation, are the established treatment for atrial fibrillation that doesn't respond to medication [1]. These techniques aim to focus thermal energy on the irregular tissue, but sometimes, the lack of tissue specificity can inadvertently harm surrounding areas as temperature gradients extend beyond the intended ablation site. In contrast, irreversible electroporation (IRE) can cause cardiac cell death by applying short, high-intensity pulsed electric fields (PEF) within a specified region defined by the lethal electric field threshold (EFT) for a particular tissue type [1]. While IRE ablation devices are in advanced clinical development, the understanding of how PEF treatment outcomes depend on waveform parameters and the evidence for tissue-specific electroporation remains limited. Therefore, we created a standardized *in vitro* model using human cells to investigate the impact of waveform parameters on the lethal EFT and to compare the effects of IRE on different neighboring tissues such as the heart, esophagus, and lungs, all under consistent experimental conditions [2,3].

METHODS

Propidium iodide (PI) uptake 4h post treatment was used as indicator of cell permeabilization. Electroporation regions stained with PI were imaged and their areas (i.e., IRE area), quantified to evaluated IRE EFTs (Figure 1). Experiments were conducted in parallel in human-induced pluripotent stem cell-derived cardiomyocytes (hiPSC-CMs), human esophageal smooth muscle cells (hESMCs), and human bronchial epithelial cells (hBEC3-KTs).

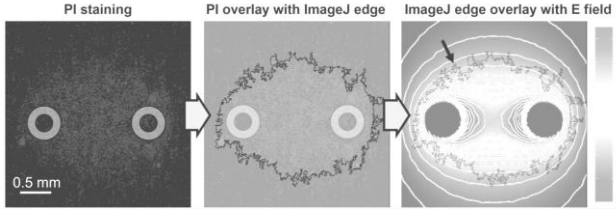

Figure 1. Fluorescent staining by PI of cell monolayers 4 h after PEF treatment; the IRE areas were compared with the electric field distribution generated by the electrodes (COMSOL Multiphysics) for the determination of the lethal EFT.

RESULTS

First, we quantified the EFT for cell death in hiPSC-CMs for a broad range of pulse parameters: 50 – 400 biphasic pulses, phase duration t_p = 0.2–10 µs, pulse repetition frequency PRF = 0.01–200 kHz). The lethal EFT was inversely proportional to t_p and pulse number, with t_p being the most influential parameter (Figure 2). The PRF did not have a significant effect, with minor variation of the EFT over the range of frequencies investigated. Together with temperature assessment, and treatment time, this data can be used to inform early-stage device development, reducing the burden on animals for the optimization of PFA waveform.

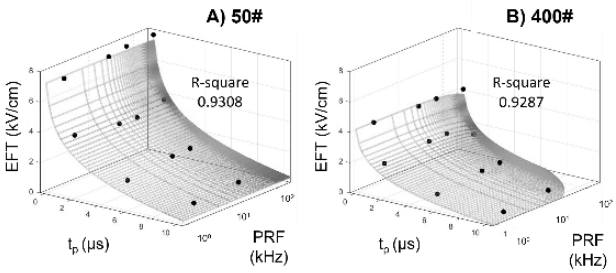

Figure 2. IRE EFT in hiPSC-CMs for a broad range of pulse parameters (only 50 and 400# shown for simplification). Fitting was obtained with multi variable logarithmic function.

Then, we compared the IRE areas in hESMCs, HBEC3-KT and hiPSC-CMs for the same PEF treatment applied (Figure 3). Cardiac models displayed significantly larger areas of dead cells in the range of parameters investigated, suggesting cell type sensitivity to PEF *in vitro*. Higher phase amplitudes tested, i.e. 400 and 600 V, caused monolayer disruption in hiPSC-CM monolayers.

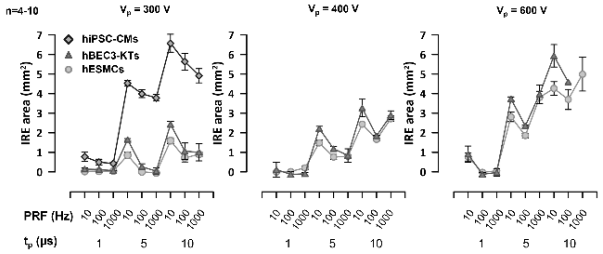

Figure 3. IRE areas measured for the tested range of PEF parameter combinations.

CONCLUSIONS

This regulatory science research establishes a standardized preclinical assay, facilitating the initial non-clinical advancement of PEF-based cardiac ablation devices and providing valuable insights for regulatory evaluation. Furthermore, our findings demonstrate that identical PEF treatments result in more extensive IRE areas in hiPSC-CMs than in HESMCs and HBEC3-KTs *in vitro*. Future investigations will concentrate on verifying these outcomes within actual tissues to evaluate the safety of IRE cardiac ablation devices.

Disclaimer: This article reflects the views of the authors and should not be construed to represent the U.S. Food and Drug Administration's views or policies. The mention of commercial products, their sources, or their use in connection with material reported herein is not to be construed as either an actual or implied endorsement of such products by the HHS.

REFERENCES

[1] A. Verma *et al*. "Primer on pulsed electrical field ablation: Understanding the benefits and limitations", *Circ Arrhythm Electrophysiol* vol. 14, p. e010086, 2021.

[2] M. Casciola *et al*. "Human in vitro assay for irreversible electroporation cardiac ablation", *Front* Physiol, vol. 13, 2023.

[3] M. Casciola *et al*. "Human cardiomyocytes are more susceptible to irreversible electroporation by pulsed electric field than human esophageal cells", *Phys Rep*, vol. 10, 2022

The use of moderate and high voltage electric fields in food processing and the circular bioeconomy

James Lyng, Ajay Menon and Norman Maloney; *School of Agriculture and Food Science, University College Dublin, Belfield, Dublin 4, IRELAND*

INTRODUCTION

In food processing operations and biorefineries electrical energy can be applied directly to foodstuffs/feedstocks to induce movement at a subcellular level which can lead to appreciable heating (i.e. electro heating) but can also be applied to foodstuffs/feedstocks to induce structural changes with minimal heating (i.e. non-thermal electro-processing). This presentation will distinguish between two forms of electro-processing technologies, namely moderate electric fields (MEF) and high voltage pulsed electrical fields (PEF). It will overview the present status of both technologies in terms of research vs commercial applications and their usage in thermal and non-thermal applications to date. It will also discuss the prospects of both technologies in terms of sustainable processing of foods and in biorefineries in the future.

DISTINGUISHING MEF FROM PEF

The definition of Sastry et al [1] will be used to distinguish MEF from PEF. In this definition MEF processing is described as "the use of electric fields at levels ranging from about 1 to 1000 V/cm (considerably lower than PEF) of arbitrary waveform and frequency with or without the attendant ohmic heat effect, to achieve interesting effects on biological materials". The main milestones in the history of MEF and PEF and a comparison of the number of publications will be provided.

THERMAL AND NON-THERMAL APPLICATIONS

The presentation will initially discuss the use of these technologies in thermal applications including their benefits in terms of greener heating and process intensification. Examples of thermal applications will also be provided. The presentation will then discuss the use of these technologies in non-thermal applications. Non thermal mechanisms of action will be discussed.

THE VALLEY OF DEATH

Increasing circularity, the bioeconomy and innovations in food processing are all essential to counteract emerging challenges of improving global food security, enhancing sustainability, green transformation and increasing consumer demands for nutritious, high quality safe food products [2]. However, it is long accepted that slow adoption rates can delay or prevent new technologies from successfully diffusing, with 40-90% of new products and technologies failing [3]. MEF and PEF electro-processing technologies have huge potential in food processing and the circular bioeconomy though they face the 'valley of death' between research knowledge and commercial adoption in the market place. Using PEF as an example a comparison of the success of two applications which have been adopted commercially (i.e. potato softening vs beverage preservation) will be compared in terms of their levels of commercial uptake.

WHAT DOES THE FUTURE HOLD

MEF and PEF are not silver bullet technologies compared to conventional processing methods. However, they can have definite niche applications where they can enjoy considerable success. Such niches can emerge where they are found to be considerably greener than conventional methods or where they can maintain or enhance the quality of food and feedstocks. Continued research and publications on these technologies is essential to enhance knowledge on their capabilities and potential. However, publications alone will not ensure commercial uptake or success. To catalyse such uptake research performing organisations need to interact more with equipment and food/feedstock processors to demonstrate their potential in an applied environment. Such activities are essential to facilitate the uptake of these technologies and educate industry as to the benefits that these technologies hold for the future of food processing and the circular bioeconomy.

REFERENCES

[1] S. Sastry. "Ohmic Heating and Moderate Electric Field Processing", *Food Sci Tech Int*, vol. 14, pp. 419-422, 2008.

[2] M. Oliveira *et al.* "Plasma-activated water: A cutting-edge technology driving innovation in the food industry", *Food Res Int*, vol. 156, p. 111368, 2022.

[3] K. Judson *et al*. "The new product development process", *J Prod Brand Manag*, vol. 15, pp. 194-202, 2006.

Advances in irreversible electroporation technology and novel clinical applications

Rafael V. Davalos[1], Nastaran Alinezhadbalalami[1], Kailee M. David[1], Irving Coy Allen[2];
[1]*Department of Biomedical Engineering and Mechanics, Virginia Tech, Blacksburg, VA 24061*
[2]*Department of Biomedical Sciences and Pathobiology, Virginia Tech, Blacksburg, VA 24061*

INTRODUCTION

Irreversible Electroporation (IRE) is a minimally invasive tissue ablation technique that involves applying low-energy pulses to create defects in the lipid bilayer, inducing cell death. [1]. IRE is unique among ablation techniques in affecting only the cell membrane while tissue molecules such as collagen structures and proteins; remain intact, thereby making treatment near critical structures possible. We developed an advanced form of the technology, high frequency irreversible electroporation (H-FIRE) [2], that is being used for the treatment of cardiac disease, cancer and other malignancies. This new therapy alleviates the need for a paralytic.

Different waveforms and fields elicit different cell death mechanisms, including necrosis, apoptosis, pyroptosis, and necroptosis [4]. These pulses have been shown to increase antigen activity with the release of damage associated molecular pathways (DAMPs) and proteins [3]. By modifying the pulse parameters and field strength, specific modes of cell death can be triggered [5]. We will discuss such mechanisms and modeling techniques to avoid thermal damage. We will also discuss recent advances in pulsed electric field therapies to target other aspects of the tumor microenvironment and potential clinical applications.

METHODS

A human glioblastoma cell line, U251, was cultured in a 2D monolayer cell culture platform and covered in low conductivity buffer for electroporation treatments. Ablation areas (n=5) were measured using fluorescent imaging to determine electric field thresholds for each waveform. To normalize the level of cell death, energy matching was used across all chosen waveforms. Cell samples were collected at 6h for a colorimetric Caspase 3/7 assay to quantify apoptotic activity. A fluorometric Caspase 1 assay was used on samples collected 30 min after treatment to quantify pyroptotic activity.

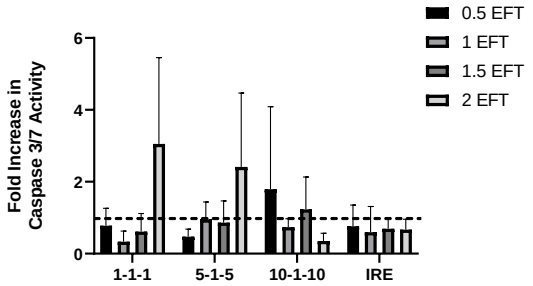

Figure 1. Apoptotic caspase 3/7 cleavage. (n=3)

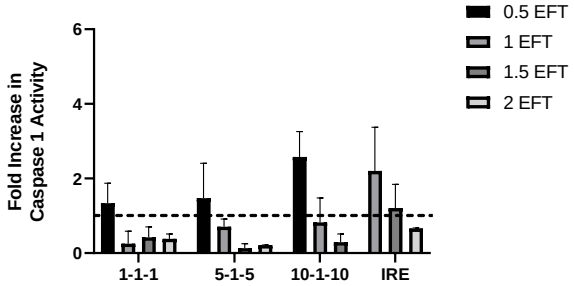

Figure 2. Pyroptotic Caspase 1 cleavage. (n=3)

RESULTS

We found that Caspase 3/7 activation (Figure 1) was significantly higher for shorter pulse widths (1 and 5μs) and stronger electric fields. Minimal caspase 3/7 activation was observed with higher pulse widths (10μs and IRE). Caspase 1 activation (Figure 2) displayed opposite trends from that of Caspase 3/7 as it was significantly higher at sublethal electric fields. Our results indicate that higher levels of apoptotic cell death occur at shorter pulse widths and increasing in electric field magnitude, and higher levels of pyroptotic cell death occur at longer pulse widths and lower field strengths.

CONCLUSION

We determined that we can activate specific cell death mechanisms by altering the applied pulse parameters. With this information, we can develop treatment plans to control the strength of an immune response to therapy to optimize patient recovery times and overall survival.

REFERENCES

[1] R. V. Davalos *et al.* "Tissue ablation with irreversible electroporation", *Ann Biomed Eng*, vol. 33, pp. 223-231, 2005.

[2] C. B. Arena *et al.* "High-frequency irreversible electroporation (H-FIRE) for non-thermal ablation without muscle contraction", *Biomed Eng Online*, vol. 10, 2011.

[3] V. M. Ringel-Scaia *et al.* "High-frequency irreversible electroporation is an effective tumor ablation strategy that induces immunologic cell death and promotes systemic anti-tumor immunity", *EBioMedicine*, vol. 44, pp. 112-125, 2019.

[4] B. Mercadal *et al.* "Dynamics of cell death after conventional IRE and HFIRE treatments", *Ann Biomed Eng*, vol. 48, pp. 1451-1462, 2020.

[5] T. Polajzer *et al.* "Immunogenic cell death in electroporation-based therapies depends on pulse waveform characteristics", *Vaccines*, vol. 11, p. 1036, 2023.

Collateral Effects of Electroporation: Heating, Electrical Stimulation, and Electrochemical Reactions

Antoni Ivorra; *Department of Information and Communication Technologies, Universitat Pompeu Fabra, Carrer Roc Boronat 138, 08018 Barcelona, SPAIN*

INTRODUCTION

Applying electrical energy to living tissues for inducing electroporation can cause diverse phenomena in addition to electroporation. Three well-identified collateral phenomena, which in most cases are undesired, are heating, electrical stimulation, and electrochemical reactions.

HEATING

Except for superconductors, all electrical conductors dissipate electrical energy in the form of heat when current flows through them. This phenomenon is known as Joule heating or resistive or Ohmic heating and obeys:

$$P = I^2 R$$

where P is the power of heating, I is the current flowing through the conductor and R is its resistance. This equation, known as Joule's law, can also be expressed for infinitesimal volumes at each point of space:

$$p = \frac{\left|\vec{J}\right|^2}{\sigma} = \left|\vec{E}\right|^2 \sigma$$

where σ is the electrical conductivity and $\vec{J}$ and $\vec{E}$ are the current density and electric field respectively. In electroporation scenarios, with field magnitudes in the order of hundreds of V/cm and conductivities in the order of S/m, Joule heating would cause harmful temperatures if very short exposures, much shorter than a second, were not used. The dependence of heating on the square of the electric field is relevant because it implies that heating is particularly high where the electric field is larger, typically at the periphery of the electrodes due to the edge effect. This is further exacerbated by the increase of σ with the temperature.

The temperature increase due to the Joule effect can be accurately predicted with numerical models, even for complex tissues. However, thermal damage models used to predict the physiological impact of the intense temperature peaks caused during electroporation are intended for longer exposures and, although are used by the electroporation community, their accuracy is still unknown.

ELECTRICAL STIMULATION

The nervous system transmits signals in the form of action potentials. Action potentials are sudden transitions in transmembrane resting voltage that propagate along the cell. Electrical stimulation consists in nonphysiologically triggering action potentials by delivering electric fields.

In clinical applications of electroporation, electrical stimulation is not desired because, by exciting efferent nerves, it causes muscle contractions and, by exiting afferent nerves, it causes pain [1].

Both electroporation and electrical stimulation occur when the transmembrane voltage is artificially increased above a threshold due to the presence of the electric field. This implies that unsought stimulation occurs very frequently when electroporation is intended. Advantageously, high-frequency biphasic fields can cause electroporation whilst minimizing electrical stimulation [2].

ELECTROCHEMICAL REACTIONS

Electrical conduction in metallic electric circuits is provided by the flow of electrons whereas in living tissues (and in suspensions) the moving charge carriers are ions. Conduction across the interface between the electronic conductor and the ionic conductor, that is, across the electrode, can be capacitive or electrochemical. Capacitive conduction is only substantial for very brief or ac currents of small magnitude. In most electroporation scenarios, conduction across the electrode is mediated by electrochemical reactions. In electrochemical reactions, the chemical species in the living tissue and the electrode exchange electrons thus altering their chemistry.

Electrochemical reactions are generally deleterious for electroporation applications because they modify pH and cause the release of gases and metallic ions. (However, it is worth noting that it has been proposed their synergy with electroporation to achieve large ablation volumes [3]).

Electrochemical reactions are a surface phenomenon (occur at the electrode) and, because of that, are of particular concern when the electrode area is large compared to the treated volume, as is typically the case in microfluidic setups.

Electrochemical reactions are difficult to model, particularly at the anode (positive electrode) because multiple reactions can occur concurrently.

Interestingly, high-frequency biphasic currents minimize electrochemical reactions. This effect, combined with lower stimulation, explains the emergence of high-frequency biphasic fields for electroporation-based ablation.

REFERENCES

[1] A. Cvetkoska *et al*. "Muscle contractions and pain sensation accompanying high-frequency electroporation pulses", *Sci Rep*, vol. 12, p. 8019, 2022.

[2] B. Mercadal *et al*. "Avoiding nerve stimulation in irreversible electroporation: a numerical modeling study", *Phys Med Biol*, vol. 62, pp. 8060-8079, 2017.

[3] N. Klein *et al*. "Single exponential decay waveform; a synergistic combination of electroporation and electrolysis (E2) for tissue ablation", *PeerJ*, vol. 5, p. e3190, 2017.

Will pulsed field ablation change the treatment of arrhythmias?

Atul Verma, *Faculty of Medicine, McGill University, Montreal, Quebec, CANADA*

INTRODUCTION

Percutaneous catheter ablation has emerged as a very effective means of treating arrhythmias including atrial fibrillation, ventricular tachycardia, and other supraventricular arrhythmias. Thermal ablation has been the mainstay of catheter ablation of arrhythmias. Radiofrequency energy is the longest used energy source, heating the tissue and thus eliminating sites that trigger arrhythmias in the heart. Cryothermy has emerged more recently and freezes the tissue instead of burning. Both of these energies have been refined over 2 decades and have provided good efficacy. However, the risks of collateral damage remain including cardiac perforation, phrenic nerve damage, pulmonary vein stenosis, and esophageal erosion and fistula.

Pulsed field ablation using irreversible electroporation may change the field of treatment for arrhythmias. First, cardiac tissue seems to be more sensitive to the effects of electroporation compared to nerve, smooth muscle, or vascular tissue. This may help target the desired cardiac triggers while minimizing the risk of collateral damage. Second, pulsed fields can be delivered within 5 seconds, compared to thermal tissue which often requires many seconds or even minutes to deploy. This may help the procedures become much more time efficient. Finally, the mechanism of cell death in electroporation appears to be predominantly apoptosis which preserves the extra-cellular matrix. This allows tissues like the esophagus or myelin layer of nerves to regenerate which also minimizes the risk of collateral damage. Cardiac cells are terminal which means they cannot regenerate. However, preservation of the matrix may help avoid cardiac chamber stiffness after extensive ablation.

RESULTS

Many pre-clinical studies have demonstrated the safety profile of pulsed field ablation compared to thermal ablation. Early human studies in which the esophagus, phrenic nerves, and pulmonary veins have been assessed post-ablation also seem to reinforce the safety of the technology.

Now that the technology has received limited market release in Europe, many thousands of procedures have been performed. Again, the safety profile appears to be good, except for some early reports of coronary vessel spasm causing ischemia. This tends to happen on the tricuspid and mitral isthmuses which are close in proximity to the coronaries. However, the efficiency of the procedures has borne out. Procedures which once took 1.5-2 hours to perform are now routinely taking under 1 hour.

Early clinical trials with one-year follow-ups have shown that the efficacy of pulsed field ablation seems equivalent to thermal ablation. This should not be surprising since tissue depths achieved from pulsed field technologies in their present form are about 4 mm – the same as thermal.

Technological advancements, unipolar and modified bipolar energy deliveries, and alternative catheter designs will be needed if lesion depth is to be improved. This will be very important for thicker tissues like the left atrial ridge, the mitral isthmus, or the ventricles.

REFERENCES

[1] A. Verma *et al*. "Primer on Pulsed Electrical Field Ablation: Understanding the Benefits and Limitations", *Circ Arrhythm Electrophysiol*, vol. 14, p. e010086, 2021.

[2] A. Verma *et al*. "Combined pulsed field ablation with ultra-low temperature cryoablation: A preclinical experience", *J Cardiovasc Electrophysiol*, vol. 34, pp. 2124-2133, 2023.

[3] M. Stewart *et al*. "Safety and chronic lesion characterization of pulsed field ablation in a Porcine model", *J Cardiovasc Electrophysiol*, vol. 32, pp. 958-69, 2021.

[4] A. Verma *et al*. "Pulsed Field Ablation for the Treatment of Atrial Fibrillation: PULSED AF Pivotal Trial", *Circulation*, vol. 147, pp. 1422-1432, 2023.

[5] V. Reddy *et al*. "Pulsed field or conventional thermal ablation for paroxysmal atrial fibrillation", *N Engl J Med*. doi: 10.1056/NEJMoa2307291, 2023.

SHORT PRESENTATIONS

A review of electroporation studies on black lipid membrane models

Burak Altun[1], Antoni Ivorra[1]; [1] *Department of Information and Communication Technologies, Universitat Pompeu Fabra, Barcelona, SPAIN.*

INTRODUCTION

Black lipid membrane (BLM) models have been utilized to investigate cell membrane processes for more than 60 years [1]. Electroporation studies explore these artificial membranes to understand membrane permeability changes when exposed to high electric field pulses [2].

We have studied the electroporation literature using BLMs with the main aim of understanding the transmembrane voltage thresholds to initiate electroporation and the factors they depend on.

METHODS

We have used "black lipid membrane models" and "planar lipid bilayer" as keywords since black lipid membranes are also referred to as planar lipid bilayers. We have found 30 research articles and considered only experimental studies. Theoretical and numerical modelling studies were disregarded.

RESULTS AND DISCUSSION

We aimed to understand the findings of different studies regarding the threshold voltages for initiating electroporation. Consequently, we also focused on the factors conducting pore opening under an applied electric field [3].

Most studies indicate thresholds in the order of a few hundreds of millivolts. Remarkably, one recent study indicates that pores can be created at transmembrane voltages lower than 100 mV [3].

However, it must be noted that while some studies consider that electroporation only occurs when stable membrane conductivity increases are achieved or even when the membrane collapses, other studies consider that electroporation occurs at the moment the membrane conductivity exhibits a conductivity larger than its resting conductivity. This issue hinders comparison between studies. In fact, during our research, we came across a double use of the term breakdown voltage. The term refers to a voltage that leads to a considerable increase in membrane conductivity due to electroporation. However, it was also indicated as a voltage that causes lipid bilayer rapture [4,5].

Some studies examine how chemical additives at different concentrations affect the electroporation threshold [6,7]. One of these studies found that the addition of surfactant caused an increase in the electroporation thresholds [6]. Furthermore, we found studies that investigated the electroporation of lipid membranes at different temperatures and focused on their temperature dependence [8,9].

Lastly, we have found studies that examine the changes in electropermeabilization due to lipid oxidation, peroxidation, and hydroperoxidization, separately [3,10]. Researchers in one of the studies observed alterations in the electrical properties of lipid bilayers [10]. They found that lipid oxidation causes an increase in the conductance of the bilayers compared to non-oxidized ones [10].

CONCLUSIONS

In the literature, we found a broad range of threshold transmembrane voltages from tens of millivolts to one volt. To a large extent, this very broad range is explained by differences in terminology and by the fact that electroporation exhibits gradation with the applied voltage (i.e., its depiction as a threshold mechanism is a simplification).

REFERENCES

[1] A. Ottova *et al.* "The 40th anniversary of bilayer lipid membrane research", *Bioelectrochemistry*, vol. 56, pp. 171-173, 2002.

[2] A. Ivorra. "Tissue Electroporation as a Bioelectric Phenomenon: Basic Concepts", in *Irreversible Electroporation*, Series in Biomedical Engineering, B. Rubinsky, Ed. Berlin: Springer, 2010, pp. 23-61.

[3] E. J. Lafarge *et al.* "Activation energy for pore opening in lipid membranes under an electric field", *Proceedings of the National Academy of Sciences*, vol. 120, 2023.

[4] P. Kramar *et al.* "Determination of the lipid bilayer breakdown voltage by means of linear rising signal", *Bioelectrochemistry*, vol. 70, pp. 23-27, 2007.

[5] P. Kramar *et al.* "A system for the determination of planar lipid bilayer breakdown voltage and its applications", *IEEE Trans Nanobioscience*, vol. 8, pp. 132-138, 2009.

[6] L. Tung *et al.* "Changes in electroporation thresholds of lipid membranes by surfactants and peptides", *Annals of the New York Academy of Sciences*, 1999.

[7] A. Polak *et al.* "Electroporation threshold of POPC lipid bilayers with incorporated polyoxyethylene glycol (C12E8)", *J Phys Chem B*, vol. 119, pp. 192-200, 2014.

[8] A. Blicher *et al.* "The temperature dependence of lipid membrane permeability, its quantized nature, and the influence of anesthetics", *Biophys J*, vol 96, pp. 4581-4591, 2009.

[9] A. Polak *et al.* "System for measuring planar lipid bilayer properties", *J Membr Biol*, vol. 245, pp. 625-632, 2012.

[10] K. Balantič *et al.* "The role of lipid oxidation on electrical properties of planar lipid bilayers and its importance for understanding electroporation", *Bioelectrochemistry*, vol. 153, p. 108498, 2023.

Beyond Transient Pores: Unveiling the Sustained Permeability in Electroporated Cell Membranes through Secondary Oxidation Insights

Daniel Wiczew[1,2], Natalia Szulc[1,2], Mounir Tarek[2]; *[1] Wroclaw University of Science and Technology, Department of Biomedical Engineering, 50-370 Wroclaw, POLAND [2] Université de Lorraine, CNRS, LPCT, F-54000 Nancy, FRANCE.*

INTRODUCTION

There is a large discrepancy with electroporation induced pore lifetime between experiment and Molecular Dynamics (MD) simulations; those in MD live few orders of magnitude less than in experiments [1]. Nevertheless, there are many studies showing lipid oxidation of the lipid membrane during electroporation [2]. Study [3] thoroughly explores pore dynamics in various bilayer systems. These investigations provide vital insights into the processes of pore formation, size, and lifetime.

METHODS

Model and MD Simulations

Two main systems were established using PACKMOL: SYST I with a central PoxnoPC (Figure 1) bilayer patch and SYST II, similar to SYST I, but with 40 mol% cholesterol. Simulations were performed using GROMACS with CHARMM36 lipid force field for POPC and cholesterol, and a special force field for PoxnoPC. TIP3P model and ECC correction were used for water and ions respectively.

RESULTS AND FIGURES

Pore formation (**in absence of Electric Field**) occurs (see Figure 2) within tens of nanoseconds in both SYST I and SYST II, with maximum sizes of 7 nm and 5 nm, respectively. Cholesterol presence in SYST II results in a smaller pore size and a prolonged pore lifetime, with the **pore not closing completely**, maintaining an aperture of about over 5 µs. We show that the findings align with the observed membrane conductance changes in GH3 cells, indicating that the pores formed are large enough to facilitate significant molecular transport. The addition of cholesterol in SYST II notably extends the pore lifetime, aligning more with experimental observations.

REFERENCES

[1] W.F.D. Bennett *et al*. "Atomistic simulations of pore formation and closure in lipid bilayers", *Biophys J*, vol. 106, pp. 201-219, 2014.

[2] M. Breton *et al*. "Optimization of the Electroformation of Giant Unilamellar Vesicles (GUVs) with Unsaturated Phospholipids", *J Membr Biol*, vol. 248, pp. 827-835, 2015.

[3] D. Wiczew *et al*. "Molecular dynamics simulations of the effects of lipid oxidation on the permeability of cell membranes", *Bioelectrochemistry*, vol. 141, p. 107869, 2021.

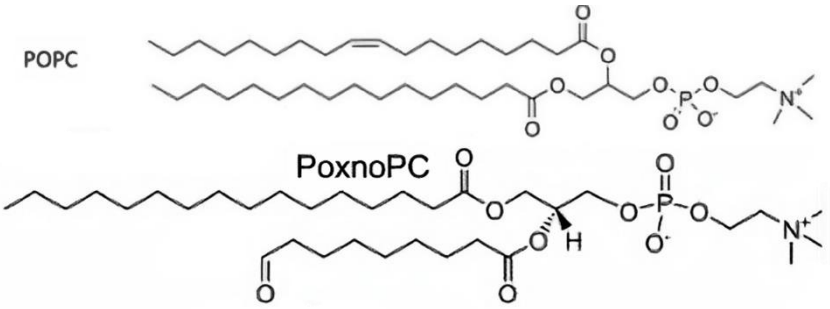

Figure 1. POPC together with its second order oxidation product – PoxnoPC.

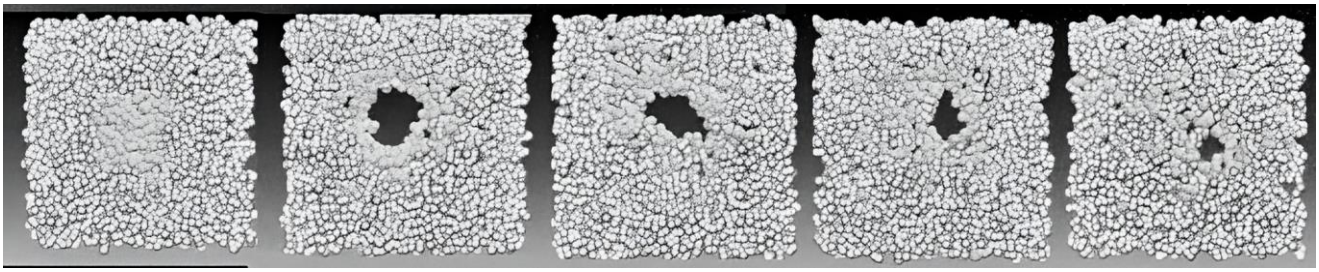

Figure 2. Depiction of the trajectory of the SYST II from the beginning (left-top frame) till the end of the 5 µs simulation. The simulation is done in absence of electric field.

Generators of PEF to biological samples for biomedical applications

Lionel Michard[1], Claire Dalmay[1], Philippe Leveque[1], Delia Arnaud-Cormos[1,2]; *[1] University of Limoges, CNRS, XLIM, UMR 7252, F87000 Limoges, FRANCE [2] Institut Universitaire de France (IUF), Paris, FRANCE.*

INTRODUCTION

In the last decades, the bio-effects of high-voltage short pulsed electric field (PEF) on biological cells and their potential therapeutic applications constituted the interest numerous research studies in the bioelectrics community. One main effect, i.e., "electroporation", can be observed when a cell is subjected for sufficient duration (milliseconds to nanoseconds range) to high intensity PEF (spanning from kV/cm to MV/m). This phenomenon is based on the permeability increase of the cell membrane, leading to a temporary (reversible) or permanent (irreversible) nano-pores formation in the membrane, which allows the exchange of molecules from and into the cytoplasm [1]. Reversible and irreversible electroporation were found to be beneficial for several therapeutic and biological applications, such as electrochemotherapy and electrogene therapy [2]. The delivery of short, nanosecond duration, intense PEF requires specific generators taking in consideration pulse's characteristics such as shape, duration, and amplitude. In this paper, we briefly describe the principle of a nsPEF optoelectronic generator.

Optoelectronic Generators

nsPEF can be generated using a high voltage DC power source and optoelectronic switches such as photoconductive semiconductor switches (PCSS) [3], [4]. DC energy is stored in a transmission line which acts as a capacitor. Ultra-low response time PCSS switches are then triggered allowing the generation of nanosecond pulses. A common architecture using a 3-ports structure and 2 PCSSs has been reported to be capable of generating 1 ns pulses with amplitudes up to 16 kV [3]. On these 3-ports structures, changing the termination on one of the ports to a short circuit, open circuit or matched load allows for modification of the reflection conditions of the incident wave, thus creating different resulting pulse shapes. Fig 1(a) shows examples of bipolar, unipolar and paired pulses obtained respectively for the short, matched load and open termination [3]. Additionally, it is possible to generate adjustable delayed pulses by changing the length of the coaxial transmission line separating the 3-ports structure and the reflection termination [3]. Fig 1(b) shows bipolar and paired pulses obtained for different coaxial cable lengths leading to different delays. This type of generator is thus capable of generating pulses of different shapes and amplitudes with adjustable delays. The generation of sub-nanosecond duration pulses will be further explored with this technology. These short, high intensity PEF might be applied to biomedical exposure systems such as miniaturized CPW [5] and could lead to the discovery of new bio-effects.

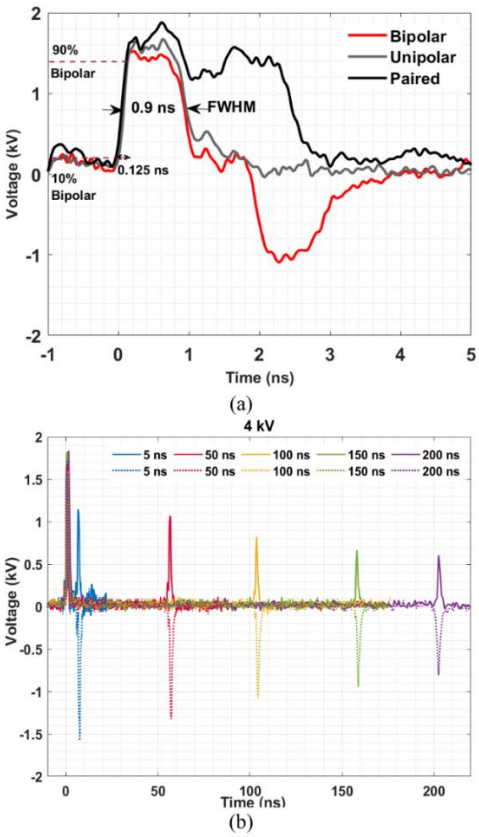

Figure 1. Electrical pulses created by the generator (a) unipolar, bipolar, and paired 0.9 ns pulses for a bias voltage of 4 kV. (b) Bipolar and paired pulses for 4 kV bias voltage with delays of 5 ns, 50 ns, 100 ns, 150 ns, and 200 ns [3].

REFERENCES

[1] L. Gibot. "3D Tissue Models to Bridge the Gap Between Cell Culture and Tissue in Assessing Electroporation," in *Handbook of Electroporation*, D. Miklavčič, Ed., Cham: Springer International Publishing, pp. 255-269, 2017.

[2] F. Apollonio *et al.* "Electroporation mechanism: Review of molecular models based on computer simulation", *6th European Conference on Antennas and Propagation (EUCAP)*, pp. 356-358, 2012.

[3] N. Tabcheh *et al.* "High Voltage Generator with Adjustable Delay Between Two Nanosecond Pulses", *IEEE Photonics Technol. Lett*, vol. 34, pp. 553-556, 2022.

[4] R. Orlacchio *et al.* "High-voltage 10 ns delayed paired or bipolar pulses for in vitro bioelectric experiments", *Bioelectrochemistry*, vol. 137, p. 107648, 2021.

[5] C. Dalmay *et al.* "A microfluidic biochip for the nanoporation of living cells", *Biosens Bioelectron*, vol. 26, pp. 4649-4655, 2011..

Delivery systems of PEF to biological samples for biomedical applications

Hafsa Tjiou[1], Claire Dalmay[1], Philippe Leveque[1], Delia Arnaud-Cormos[1,2]; *[1] University of Limoges, CNRS, XLIM, UMR 7252, F87000 Limoges, FRANCE [2] Institut Universitaire de France (IUF), Paris, FRANCE.*

INTRODUCTION

In the last decades, the bio-effects of high-voltage short pulsed electric field (PEF) on biological cells and their potential therapeutic applications constituted the interest of numerous research studies in the bio-electrics community. One main effect, i.e., "electroporation", can be observed when a cell is subjected for sufficient duration (milliseconds to nanoseconds range) to high intensity PEF (spanning from kV/cm to MV/m). This phenomenon is based on the permeability increase of the cell membrane, leading to a temporary (reversible) or permanent (irreversible) nano-pores formation in the membrane, which allows the exchange of molecules from and into the cytoplasm [1]. Reversible and irreversible electroporation were found to be beneficial for several therapeutic and biological applications, such as electrochemotherapy and electrogene therapy [2]. The delivery of short, nanosecond duration, intense PEF requires specific generators taking in consideration pulse's characteristics such as shape, duration, and amplitude. Moreover, delivery devices based on reduced gap distance between the electrodes in direct contact with the biological sample are explored for their ability to generate high electric field intensity [3]. In this paper, we briefly a proposed nsPEF delivery device, i.e., a miniaturized coplanar waveguide transmission line (CPW TL).

Coplanar waveguide transmission line for PEF delivery

A coplanar waveguide is a form of planar transmission line, based on a conductor printed on a dielectric two-dimensional substrate, called printed circuit board (PCB). The CPW are widely used in radio-frequencies and microwaves applications. Nefzi et al in [4] proposed a microfluidic microsystem based on a CPW TL (figure 1). The miniaturized structure, i.e., the reduced gap distance between the electrodes (130 µm), allows the generation of high intensity PEF, in the range of ~kV.

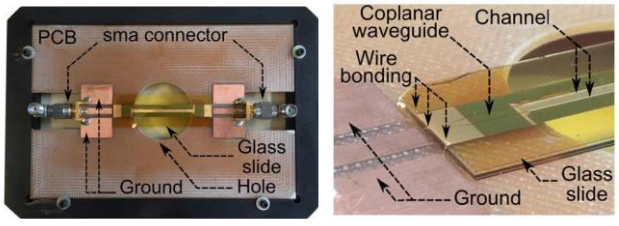

Figure 1. Photographs of the microfluidic microsystem based on CPW electrodes and of the microsystem mounted on a printed circuit board (PCB).

A wide frequency bandwidth, was proved by the electrical measurements (S parameters) of this system (figure 2). The reflection coefficient S11 is inferior to -10 dB, and

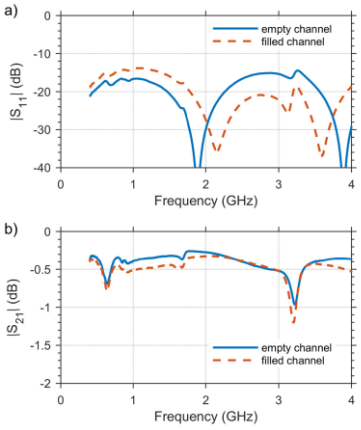

Figure 2. S-parameter measurement of the CPW, with empty (line), and filled (dots) channel; a) Reflection coefficient, b) transmission coefficient.

the transmission coefficient S21 is superior to -1 dB up to 3 GHz; it is possible to deliver electric field pulses with a

duration of ~1 ns. In this study, the CPW was employed to assess the exposure of biological samples to a continuous wave (CW) signal at 1.8 GHz. In our perspective, and due to its characteristics (frequency bandwidth and reduced inter electrode gap), a delivery device based on a miniaturized CPW TL will be designed and the generation of short duration (~ ns), intense (~ MV/m) electric field pulses will be investigated.

REFERENCES

[1] L. Gibot. "3D Tissue Models to Bridge the Gap Between Cell Culture and Tissue in Assessing Electroporation," in *Handbook of Electroporation*, D. Miklavčič, Ed., Cham: Springer International Publishing, pp. 255–269, 2017.

[2] F. Apollonio *et al.* "Electroporation mechanism: Review of molecular models based on computer simulation," in *2012 6th European Conference on Antennas and Propagation (EUCAP)*, pp. 356-358, 2012.

[3] D. Arnaud-Cormos *et al.* "Delivery system setup and characterization for biological cells exposed to nanosecond pulsed electric field," in *2015 IEEE MTT-S International Microwave Symposium*, pp. 1-4, 2015.

[4] A. Nefzi *et al.* "Microdosimetry Using Rhodamine B Within Macro- and Microsystems for Radiofrequency Signals Exposures of Biological Samples", *IEEE Trans. Microw. Theory Tech*, vol. 68, pp. 1142-1150, 2020.

PDMS-free microphysiological system to study the effects of pulsed electric fields

Neringa Bakute[1], Eivydas Andriukonis[1], Kamile Kasperaviciute[1], Martynas Sapurov[1], Jorunas Dobilas[1], Vilius Vertelis [1], Skirmantas Kersulis [1], Gatis Mozolevskis[2], Arunas Stirke[1,2]; [1] *State Research Institute, Center for Physical Sciences and Technology, Sauletekio ave. 3, LT-10257, Vilnius, LITHUANIA* [2] *Institute of Solid State Physics, University of Latvia, Kengaraga str. 8, LV-1063, Riga, LATVIA.*

INTRODUCTION

Batch electroporation, the conventional method of PEF treatment, typically involves a cuvette with embedded electrodes. Although the use of commercially available cuvettes is a simple, routine procedure, it does have certain drawbacks, including distortions in the electric field, local pH variation, excessive heat generation, and the dissolution of metal ions which in turn leads to reduced electroporation efficiency and cell viability [1]. To overcome these drawbacks, conventional batch pulsed electric field (PEF) technology has shifted toward the microscale and integration with microfluidic devices [2], also known as 'lab-on-a-chip', 'organ-on-a-chip' and microphysiological system (MPS).

In microfluidics, most soft-lithography microchips are made of polydimethylsiloxane (PDMS). However, an off-stoichiometry thiol-ene (OSTE) has emerged as an alternative to PDMS maintaining essential characteristics for microfluidics, such as transparency, biocompatibility, and repeatability and lacking the disadvantages of PDMS [3].

We present an MPS with an OSTE-based microfluidic chip for the PEF treatment of mammalian cells while monitoring their physiological parameters such as oxygen content, pH and trans-epithelial/endothelial electrical resistance (TEER).

METHODS

Microchip was fabricated by a soft-lithography technique. C6 cells were PEF treated in a stop-flow and continuous flow experiments at various electric fields 100-µs 1 Hz using the high-power square wave pulse electroporator; permeability and viability were determined by fluorescent spectrophotometry with DapI and trypan blue exclusion assay. Oxygen concentration was determined with oxygen measurement system Oxy-4 (PreSens, Germany); pH measurement was performed with developed pH sensor module and RealTerm software. TEER measurement was performed with LCR-6000 meter (Gwinstek, USA), connected to two adjacent electrodes in one plane.

RESULTS AND FIGURES

A microfluidic chip was fabricated in the format of a microscopy slide, its design is presented in Figure 1.

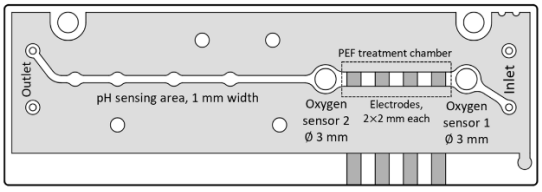

Figure 1. Schematic cross-sections of the microchip.

PEF treatment in stop-flow experiments revealed cell permeability to DapI (Figure 2) but did not affect cell viability at the electric field of 1.8-10 kV/cm. Oxygen concentration increased in the samples with cells during PEF treatment, meanwhile decreased if no cells were present. pH has increased during the PEF treatment. Lastly, we have demonstrated the ability to measure TEER.

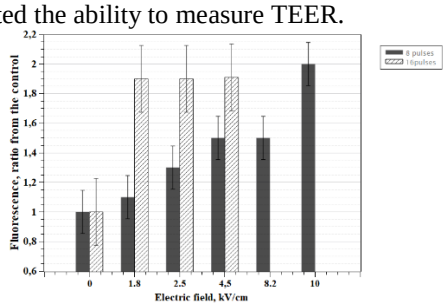

Figure 2. Permeability to DAPI in stop flow experiments at 1,8 kV/cm, 1 Hz. Fluorescence intensities expressed as a percentage of the fluorescence of the non-electroporated control for each electric field.

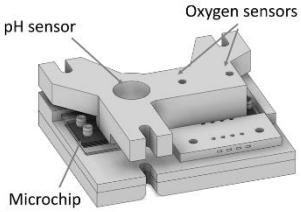

Figure 3. Schematic representation of MPS.

CONCLUSIONS

We have demonstrated our proof-of-concept technology works for PEF treatment of mammalian cells, measurement of oxygen, pH and TEER. Thus, our system (Figure 2) can be considered as an MPS by monitoring cell physiological parameters *in situ*.

REFERENCES

[1] G. Saulis *et al.* "Cytotoxicity of a Cell Culture Medium Treated with a High-Voltage Pulse Using Stainless Steel Electrodes and the Role of Iron Ions", *Membranes*, vol. 12, p. 184, 2022.

[2] T. Geng *et al.* "Microfluidic electroporation for cellular analysis and delivery", *Lab Chip*, vol. 13, pp. 3803-3821, 2013.

[3] C. F. Carlborg *et al.* "Beyond PDMS: OSTE based soft lithography for rapid prototyping of microfluidic devices", *Lab Chip*, vol. 11, pp. 3136-3147, 2011.

Microwave Sensors for Probing Effects of Pulsed Electric Field

Petr Kurka, Daniel Havelka, Michal Cifra; *Institute of Photonics and Electronics of the Czech Academy of Sciences, Chaberská 1014/57, 182 00 Prague, CZECH REPUBLIC.*

INTRODUCTION

Pulsed Electric Field (PEF) has gained substantial recognition in diverse scientific domains, especially in applications like cell electroporation. Still, a central challenge remains: How to monitor the real-time impacts of PEF? The answer could be by monitoring sample dielectric permittivity in the microwave range [1]. An advantage of permittivity measurement is its non-invasiveness and the ability to operate on different frequencies than the PEF. Therefore, no interference between the PEF application and the permittivity measurement arises.

METHODS

Planar microwave chips can be used as the sensor. In Figure 1 and Figure 2, you can see such examples from our lab. It is a split-ring resonator that was developed and tested in a previous work [2].

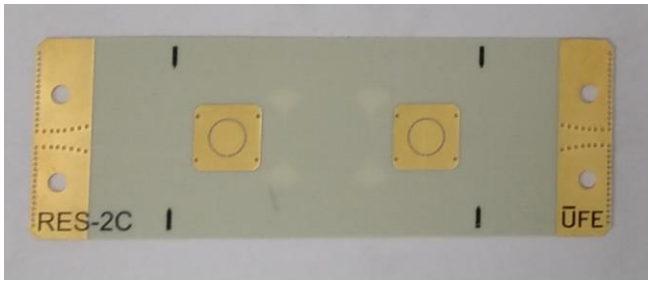

Figure 1. Split-ring resonator – top side.

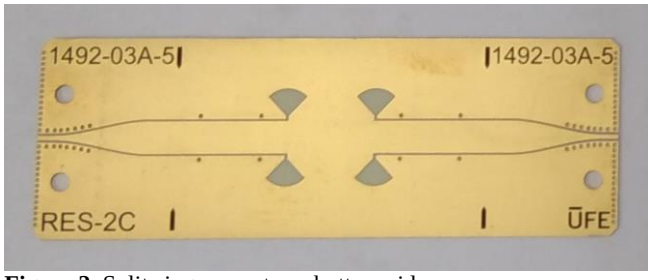

Figure 2. Split-ring resonator – bottom side.

A Vector Network Analyzer (VNA) was used as a measuring device. The samples were positioned on the Microwave Chip for characterization. In Figure 3, you can see the chip loaded with a sample of pure water. S-parameters were acquired using the VNA. Advanced numerical techniques were used to translate the S-parameters into permittivity.

RESULTS

There are three primary mechanisms driving the changes in permittivity in biomolecular water-based samples during and after PEF treatment, irrespective of the presence or absence of membrane compartments:

1. The unfolding and aggregation of protein samples, electrochemically induced changes, and consequent changes in effective dissolved biomolecules concentration.
2. Local temperature fluctuations. The higher the temperature change, the more significant the change in the sample permittivity is.
3. A formation of microbubbles due to sample heating or electrochemical generation of gasses. The microbubbles can alter the measured permittivity significantly.

The combination of all these effects results in a measurable change in the permittivity of the sample during PEF treatment.

Figure 3. Split-ring resonator loaded with a 130 uL water sample.

CONCLUSION

This work aims to demonstrate the connection behind quantifying PEF effects through permittivity changes and its potential for permittivity-based real-time monitoring of PEF effects in future applications.

ACKNOWLEDGEMENTS

We acknowledge support from the Czech Science Foundation, project no. GX20-06873X.

REFERENCES

[1] A. Tamra *et al.* "Single Cell Microwave Biosensor for Monitoring Cellular Response to Electrochemotherapy," *IEEE Trans Biomed Eng*, vol. 69, pp. 3407-3414, 2022.

[2] A. K. Jha *et al.* "A Resonant Reflection Type Microwave Reference Sensor for Testing of Small Biomolecules," in Proceedings of EuMCE, Prague, pp. 629-632, 2019.

The effects of a microsecond pulsed electric field on tubulin

Michaela Poplová[1*], Tomáš Zakar[1*], Viliam Kolivoška[2], Michal Cifra[1]; *[1] Institute of Photonics and Electronics, The Czech Academy of Sciences, Chaberská 57, 18200, Prague, CZECH REPUBLIC [2] J. Heyrovsky Institute of Physical Chemistry, The Czech Academy of Sciences, Dolejškova 2155/3, 18223, Prague, CZECH REPUBLIC. * equal contribution*

INTRODUCTION

Tubulins serve as the fundamental constituents of the largest class of filaments, known as microtubules (MTs), which play an indispensable role in a multitude of vital cellular processes. Notably, the tubulin protein exhibits an exceptionally high structural electric charge and dipole moment [1]. The functioning and interactions of tubulin proteins are greatly influenced by the electric charge present on the amino acid residues and atomic groups within them. Consequently, the application of an external electric field offers a promising approach to manipulating the functionality of cytoskeletal proteins such as tubulin [2].

METHODS

Initially, the tubulin protein was transferred to ddH_2O by centrifugal filtration. After setting the proper concentration, the tubulin was treated by a microsecond pulsed electric field (1500 V / 1 mm gap, unipolar 100 µs, 1 Hz firing frequency, 20 pulses in one series) in a standard 1 mm gap electroporation cuvette. Figure 1. shows the schematic diagram of the pulse setup. After the pulse treatment, tubulin was transferred into the BRB80 medium for further analysis. Particle size distribution was measured by Dynamic Light Scattering (DLS) spectroscopy. For further examinations, samples were filtered by ultracentrifugation to eliminate larger particles-aggregates being formed during the µsPEF treatment and to set the same initial concentration for all the samples. The treated and untreated tubulin was investigated by ANS fluorescence (1-anilino-8-naphthalene sulfonate) assay, Ellman's assay (DTNB reagent), TRP/TYR fluorescence spectroscopy, and polymerization assay.

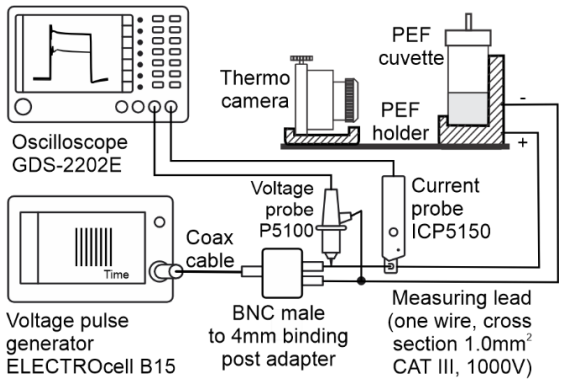

Figure 1. PEF treatment schematic diagram of the tubulin inside the electroporation standard cuvette.

RESULTS

The DLS analysis revealed that the number of large particles increases in the PEF-treated tubulin samples. We observed a significant drop in the protein concentration as well in all the PEF-treated samples after the vast majority of aggregates were removed by ultracentrifugation. Polymerization (seen in Fig.2) assay proved that the 3 times PEF-treated tubulin lost the ability to form microtubules. The results were verified by phase contrast microscopy. The results of the ANS fluorescence spectroscopy showed an increasing trend in the fluorescence intensity at the treated tubulin samples, indicating that PEF might alter the structure of tubulin allowing the ANS to access more hydrophobic groups in the protein. However, the structural changes in the protein caused by PEF treatment decreased the ability of Ellman's reagent (DTNB) to interact with the tubulin's sulfhydryl groups. The PEF treated samples exhibited decreased TRP/TYR autofluorescence.

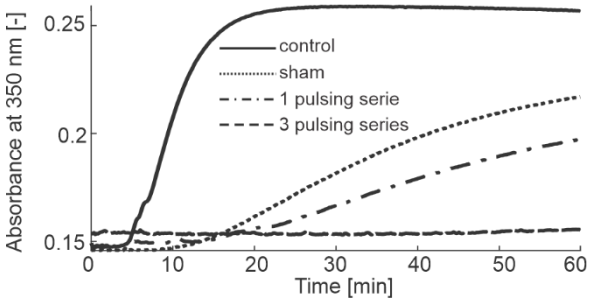

Figure 2. Polymerization curves of control sample incubated directly in BRB80; sham sample with the same procedure as pulsed samples (transferring into ddH_2O but without pulsing), and sample in ddH_2O during the pulsed period.

CONCLUSION

Our results contribute to the development of novel electromagnetic methods for modulating the function of biomolecular matter at the nanoscale. The PEF treatment causes structural changes in tubulin while preserving its basic ability to polymerize. We also found out the threshold of the irreversible function of tubulin and observed the aggregation effect of PEF treatment on tubulin.

ACKNOWLEDGEMENTS

We acknowledge support from the Czech Science Foundation, project no. GX20-06873X.

REFERENCES

[1] P. Marracino *et al.* "Tubulin response to intense nanosecond-scale electric field in molecular dynamics simulation", *Sci Rep*, vol. 9, p. 10477, 2019.

[2] D. E. Chafai *et al.* "Reversible and Irreversible Modulation of Tubulin Self-Assembly by Intense Nanosecond Pulsed Electric Fields", *Adv Mater*, vol. 31, p.1903636, 2019.

Study on the combined effect of Electroporation and Radiofrequency

Borja López-Alonso[1], Matej Reberšek[2], Héctor Sarnago[1], Óscar Lucía[1], Damijan Miklavčič[2]; *[1] Escuela de Ingeniería y Arquitectura, University of Zaragoza, C/ Mª de Luna 1, Zaragoza, SPAIN [2] Faculty of Electrical Engineering, University of Ljubljana, Trzaska 25, Ljubljana, SLOVENIA.*

INTRODUCTION

Electroporation (EP) has a wide range of applications, including medicine and food processing. In the food industry, the synergy between the effects of electroporation and temperature increase has already been demonstrated in some applications [1]. However, in medicine, electroporation is typically used to minimize thermal effects, and the effects of the combination of cell permeability change and heating have not been studied in depth.

In medicine, there are already treatments based on heating within which radiofrequency (RF) is applied in a similar way to electroporation. As in EP, in RF bipolar electrodes are used between which a voltage wave is applied, but at a higher frequency than the one used in EP. This makes it possible to design a system capable of combining the waves used in EP and RF to generate the electric field required for produce electroporation and at the same time increasing the temperature.

The aim of this study is to develop a power electronics system to study the effects of the combination of RF and EP in vitro. The requirements for the system and the solutions to the problem are presented below.

PROBLEM DESCRIPTION

Although RF and EP are based on the generation of a voltage wave, their properties are different and there are several ways to combine them. Firstly, EP [2] is based on generation of an electric field of the order of KV/cm at typical frequencies of the order of KHz, whereas RF requires the generation of currents in the order of tens of A at frequencies in the MHz range. Three main strategies for combining these treatments have been identified: harmonic summing, PWM control and amplitude modulation. The first, as shown in Figure 1 (a), is the direct sum of two pure harmonics, one with frequency and amplitude in the EP range, and the other with the parameters of the RF. The second strategy is the generation of a PWM wave (Figure 1 (c)), that contains two necessary harmonics, but as shown in Figure 1(d), it also contains other lower-order harmonics. Finally, a harmonic with frequency in the RF range and amplitude in the EP range can be generated and modulated in amplitude by a frequency wave in the EP range, as shown in Figure 1 (e). In contrast to the previous strategies, as shown in Figure 1 (f), this wave does not have the EP harmonic, so its response to tissue impedance should be different from the previous two. A priori, each strategy to combine both treatments could lead to different results. Therefore, the ideal system must have a high output power to supply the necessary current of the RF, it must also be able to work with voltages of the order of KV to generate the necessary fields to EP phenomenon occur, and finally, it must have a versatility that allows testing all the proposed strategies.

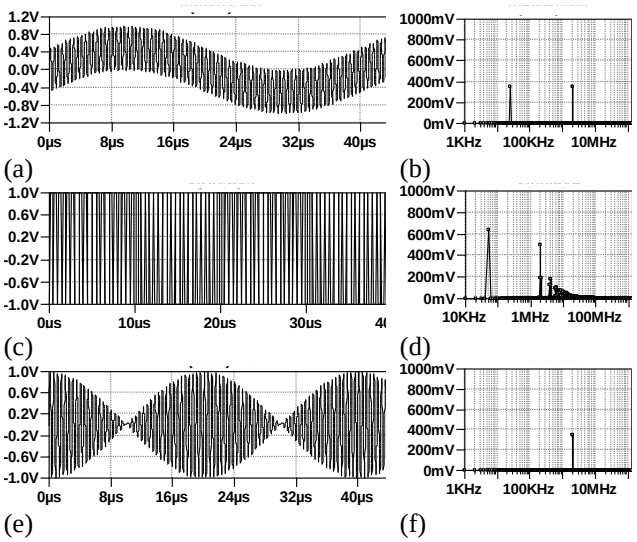

Figure 1. Voltage waveform and harmonic content for the combination of a 2 MHz RF treatment and a 50 KHz EP treatment: (a) and (b) by direct harmonic summation, (c) and (d) by PWM control, and (e) and (f) by amplitude modulation.

SYSTEM PROPOSAL

The easiest system to carry out a proof of concept with electrode spacing less than millimetres is the use of a high frequency analog digital converter (DAC) together with a high-power operational amplifier. However, to work with tissues or electrodes with larger distance, a design based on two independent inverters, or a multilevel design of high power and high frequency DAC is required.

CONCLUSIONS

The combination of EP with RF could improve the efficacy of current EP treatments, but a technological development is needed to study it, and these are the goals of the research presented.

ACKNOWLEDGEMENTS

This work was partly supported by Projects PID2022-136621OB-I00, PDC2021-120898-I00, TED2021-129274B-I00 and ISCIII PI21/00440, co-funded by MCIN/AEI/10.13039/501100011033, and by Margarita Salas fellowship by the MIU and NextGenerationEU, convocatoria 2021-2023.

REFERENCES

[1] G. Saldana *et al.* "Microbiological Aspects Related to the Feasibility of PEF Technology for Food Pasteurization", CRFSN, vol. 54, pp. 1415-1426, 2014.

[2] T. Garcia-Sanchez *et al.* "Successful Tumor Electrochemotherapy Using Sine Waves," *IEEE Trans Biomed Eng*, vol. 67, pp. 1040-1049, 2020.

.

PEF application enables extraction of phytochemicals from *Scutellaria baicalensis* roots to a Deep Eutectic Solvents (DES) medium

Kajetan Grzelka[1*], Sylwester Ślusarczyk[1], Adam Matkowski[1]; [1] *Department of Pharmaceutical Biology and Biotechnology, Wroclaw Medical University, POLAND.*
* - corresponding author

INTRODUCTION

Exposing biological tissue to pulsed electric field (PEF), after properly adjusting its parameters, leads to cell electroporation. Increased permeability of the membrane then results in increased exchange of intra- and extracellular compounds, enabling extraction of compounds from plant tissue. Our aim is to further study the effect of PEF on plants, especially regarding extraction. In available literature [1], [2] authors have already shown that electroporation can be successfully used in extraction of compounds from plant tissue. In our research we hope to expand on these findings and further optimize the treatment parameters, so that after pulse administration and successful extraction of phytochemicals the survival of treated plants is ensured and this process can be regularly repeated. Additionally, we used deep eutectic solvents (DES) as a green alternative to conventionally used aggressive chemicals such as methanol. Plants used in this study were cultivated in aeroponic systems, which adds to eco-friendly character of our work.

MATERIAL AND METHODS

Aeroponically cultivated 3 months old *Scutellaria baicalensis* (Sb) was used as a model plant in this study. Two variants of PEF were applied: E = 0.5 kV/cm N = 100 f = 1 Hz t = 100 us **(A)** and E = 0.5 kV/cm N = 200 f = 10 Hz t = 50 us **(B)**, where E – electrical field strength, N – no. of pulses f – frequency, t – pulse length. The following solvents were used: choline chloride: glucose (1:2) + 30% water; choline chloride: ethylene glycol (1:2); choline chloride : fructose (1:2) + 30% water; choline chloride : saccharose (1:2) + 40% water; tap water. After pulse administration to the plants' roots, the medium was collected from the cuvette and antioxidant DPPH (radical scavenging activity) tests were conducted, using baicalin (concentration range 5-500 μg/mL) as reference. The change in electrical conductivity of solvents was also noted and membrane disintegration index Z was calculated.

RESULTS

There are statistically significant differences of medium conductivity and antioxidant activity between samples, being generally higher for PEF treatment **(B)**. The highest disintegration index Z (40%) was noted for a DES mixture of choline chloride: glucose (1:2) + 30% distilled water, and the lowest when using tap water (11%). None of the treated specimens survived the process, clearly showing that the applied PEF conditions were too severe and need to be further adjusted.

DPPH test indicated that the most active extract was obtained in a DES mixture of choline chloride: ethylene glycol (1:2), where almost 50% of free radicals were scavenged and corresponded to antioxidant activity of 300 μg/mL baicalin concentration. The HPLC-MS analysis of exact composition of the extracts is in progress and will be followed by quantitative analysis.

CONCLUSION

PEF assisted extraction of Sb flavonoids is promising but its efficiency varies depending on DES composition and treatment parameters.

ACKNOWLEDGEMENTS

The research was funded in whole of the National Science Center POLAND basis of the decision number National Science Centre Poland; UMO-2020/39/D/NZ9/01402 and grant to K. Grzelka funded by Empiria i Wiedza foundation in Talenty Jutra program, 2023 edition.

REFERENCES

[1] Y. N. Kim *et al*. "Effects of pulsed electric field (PEF) treatment on physicochemical properties of Panax ginseng", *Innov Food Sc. Emerg Technol*, vol. 58, p. 102232, 2019.
[2] M. Fincan *et al*. "Pulsed electric field treatment forsolid-liquid extraction of red beetroot pigment", *J. Food Eng*, vol. 64, pp. 381-388, 2004..

Growth properties enhancement of oleaginous yeasts in bioreactors by nanosecond pulsed electric fields (nsPEF)

Marco S. Fluri[1], Katharina Übelhör[1], *Lya Siegenthaler[2]*, *Leandro Buchmann[2]*, Lukas Neutsch[1]; [1] *Zürcher Hochschule für angewandte Wissenschaften, Bioprocess Technology Research Group, Grüntalstrasse 14, 8820 Wädenswil, SWITZERLAND* [2] *Bühler Group, Gupfenstrasse 5, 9240 Uzwil, SWITZERLAND.*

INTRODUCTION

The increasing need in biotechnology for more sustainable solutions, whilst boosting the spacetime-yield of the production is a demanding challenge. A promising way to achieving this goal is the application of nsPEF (nanosecond Pulsed Electric Field) to boost yield or growth properties [1]. In this paper *Yarrowia lipolytica* is used as a model organism for the production of natural lipids, with e.g. application in food biotech. The production takes place in a in a highly monitored biotechnological batch process with state-of-the-art process analytic technologies. The effect of nsPEF and its challenges in application will be pointed out and discussed.

METHODS

Yarrowia lipolytica was cultivated in a 2.5L glass bioreactor (Labfors 5, Infors HT, Switzerland) in batch mode. Based on pre-assessments for the most suitable biological treatment time point of when to apply nsPEF to the cells (single treatment time point), composed of multiple experiments in a miniaturized manner: At this timepoint the reactor was split in two 1L reactors (Minifors 2, Infors HT, Switzerland). The cell suspension transferred into the first reactor was treated with nsPEF. 0.7kW/mL were applied using the Stellar™ Gemini system, an industrialized product based on previous work of L. Buchmann [2]. The cell suspension of the second reactor was not treated during the transfer and acted as control. The two cultivations ran for 48h and further monitoring of inline optical density (OD), dissolved oxygen (pO2), pH and offline CDW (Cell Dry Weight), offline OD and substrate composition were performed. For comparability and additional verification of the reactor-run experiment, monitored shake flask cultivations were conducted with the treated and control cell suspension.

RESULTS

The behaviour known from pre-trials, that cells show a lag phase after treatment which lasts approx. 1.5h was observed both in reactor and shake flask trials. After that period, both cultivations were growing with approx. the same growth rate at 0.21 h^{-1} for 8h. After the exponential growth phase, the treated cells were still metabolically active, whereas the control showed only minor metabolic activities. The exhaust CO_2 stayed on a level of 0.2%, pO2 around 80% and the respiratory index (RQ) at 0.35 mol mol^{-1} for the next 33h in the nsPEF treated reactor. During this time OD and CDW kept increasing in the treated reactor. In Figure the CDW measurements of the two reactors are shown. The increasing values in the treated reactor after the exponential phase (15h +) are displayed and the percentual increase compared to the untreated rector are indicated. An increase in CDW of almost 50% and an increase in OD of 61% was achieved.

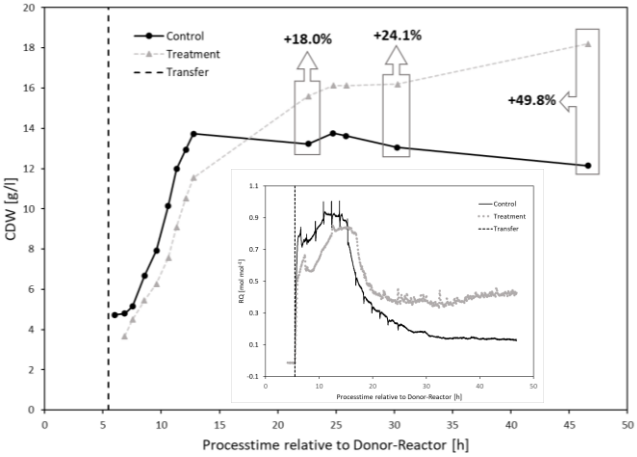

Figure 1. Cell Dry Weight (CDW) of two reactors inoculated with cell suspension of *Yarrowia lipolytica*. One was treated with nsPEF (black line), the other wasn't (grey dotted line). The small, embedded graph shows the RQ, to highlight the shift in growth due to the nsPEF treatment.

Comparing previous conducted shake flask trials (data not shown) to the results obtained in the reactor, it can be concluded that the growth enhancing effect is much larger in the controlled environment of a reactor. Hence, we point out that the growth enhancement effect of nsPEF on *Yarrowia lipolytica* shows a much more significant behaviour when increasing the scale and process control.

CONCLUSION AND OUTLOOK

Besides the promising growth enhancement results for *Y. lipolytica*, this project shall lead to a generalized approach to determine the optimal biological treatment timepoint and optimal nsPEF parameters for a broad range of biological systems. The combination of a miniaturized approach with a multistage reactor setup, holds as a generic approach to investigate further strains and provides the toolkit to establish a rapid screening to determine the most favourable settings for nsPEF treatment. Additional investigations are still needed to further develop this approach.

REFERENCES

[1] L. Buchmann *et al*. "Effect of nanosecond pulsed electric field treatment on cell proliferation of microalgae", *Bioresour Technol*, vol. 271, pp.402-408, 2019.

[2] L. Buchmann *et al*. "Comprehensive pulsed electric field system analysis for microalgae processing", *Bioresour Technol*, vol. 265, pp. 268-274, 2018.

In vivo microscopy imaging of two model plants *Iris domestica* and *Scutellaria baicalensis* after Pulse Electric Field (PEF) treatment

Sylwester Ślusarczyk[1], Kajetan Grzelka[1], Grzegorz Chodaczek[2], Adam Matkowski[1,3]; *[1] Department of Pharmaceutical Biology and Biotechnology, Wroclaw Medical University, POLAND [2] Bioimaging Laboratory at Łukasiewicz Research Network - PORT Polish Center for Technology Development,Wroclaw, [3] Medicinal Plants Botanical Garden, Wroclaw Medical University, POLAND.*

INTRODUCTION

The aim of this work was to develop and optimize a PEF treatment for the vital microscopy imaging and reversible electroporation from the roots and rhizome of *Iris domestica* (syn. Belamcanda chinensis L. DC. Iridaceae) and *Scutellaria baicalensis* L. cultivated in aeroponic system.

MATERIAL AND METHODS

7 weeks old aeroponic cultivar both plants were electroporated (4 mm gap cuvette) using different pulsed electric field strength 1, 3 and 7.5 kV/cm with constant 50 μs duration of pulse and repetition (N=50) of pulse. Roots were electroporated in the presence of propidium iodide (PI) using as a medium pure water and HEPES buffer and directly imaged after the electroporation on the Leica SP8 confocal microscope. PI was excited with a 552 nm laser line and the collected emission range was 560-680 nm. Six to eight areas were imaged with volumes up to 146 um^3 and a 2 um Z step. Nuclei were marked with a paintbrush tool in a separate empty channel and upon channel binarization counted with the Analyze Particle function (Figure 1). Than plants were cultivated in aeroponic systems and observed throughout the next 4 months, compare to control.

RESULTS

Experiment proved that live roots electroporation in 1 and 3 kV/cm is reversible (plants survived and still grow for next 4 month) but 7.5 kV/cm is irreversible (no plants survived). *I.domestica* is less sensitive to PEF treatment than *S.baicalensis*, however we previously showed that electroporation of *S.baicalensis* significantly impacted plant growth and the content of flavonoids, especially baicalein and wogonin, depending on the treatment parameters [1].

CONCLUSION

We can conclude that 1 kV/cm electric field improved plants growing compared to control. Confocal microscopy show simple linear relationship of stained cell nuclei was proportional to the strength of the electric field and nuclei membrane were observed per 3 mm deep in the root.

ACKNOWLEDGEMENTS

The research was funded in whole of the National Science Center POLAND basis of the decision number National Science Centre Poland; UMO-2020/39/D/NZ9/01402

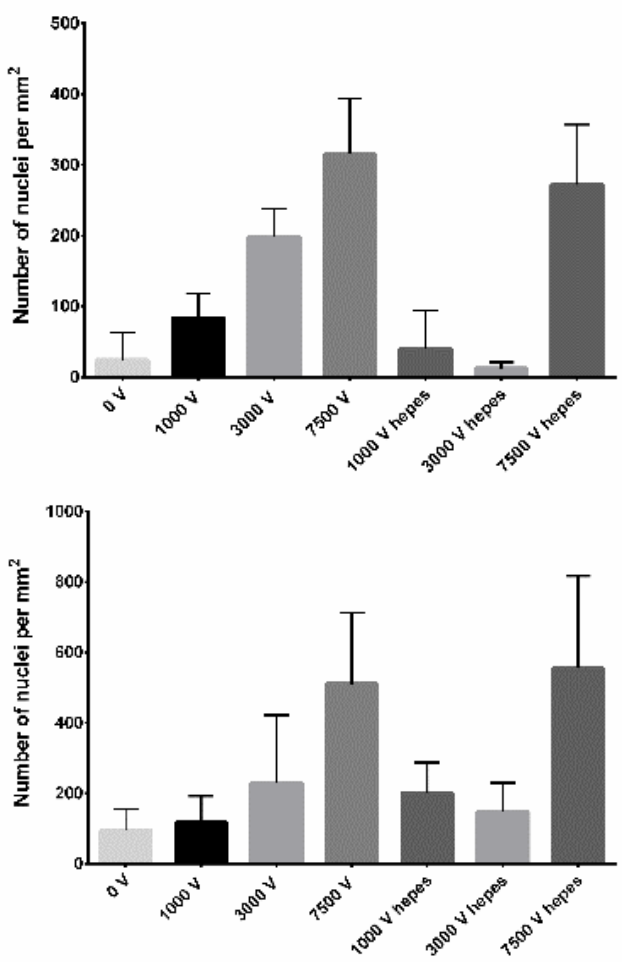

Figure 1. Calculated nuclei of *I.domestica* (uper) and *S.baicalensis* (lower) roots tissue after PEF tretment in water and hepes buffer.

REFERENCES

[1] K.Grzelka *et al*. "Electrostimulation improves plant growth and modulates the flavonoid profile in aeroponic culture of Scutellaria baicalensis Georgi", *Front Plant Sci*, vol. 14, p. 1142624, 2023.

Investigation of osmotic shock effect on pulsed electric field treated *S. cerevisiae* yeast cells

Greta Gančytė[1], Povilas Šimonis[1], Arūnas Stirkė[1,2]; [1]*Laboratory of Bioelectrics, Center for Physical Sciences and Technology, State Research Institute, Sauletekio Ave. 3, 10257, Vilnius, LITHUANIA* [2]*Micro and Nanodevices Laboratory, Institute of Solid State Physics, University of Latvia, Kengaraga Str. 8, Riga, 1063, LATVIA.*

INTRODUCTION

Saccharomyces cerevisiae yeasts are single-celled eucaryotic fungus microorganisms. During the course of evolution yeast adapted to employ the high osmolarity glycerol (HOG) pathway to recover after dangerous cell shape modifications and intracellular water imbalance caused by environmental osmotic pressure changes. Pulsed electric field (PEF) treatment is known to cause plasma membrane permeabilization, an effect known as electroporation, yet at the moment there is no information on whether biochemical pathways responsible for intracellular osmotic balance have a role in yeast response to PEF treatment. In this study, we set out to employ osmotic shock treatment to elucidate its effect on 1) viability, 2) permeability and recovery PEF-treated yeast cells as well as 3) to investigate involvement of HOG in yeast cell responses to PEF and osmotic shock treatments.

METHODOLOGY

Experiments were performed with wild type (WT) Y00000 yeast and a mutant strain derived from WT, Y02724, with no active HOG1 gene. In this study mutant strain will be referred to as Δhog.

Cell suspension was placed into a cuvette with a 0.2 cm gap between electrodes and exposed to a single square-shaped pulse with pulse length of 150 µs and an electric field strength (E) of up to 10 kV/cm.

5s after the pulse, to 500 µL electroporated cell suspension 1500 µL of either (1) distilled water, (2) 20 mM Tris, 0.5 M sorbitol, pH 7.4, as a hypoosmotic solution and 3) 20 mM Tris, 1.5 M sorbitol, pH 7.4, (4) 20 mM Tris, 2 M sorbitol, pH 7.4 as a hyperosmotic solution was added. Final sorbitol concentration in respective samples was (1) 0.25 M ($\pi = 6.11$ atm), (2) 0.625 M ($\pi = 15.28$ atm), (3) 1.375 M ($\pi = 33.62$ atm), (4) 1.75 M ($\pi = 42.79$ atm).

The osmotic pressure of each solution was calculated by:

$$\pi = iMRT \quad (1)$$

where π is osmotic pressure, i is van't Hoff's factor (for this solution i = 1), M is Molar concentration of the solution (mol/L), R is the ideal gas constant (0.08206 L atm mol^{-1} K^{-1}) and T is the temperature in Kelvin (K).

RESULTS

Results showed that Hog1 deficient *S. cerevisiae* cells were considerably more sensitive to electric field treatment, confirming a link between the HOG pathway and *S. cerevisiae* recovery process after electroporation. By suddenly changing the osmolarity of the media after PEF we influenced the cells' plasma membrane recovery rate, severity of permeabilization and survivability of yeast cells [1].

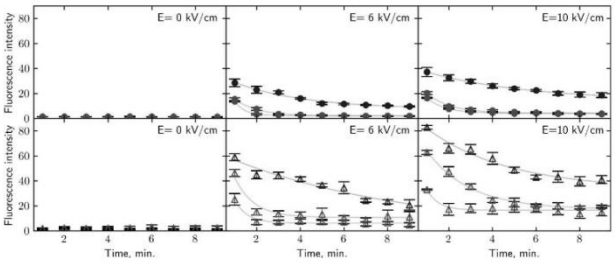

Figure 1. Fluorescence intensity dependence on time after PEF.

Our proposed mechanism is summarised in Fig. 2.

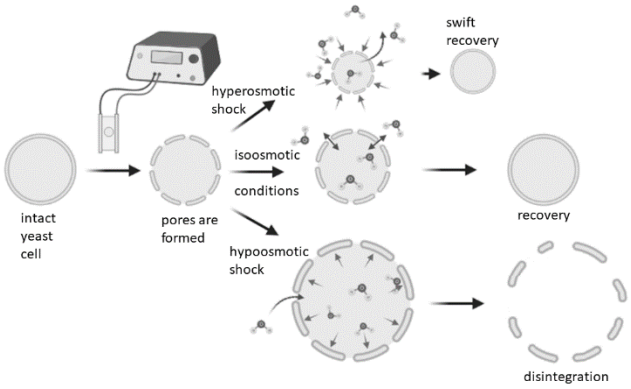

Figure 2. Schematic representation of post-PEF osmotic shock impact on yeast cell.

REFERENCES

[1] G. Gančytė *et al*. "Investigation of osmotic shock effect on pulsed electric field treated S. cerevisiae yeast cells", *Sci Rep*, vol. 13, p. 10573, 2023.

Pulsed electric fields assisted gentle cell disruption for microalgae biorefinery

Byron Perez[1,2], Iris Haberkorn[2], Carole Zermatten[1,2], Alexander Mathys[1,2]; *[1] Sustainable Food Processing Laboratory, ETH Zürich, Zürich, SWITZERLAND [2] ETH Singapore Centre (SEC), SINGAPORE.*

INTRODUCTION

The increasing global population poses a significant challenge, as the surge in resource demand is anticipated to reach 50% to 60% by 2050. Microalgae, with their minimal land needs and metabolic flexibility, offer a more efficient way to produce valuable bioresources compared to traditional crops [1]. However, challenges during the downstream processing of microalgae derivatives hinder their industrial potential. Microsecond pulsed electric field (PEF) can gently disrupt cells, facilitating extraction selectivity and reducing cell debris formation. This selectivity facilitates a biorefinery cascade, enabling the isolation of proteins and lipids without cross-contamination despite modest extraction yields [1]. A subsequent incubation step holds promise for enhancing cell permeability and intracellular compound extraction through PEF-triggered processes [2], [3]. While the impact of pulse width has been explored in various PEF applications, its influence on the incubation outcome remains uncharted. This study investigates the effect of pulse width on PEF-assisted protein extraction yield and cell permeability in highly concentrated, heterotrophic *Auxenochlorella protothecoides* during the post-PEF incubation phase.

METHODS

Auxenochlorella protothecoides suspension (40±3 g L^{-1}) was treated in a continuous plate-plate treatment chamber. An electric field of 25 kV cm^{-1} (10±0.1 kV) was applied by a RUP6-15CL square pulse generator and monitored using a voltage probe and oscilloscope. The frequency was adjusted to apply 12 or 36 pulsed of 15 µs or 5 µs, respectively, with an equivalent energy input of 1720±30 kJ kg^{-1}_{DW}. Samples post-PEF treatment were adjusted to pH 4 and incubated in the dark at 25 ± 1 ºC. Microalgae permeabilization was assessed using Sytox Green® dye on an Attune-NxT Flow Cytometer. Protein was analyzed as total nitrogen using a Shimadzu TOC/TN analyzer

RESULTS AND DISCUSSION

Initial permeabilization levels were 63±0.89% and 64.61±0.95% for 5 and 15 µs pulses, respectively, with comparable initial extraction yields across both pulse durations. Subsequent to a 5 h incubation interval, cell permeabilization nearly reached 96% for both pulse widths. This enhancement might be attributed to PEF-triggered sensitization of microalgae cells to the acidic incubation conditions or incomplete membrane recovery in reversibly electroporated cells. Protein yields 71% higher than the pre-incubation levels were observed for both pulse widths following PEF treatment and incubation for 5 h (from 0.122±0.017 to 0.209±0.025 kg_{EP} kg^{-1}_{TP} for 5 µs, and from 0.125±0.004 to 0.214±0.0167 kg_{EP} kg^{-1}_{TP} for 15 µs). After a 19 h incubation period, protein yield reached 0.237±0.02 and 0.260±0.019 kg_{EP} kg^{-1}_{TP} for 5 and 15 µs, respectively, corresponding to a 109% augmentation over initial extraction. These findings affirm the absence of pulse width influence within this timeframe, both for cell permeabilization and protein extraction yield pre- or post-incubation. The extraction yield enhancement is aligned with prior research attributing enhanced permeability and yield to enzymatic activity post-cell death [2].

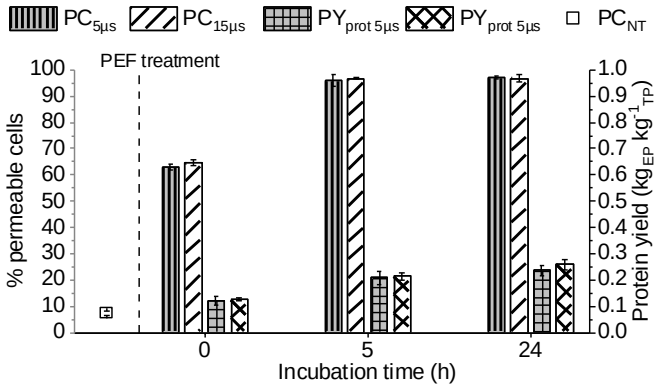

Figure 1. Percentage of permeabilized cells (PC, left y-axis) for non-treated sample (PC_{NT}) and protein extraction yield (PY, right y-axes) for samples treated with 36x5 µs pulses ($PC_{5µs}$ and $PY_{prot\ 5\ µs}$), 12x15 µs pulses ($PC_{15\ µs}$ and $PY_{prot\ 15µs}$). Data represents averages and standard deviations from three biological replicates measured in technical duplicates.

CONCLUSIONS

The post-PEF treatment incubation step exhibited no discernible pulse width dependence up to 15 µs. Remarkably, this phase could enhance cell permeability by up to 36% and boost protein yield by 109%, achieved without additional PEF treatment application. These findings underline the potential for an efficient microalgae cell disruption process for future biorefinery applications.

REFERENCES

[1] G. P.'t Lam *et al.* "Multi-Product Microalgae Biorefineries: From Concept Towards Reality," *Trends Biotechnol*, vol. 36, pp. 216-227, 2018.

[2] D. Krust *et al.* "Biological signalling supports biotechnology – Pulsed electric fields extract a cell-death inducing factor from Chlorella vulgaris," *Bioelectrochemistry*, vol. 143, p. 107991, 2022.

[3] D. Scherer *et al.* "Pulsed electric field (PEF)-assisted protein recovery from Chlorella vulgaris is mediated by an enzymatic process after cell death", *Algal Res*, vol. 41, p. 101536, 2019.

"This research is supported by the NRF, Prime Minister's Office, Singapore under its CREATE program.

Impact of pulse parameters on gene electrotransfer to Jurkat E6.1 cell line

Zala Vidic[1, 2], Damijan Miklavcic[1]; *[1] University of Ljubljana, Faculty of Electrical Engineering, Trzaska 25, SI-1000 Ljubljana, SLOVENIA [2] University of Ljubljana, Faculty of Medicine, Vrazov trg 2, SI-1000 Ljubljana, SLOVENIA.*

INTRODUCTION

Electroporation is a non-viral method for nucleic acids delivery to the cells which is a crucial step for developing gene therapies [1]. For successful gene electrotransfer (GET), the optimal pulse parameters for a particular cell type should be determined [2]. In our study, we tested different protocols for measuring effects of electroporation and tried to evaluate the impact of electric field strength on GET efficiency in human T cell line. The results could lead to a better understanding of the processes underlying the genetic manipulation of T cells, such as engineering CAR-T cells for cancer immunotherapies [1].

MATERIALS AND METHODS

Jurkat E6.1 cells (CLS, Germany) in RPMI-1640 growth medium were placed in 2 mm cuvettes at a concentration of 5×10^6 cells/ml and exposed to 8 pulses of 100 µs duration at a repetition frequency of 1 Hz. Electric fields of 0 to 3 kV/cm were tested for all experiments. Electroporation was performed using L-POR V0.1 (mPOR, Slovenia). Cell viability after electroporation was determined using the MTS-based proliferation assay (Promega, USA) 24 hours after pulse delivery. Sample absorbance was measured with an Infinite M200 spectrophotometer (Tecan, Switzerland) using different measurement parameters (single or multiple reads per well). Cell membrane permeabilization was determined using the YO-PRO-1 dye (Life Technologies, USA). The percentage of permeabilized cells was measured 3 minutes after pulse delivery using a flow cytometer (Attune NxT, Life Technologies, USA). For evaluation of GET, pEGFP-N1 was added to the cell suspension at a concentration of 100 µg/ml before pulse delivery. After 24 hours of incubation (37°C, 5% CO_2), cell viability was assessed as previously described and GET efficiency was measured using a flow cytometer. Overall GET efficiency was calculated as: GFP positive cells (%) × viable cells (%) / 100.

RESULTS

The experiments provided us with the membrane permeabilization and cell viability curves (Figure 1), which give us information about the electric field that supposedly results in the highest survival and permeabilization rate and thus optimum outcome of overall GET efficiency in the Jurkat E6.1 cell line. Furthermore, we have shown that the parameters tested for absorbance measurements had only a minor effect on the results of the viability measurements. When testing the impact of different electric field strengths on GET outcome, we achieved the overall GET efficiency of 37 % when the cells were exposed to 2 kV/cm (Figure 2). Results in both pictures are represented as an average of 3 repetitions.

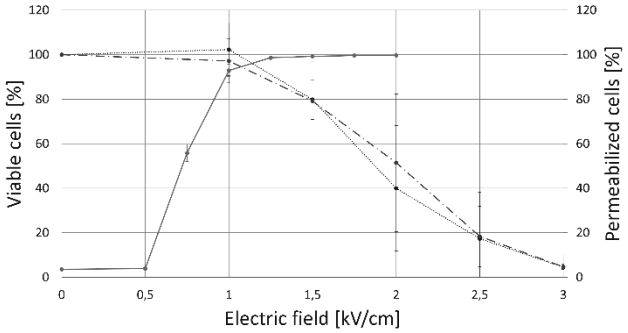

Figure 1. Survival (solid line – single read per well; dashed line – multiple reads per well) and permeabilization (bold line) of Jurkat cells exposed to different electric fields.

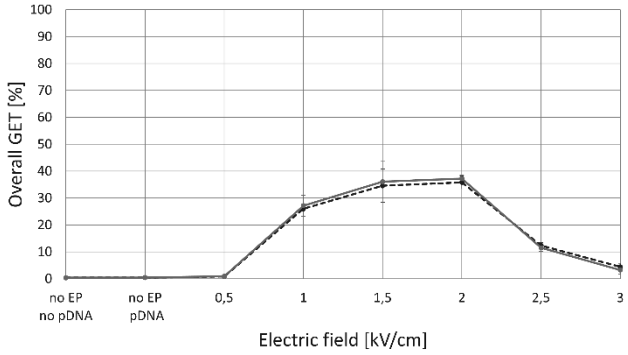

Figure 2. Overall pEGFP-N1 electrotransfer efficiency in Jurkat cells exposed to different electric fields (dashed line – 2 hours; solid line - 3 hours of cell incubation with MTS).

CONCLUSIONS

Our results give us insight into the behaviour of Jurkat T cells when exposed to electric fields of different strengths. However, further studies are needed to understand the mechanisms of gene manipulation by electroporation since many factors may influence the final outcome of GET.

ACKNOWLEDGMENTS

This study was funded by Slovenian Research Agency (ARRS) with grant P2-0249 and Junior Researcher funding to ZV. The experiments were performed in the Infrastructure Programme "Network of research infrastructure centres at the University of Ljubljana (MRIC UL, grant IP-0510).

REFERENCES

[1] E.S. Atsavapranee *et al*. "Delivery technologies for T cell gene editing: Applications in cancer immunotherapy", *EBioMedicine*, vol. 67, p. 103354, 2021.

[2] T. Potocnik *et al*. "Efficient Gene Transfection by Electroporation—In Vitro and In Silico Study of Pulse Parameters ", *Appl Sci*, vol. 12, p. 8237, 2022.

Optimizing High-Voltage Pulses for Gene Electrotransfer: Balancing Transfection Efficiency and Cell Viability

Ernestas Urbanskas[1], Justinas Venckus[1], Baltramiejus Jakštys[1]; [1] *Faculty of Natural Sciences, Vytautas Magnus University, Vileikos g. 8, 44404 Kaunas, LITHUANIA.*

INTRODUCTION

Gene electrotransfection (GET) stands as a prevalent technique for gene delivery, relying on the utilization of electric fields [1]. The process of introducing genes into cells using electrical pulses has been shown to be more complex than the electrotransfer of small molecules across the cell's plasma membrane, and it includes the involvement of endocytosis [2]. GET is already established as a cost-effective and safe technology in clinical studies, since it uses plasmid DNA without the need for viruses or extra chemicals [1]. Although its effectiveness is still limited when it comes to transferring large genes and GET can reduce cells viability considerably.

The primary objective of this research was to examine the effectiveness of GET and assess cell viability. The study involved the experimentation with electric field strength and pulse number, aiming to pinpoint optimal conditions. These conditions were sought to enhance the transfection efficiency without harming cell viability.

METHODS

Experiments were conducted utilizing the Chinese hamster ovary (CHO) cell line, employing varied electroporation parameters to assess the effectiveness of GET. The efficiency of transfecting the Green Fluorescent Protein (pMAX-GFP) plasmid was examined by quantifying the count of transfected cells and the intensity of their fluorescence through the employment of a flow cytometer (AccuriTM C6, USA) after 24 hours subsequent to the application of varying quantities of high voltage (HV) pulses. Additionally, the viability of the cells after GET was determined using a clonogenic assay, performed six days post the experimental procedure.

RESULTS

Using an 800 V/cm electric field, more cells were transfected as the number of high-voltage (HV) pulses increased. At 8 HV pulses, 39% of cells were transfected with 95% viability and 1.7 million SSV fluorescence. At 32 HV pulses, transfection efficiency reached highest 68 %, cell viability 22 %.With 16 HV pulses, 56% transfection and 46% viability were observed, along with 2.0 million SSV fluorescence.

Statistically, transfection and fluorescence significantly differed from controls at 8-32 HV pulses ($p<0.001$ and $p<0.0001$, respectively). Viability was significantly lower at 16-32 HV pulses compared to controls ($p<0.001$), but not at 1-8 HV pulses.

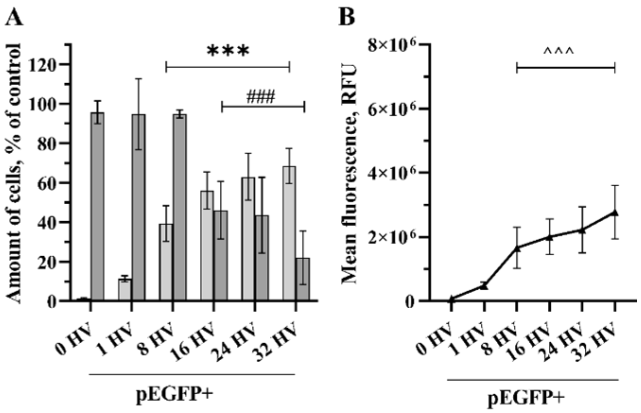

Figure 1. The efficacy of Gene Electrotransfer (GET) and the survival of CHO cells rely on the count of electric pulses. The investigations were carried out under conditions of 800 V/cm electric field strength, 100 µs pulse duration, and a 1 Hz repetition frequency. Statistical significance was assessed using the Bonferroni multiple comparison test, where *** indicates $p<0.001$, and ** indicates $p<0.05$ in relation to the comparison of transfected, fluorescent, and viable cell quantities between the control group and the ensuing experiments.

CONCLUSION

Our findings indicate that using lower electrical field strength, it takes more HV pulses to achieve optimal transfection rate and keep cell viability relatable high. Although increasing electrical field strength it takes less HV pulses to achieve same goal.

REFERENCES

[1] L. D. Cervia *et al*. "Current Progress in Electrotransfection as a Nonviral Method for Gene Delivery", *Mol Pharmaceutics*, vol. 15, pp. 3617-3624, 2018.

[2] C. Rosazza *et al*. "Endocytosis and Endosomal Trafficking of DNA After Gene Electrotransfer In Vitro", *Mol Ther Nucleic Acids*, vol. 5, p. e286, 2016.

The Influence of Electric Pulse Duration on Protein Uptake and Cell Viability in Electroporation of CHO Cells

Justinas Venckus[1], Ernestas Urbanskas[1], Baltramiejus Jakštys[1]; [1] *Faculty of Natural Sciences, Vytautas Magnus University, Vileikos g. 8, 44404 Kaunas, LITHUANIA.*

INTRODUCTION

Protein delivery into cells has potential in genome editing and cellular function studies, crucial for disease treatments. However, the plasma membrane's impermeability to proteins, due to their size and charge, presents challenges. In this regard, electroporation stands out as a versatile technique [1]. Although traditionally used for nucleic acid transfer, direct protein introduction offers immediate cellular effects, bypassing delays and potential post-transcriptional and post-translational modifications associated with DNA or RNA electrotransfection. Yet, the efficiency of electroporation with large proteins, which have low surface charges, is debated. This is because they rely more on diffusion than on the electrophoretic-driven delivery typical of highly charged nucleic acids [2]. Adjusting pulse duration might be a solution, as longer membrane pore openings could aid weakly charged protein entry. Still, there are concerns about protein conformational changes, cell viability post-electroporation, and protein retention as the cell grows.

The main goal of this research was to determine the efficiency of electroporation of proteins into cultured mammalian cells by varying the duration of electric pulse, aiming to define optimal conditions. These conditions were sought to improve the protein delivery efficiency without reducing cell viability.

METHODS

Chinese hamster ovary (CHO) cells were utilized for protein introduction experiments, following an adapted method from Lambert et al. [3]. While the foundation of our approach was based on their methodology, some modifications were implemented. CHO cells were electroporated using varying pulse durations (1, 2, 5, 10, and 15 ms) at an electric field strength of 1500 V/cm to facilitate the entry of the bovine serum albumin (BSA) Alexa Fluor 488 conjugate. The control group was not subjected to the electric pulse, nor it was treated with BSA. 24 hours post-electroporation, the viability of the CHO cells—both those treated with the labelled BSA prior to the procedure and controls without the protein—was assessed using the 3-(4,5-dimethylthiazol-2-yl)-2,5-diphenyltetrazolium bromide-phenazine methosulfate (MTT-PMS) assay. BSA delivery efficiency was determined by counting the number of fluorescent cells and quantifying their fluorescence intensity via flow cytometry, specifically employing the AccuriTM C6 cytometer (USA).

RESULTS

At 1500 V/cm electric field strength, the impact of pulse duration on protein uptake and cell viability was studied. Starting at 1 ms, 23% of cells were fluorescent, but overall cell viability dropped to 20.3%, implying cellular damage. At 2 ms, the fluorescent cell percentage increased significantly by 41.35%. A further increase to 5 ms gave a 14.12% rise in fluorescent cell percentage, but from 5 ms to 15 ms, a slight decrease was noted. The mean fluorescence intensity (MFI) peaked at 5 ms (1,24 million RFU), indicating maximum protein uptake. However, after this peak, MFI marginally decreased at 10 ms and 15 ms. Cell viability consistently decreased as pulse duration increased, with the most significant decline (40.24%) between 5 ms and 10 ms. Compared to controls, protein electroporation efficiency showed statistical significance, but cell viability was notably lower ($p<0.05$ and $p<0.001$).

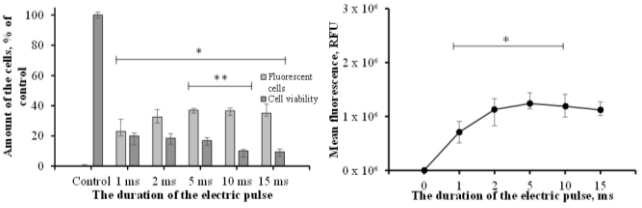

Figure 1. Dependence of cell viability, bovine serum albumin Alexa Fluor 488 conjugate electrotransfer efficiency (left) and the mean intensity of fluorescence (right) on the varying durations (1, 2, 5, 10 and 15 ms) of the single 1500 V/cm strength electrical pulse Chinese hamster ovary (CHO) cells were subjected to. Statistical significance was assessed using the Student's t-test, where * indicates $p<0.05$, and ** indicates $p<0.001$ in relation to the comparison of fluorescent and viable CHO cell quantities between the control group and the ensuing experiments. The data is shown as mean (n=3) ± standard deviation.

CONCLUSION

Our findings indicate that electroporation facilitates protein delivery into mammalian cells and its efficiency could be initially improved by widening the electric pulse, but this comes with a substantial reduction in cell viability. Prolonging pulse durations further decreases cell viability while the protein delivery remains relatively stable.

REFERENCES

[1] N. Pathak *et al*. "Cellular Delivery of Large Functional Proteins and Protein–Nucleic Acid Constructs via Localized Electroporation", *Nano Lett*, vol. 23, pp. 3653-3660, 2023.

[2] Y. Cao *et al*. "Universal intracellular biomolecule delivery with precise dosage control", *Sci Adv*, vol. 4, p. eaat8131, 2018.

[3] H. Lambert *et al*. "Electroporation-mediated uptake of proteins into mammalian cells", *Biochem Cell Biol*, vol. 68, pp. 729-734, 1990.

Role of the actin cortex in intracellular transport of electrotransferred DNA cargo

Sophie de Boer[1], Aswin Muralidharan[1], Hans Uitenbroek[1] , Bijoy Bera[1], Gijsje H. Koenderink[2], Pouyan E. Boukany[1]; [1] *Department of Chemical Engineering, Technical University of Delft, NETHERLANDS [2] Department of Bionanoscience & Kavli Institute for Nanoscience Delft, Technical University of Delft, NETHERLANDS.*

INTRODUCTION

Genome editing methods such as CRISPR-CAS can precisely alter mammalian cell genomes, driving cell biology advancement and promising treatments for congenital diseases. Efficient genome editing for therapy involves delivering nucleic acids and editing enzymes to cell nuclei by breaching the insulating cell membranes. Electroporation can permeabilize the cell membrane using high-voltage pulses but its efficacy lacks clear understanding, which hinders clinical use. While prior research studied the active and passive intracellular transport of genetic cargoes [1], our hypothesis highlights the overlooked impact of the DNA size and cell type during gene electrotransfer. This unexplored mechanism of cargo translocation explains differences in transport effects on varying live cells and cargo types.

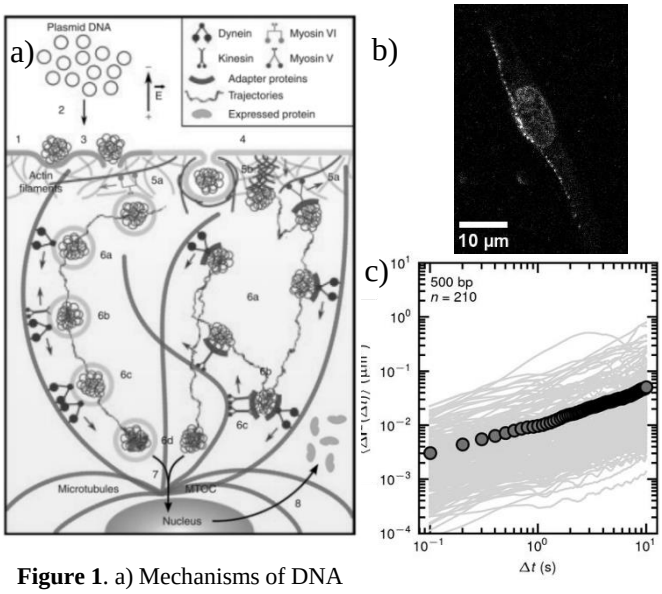

Figure 1. a) Mechanisms of DNA electrotransfer in mammalian cells, reproduced from [1]. b) DNA aggregation after electroporation on a CHO-K1 cell. c) Individual time averaged mean squared displacements of 500 bp DNA against the lag time Δt, for a measurement time T = 10 s. The circles represent the ensemble, reproduced from [2].

There are multiple intracellular pathways for cargoes to reach the nucleus, these mechanisms are shown in Fig 1a). Previous research has shown that internalized cargoes undergo anomalous diffusion [2]. Furthermore, the diffusion coefficient of electrotransferred DNA cargo decreases when the DNA size is increased, and the transport is dependent on the cell's type (benign, malignant, and metastatic) [2].

In this ongoing study, the ultimate objective of this work is to uncover how the actin cortex (a network of filaments that strengthens the cell membranes) contributes to the transport of nucleic acids in the cytoplasm after the transfer across the cell membrane. This is pertinent due to the actin cortex's effect on the resealing dynamics of electropermeabilized membranes [3], and its unclear role in intracellular transport after electroporation.

METHODS [2] & PRELIMINARY RESULTS

This study will be utilizing diverse nucleic acid sizes: 100 bp, 250 bp, 500 bp, and other cargo (e.g. CRISPR-Cas) along with a range of cell types such as benign, malignant, and metastatic breast carcinoma cell lines. In Fig 1b) aggregation of fluorescent 500 bp DNA ladders is shown at the CHO-K1 cell membrane after electroporation.

To monitor intracellular transport, the culture medium is aspirated from the Ibidi plates prior to electro-transfer. Stainless steel electrodes (placed parallel to each other and 3 mm apart) are used to apply 10 electric pulses of 350 V/cm amplitude and 5 ms duration at a frequency of 1 Hz to the cells in the chambers. After electroporation, the electrodes are removed and the cells are left to rest for 10 minutes at room temperature (~ 22◦C). Finally, the cells are incubated for 15 minutes and then imaged.

OUTLOOK

To understand the mechanism of cargo translocation, single particle tracking (SPT) will be employed to monitor the intracellular displacement of nucleic acids within cells using (photostable) Cy3 dye. By analysing mean squared displacement graphs, different diffusion regimes can be identified, and intracellular transport behaviour can be clarified as done in Fig 1c) in prior studies [2]. By validating this experimental technique with continuous random walk (CTRW) and fractional Brownian motion (FBM) models, in addition to innovations such as photostable dyes and CRISPR-Cas cargoes, we can gain insights into the dynamics and behaviour of these complex systems.

REFERENCES

[1] C. Rosazza *et al*. "Intracellular tracking of single-plasmid DNA particles after delivery by electroporation", *Mol Ther*, vol. 21, pp. 2217-2226, 2013.

[2] A. Muralidharan *et al*. "Intracellular transport of electrotransferred DNA cargo is governed by coexisting ergodic and non ergodic anomalous diffusion.", *BioRxiv* 2021.

[3] D. L. Perrier *et al*. "Response of an actin network in vesicles under electric pulses", *Sci Rep*, vol. 9, p. 8151, 2019.

Role of the Actin Cytoskeleton in Cell Membrane Electroporation and Cargo Translocation

Nikki Nafar[1], Pouyan E. Boukany[1], Gijsje H. Koenderink[1]; [1] *Faculty of Applied Sciences, Delft University of Technology, Van der Maasweg 9, 2629 HZ Delft, NETHERLANDS.*

INTRODUCTION

Genome editing technologies require intracellular delivery of nucleic acids (DNA or RNA) or proteins (e.g., CRISPR-Cas9). Electroporation, a method that transiently disrupts the cell membranes through high-voltage electric pulses, offers a potential solution. However, the biophysical mechanisms underpinning electroporation are still poorly understood, in part due to the inherent complexities of live cells and overly simplified models like giant unilamellar vesicles (GUVs) [1]. An often-underestimated factor is the actin cytoskeleton, crucial for cellular structural integrity and various cellular processes. Evidence suggests that the actin cytoskeleton plays a key role in electroporation, influencing membrane permeability, macropore formation, and resealing [1, 2]. This research aims to elucidate the role of the actin cytoskeleton in electroporation by engineering tunable actin cortices within GUVs. This effort could provide deeper insights into electroporation's biophysical principles

RESEARCH METHODOLOGY

To model the actin cortex, we will encapsulate five regulatory proteins into GUVs: ADF/cofilin for thickness control, α-actinin for crosslinking, myosin II motors for network tension, and Arp2/3 complex and mDia1 formin as nucleators [3,4]. Depending on the resolution needed, cortex assembly and structure will be assessed with various imaging techniques. The effect of cortex characteristics on surface mechanics will be evaluated using micropipette aspiration (MPA). The effects of electroporation on the structural/ mechanical integrity of the actin cortex will be studied using confocal imaging and mechanical measurements. Additionally, we will investigate the influence of membrane composition on biomechanics and electroporation susceptibility, focusing on membrane lateral organization, fluidity, and electroporation thresholds, using ternary raft mixtures (mixtures of saturated and unsaturated lipids with cholesterol). Lastly, we will examine how actin cortex variations affect the electrotransfer of DNA cargo, measuring adhesion force post-electroporation with single molecule force spectroscopy using an AFM.

RESULTS

In Arp2/3-mediated actin cortices GUVs, actin and VCA concentrations impacted actin cortex formation in a concentration-dependent manner (Figure 1). Increased actin led to more vesicles with an actin cortex, and higher VCA shifted actin from patches to a continuous cortex. In mDia1-mediated cortices, profilin promoted cortical actin localization (Figure 2). Irregular distribution of actin was seen in DOPC GUVs, while POPC led to continuous cortex but with lipid clusters (Figure 2, bottom row), necessitating GUV formation optimization.

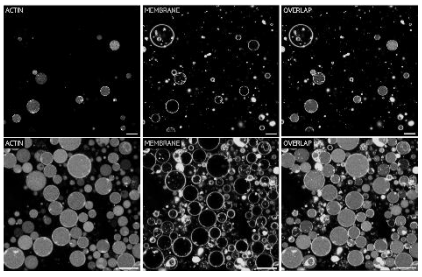

Figure 1. Confocal images of DOPC GUVs with Arp2/3-induced actin cortex. Top: 4.4 μM actin, 0.05 μM Arp2/3, 0.65 μM VCA. Bottom: 8 μM actin, 0.05 μM Arp2/3, 6.5 μM VCA.

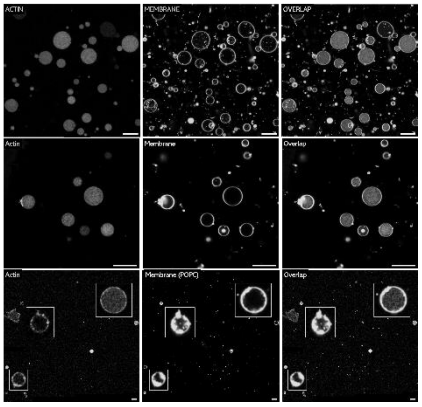

Figure 2. Confocal images of GUVs with mDia1-induced actin cortex. Top: DOPC GUVs, 4.4 μM actin, 1 μM mDia1. Middle: DOPC GUVs, 4.4 μM actin, 1 μM mDia1, 4.4 μM profilin. Bottom: POPC GUVs, 4.4 μM actin, 1 μM mDia1, 4.4 μM profilin.

REFERENCES

[1] T. Kotnik *et al*. "Membrane Electroporation and Electropermeabilization: Mechanisms and Models", *Annu Rev Biophys*, vol. 48, pp. 63-91, 2019.

[2] D. L. Perrier *et al*. "Response of an actin network in vesicles under electric pulses", *Sci Rep*, vol. 9, 2019.

[3] T. M. Svitkina. "Actin Cell Cortex: Structure and Molecular Organization", *Trends Cell Biol*, vol. 30, pp. 556-565, 2020.

[4] L. Baldauf *et al*. "Branched actin cortices reconstituted in vesicles sense membrane curvature", *Biophys J*, vol 122, pp. 2311-2324, 2023.

The effect of electroporation with different electrodes on cell viability in the incubation medium

Tina Turk, Alenka Maček Lebar; *University of Ljubljana, Faculty of Electrical Engineering, Trzaska 25, SI-1000 Ljubljana, SLOVENIA.*

INTRODUCTION

Electroporation refers to the temporary enhancement of cell membrane permeability through the application of high-voltage pulses, enabling the passage of various ions and molecules. The prevailing mechanism involves the rearrangement of lipid molecules in the cell membrane to form conductive pathways known as pores. Exposure to pulsating electric fields also induces chemical changes and affects membrane proteins, further increasing cell membrane permeability [1].

During pulse delivery electrochemical reactions occur at the interface between the electrodes and the medium. An important electrochemical process is the oxidation of the electrode metal, leading to the release of metal ions into the biological sample. Specifically, release of iron ions triggers processes that can result in cytotoxicity of the cell culture medium and affect cell viability [2].

The aim of our study was to determine how different metal electrodes influence cellular processes post-electroporation, focusing on stainless steel and aluminium electrodes.

METHODS

Experiments were performed on Chinese hamster ovary cells (CHO). Eight monopolar square-wave electrical pulses with a duration of 5 ms, an electric field strength of 0.75 kV/cm and a repetition frequency of 1 Hz were applied. Five minutes after electroporation, 400 µl of the electroporated cell suspension (4×10^6 cells) was centrifuged (5 min, 200 g) to separate the electroporation medium from the electroporated cells. The electroporation medium was removed and replaced with fresh growth medium. The electroporated cells were incubated in this medium for 2 h in an incubator (37°C, 5 % CO_2). The incubation medium was obtained by filtering this medium with a 0.8 µm filter. Cells from a freshly trypsinized cell culture were seeded into the incubation medium on a 96-well plate. Cell viability was determined after 72 h using the MTS assay.

We analysed the cytotoxicity of Fe^{2+} ions at concentrations ranging from 0.05 to 5 mM using a clonogenic assay. Furthermore, we examined how the presence Fe^{2+} ions at concentrations ranging from 1 to 5 mM in the cell suspension during electroporation in aluminium electrodes affects the viability of cells from a freshly trypsinized cell culture in the incubation medium.

RESULTS

All cells from a freshly trypsinized cell culture died in the incubation medium after electroporation when stainless steel electrodes were used, whereas the viability of freshly trypsinized cells when using aluminium electrodes was comparable to the control (Figure 1).

In the general assessment of cytotoxicity with a clonogenic assay, all cells in the sample died when exposed to a 5 mM concentration of Fe^{2+} ions. Taking into account the electrical charge delivered to the cell sample during electroporation, the toxic concentration of iron ions released from the stainless steel electrodes during electroporation should be approximately 3.2 mM. Results showed that adding a 5 mM concentration of Fe^{2+} ions to the cell suspension before electroporation with aluminium electrodes caused a significant reduction in the proportion of metabolically active cells (to 16.7 ± 5.6 %) from a freshly trypsinized cell culture in the incubation medium.

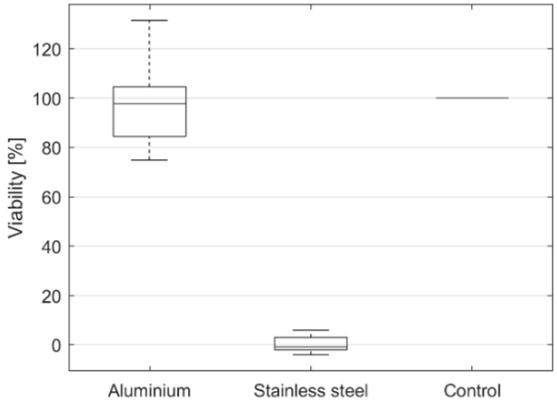

Figure 1. Viability of freshly trypsinized cells seeded in the incubation medium after electroporation with aluminium and stainless steel electrodes.

CONCLUSIONS

The incubation medium after electroporation with stainless steel electrodes is much more cytotoxic than the incubation medium after electroporation with aluminium electrodes. A 5 mM concentration of Fe^{2+} ions significantly reduces the viability of cells from a freshly trypsinized cell culture in the incubation medium after electroporation with aluminium electrodes. This value is slightly higher than expected and indicates that other factors, such as the release of Fe^{3+} or other metal ions, contribute to the cytotoxicity observed in the incubation medium after electroporation with stainless steel electrodes.

[1] T. Kotnik *et al.* "Membrane electroporation and electropermeabilization: Mechanisms and models", *Annu Rev Biophys*, vol. 48, pp. 63-91, 2019.

[2] G. Saulis *et al.* " Cytotoxicity of a Cell Culture Medium Treated with a High-Voltage Pulse Using Stainless Steel Electrodes and the Role of Iron Ions ", *Membranes*, vol. 12, p. 184, 2022.

Study of irreversible electroporation-induced cell death in spheroids derived of murine hepatocarcinoma

Nicolas Mattei, Jelena Kolosnjaj-Tabi, Marie-Pierre Rols, Muriel Golzio; *Institute of Pharmacology and Structural Biology (IPBS), 205 rte de Narbonne, 31077 Toulouse cedex 4, FRANCE (CNRS UMR 5089)*

INTRODUCTION

Irreversible electroporation (IRE) has emerged as a safe non-thermal ablation method for solid tumors, capable of preserving surrounding tissues [1]. Relapses among certain patients create a need for a better understanding of the IRE-induced cell death [2]. Indeed, it is of great interest to explore how tumors subjected to sub-therapeutic pulses regrow, and if the combination of IRE with chemotherapy or immunotherapy could improve current treatments. In this context, we assessed the growth of 3D multicellular spheroids after electric pulses exposure with or without the addition an anticancer drug (bleomycin). Then, we assessed the immunogenicity of the IRE-induced cell death by measuring the release of two major Damage Associated Molecular Patterns (DAMPs), ATP and HMGB1.

MATERIALS AND METHODS

Murine hepatoma-derived Hepa 1-6 cells expressing GFP were seeded in Ultra-Low Attachment 96-well plate with a concentration of 3000 cells for 200 µL of supplemented DMEM medium. The spheroids were treated after 4 days of incubation at 37°C with 5% CO2. The monopolar pulses were applied in low-conductivity phosphate buffer with two parallel plate stainless steel electrodes with an inter-distance of 4 mm. The IRE protocol consisted of 80 pulses of 100 µs duration applied at a pulse repetition rate of 1000 Hz. The electric field intensity varied between 0 and 2500 V/cm. For the growth analysis, the spheroids were imaged by fluorescence microscopy for the following 4 days. When mentioned, bleomycin (30 nM) was added to the medium. Released ATP and HMGB1 were measured in collected media after pulses by a bioluminescent assay and immunoblotting, respectively.

RESULTS

Applying 2500 V/cm induces a permanent loss of the GFP expression in the spheroids. The application of 1500 V/cm induces a transient loss of fluorescence, followed by a regrowth of residual cells. With the addition of bleomycin, this regrowth is completely inhibited (Figure 1).

The level of released ATP measured 10 minutes after pulses exposure correlates to the intensity of electric field applied. Six hours after the pulses exposure, no HMGB1 is observed at 1000 V/cm. Increasing HMGB1 is detected at 1500 and 2500 V/cm (Figure 2). These results indicate that IRE can induce an immunogenic cell death.

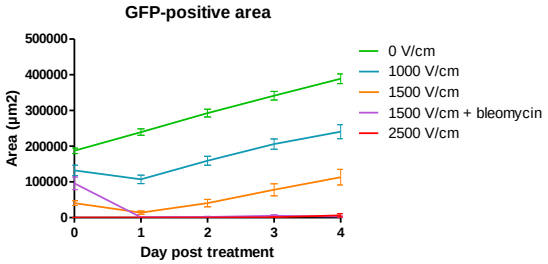

Figure 1. Growth of Hepa 1-6 spheroids after IRE pulses. GFP-positive area was measured every day. N = 4

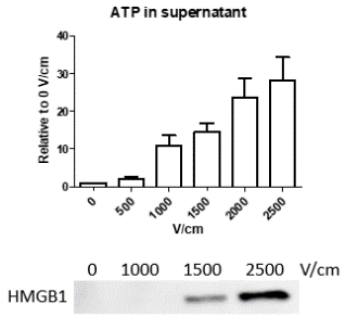

Figure 2. Released DAMPs in supernatant of pulses spheroids. (top) ATP assessed by bioluminescent assay 10 minutes after pulsing. N = 3. (bottom) HMGB1 assessed by immunoblotting 6 hours after pulsing, N = 3.

CONCLUSION

Under a certain threshold, IRE alone does not allow killing all cells constituting the spheroids. Nevertheless, this inefficiency can be compensated by the addition on an anticancer drug. Moreover, IRE-induced cell death shows characteristics of immunogenic cell death that has the potential of inducing an immune response and can thus allow the improvement of immunotherapy. These results should be considered in the future for the optimization of the timing of combined therapy involving IRE and immunotherapeutic agents.

REFERENCES

[1] B. Geboers *et al.* "High-Voltage Electrical Pulses in Oncology: Irreversible Electroporation, Electrochemotherapy, Gene Electrotransfer, Electrofusion, and Electroimmunotherapy", *Radiology*, vol. 295, pp. 254-272, 2020.

[2] N. Zhang *et al.* "Irreversible Electroporation: An Emerging Immunomodulatory Therapy on Solid Tumors", *Front Immunol*, vol. 12, p. 811726, 2021.

Electrochemotherapy for treatment of osteosarcoma tumors

Saša Kupčič[1, 2], Urša Lampreht Tratar[1], Meta Novak[3], Barbara Breznik[3], Gregor Serša[1, 4] Maja Čemažar [1, 5.]; [1] *Institute of Oncology Ljubljana, Zaloška cesta 2, 1000 Ljubljana, SLOVENIA* [2] *University of Ljubljana, Faculty of Medicine, Vrazov trg 2, 1000 Ljubljana, SLOVENIA* [3] *National Institute of Biology, Večna pot 111, 1000 Ljubljana, SLOVENIA* [4] *University of Ljubljana, Faculty of Health Sciences, Zdravstvena pot 5, 1000 Ljubljana, SLOVENIA* [5] *University of Primorska, Faculty of Health Sciences, Polje 42, 6310 Izola, SLOVENIA.*

INTRODUCTION

Osteosarcoma is a common primary bone cancer, that mainly affects children between 10 and 14 years of age [1].

Electrochemotherapy (ECT) is a local tumor ablation therapy that combines a physical delivery method; electroporation, with cytotoxic drugs. It has already proved successful in treatment of different types of tumors, but there is still a lack of information on its effect on osteosarcoma tumors [2]. Effects of ECT on osteosarcoma tumors can be studied on different preclinical models, from 2D cell cultures to homologous animal models. Therefore, the aim of our study was to develop 3D spheroids from immortalized K7M2 murine osteosarcoma cell line and evaluate the effect of electroporation on cultivated spheroids. Such established model could later help us to determine effectiveness of ECT treatment on osteosarcoma tumors.

METHODS

For formation of spheroids, 96-well plates with 5000 or 10 000 K7M2 cells per well were first centrifuged (900 g, T = 28°C, t = 90 min). Plates were then incubated in a CO_2 incubator for 72 h. After the incubation, spheroids were transfered to a plastic container, specifically designed for spheroid growth (ClinoReactor®, CelVivo, Inc, Chevy Chase, MA, USA). ClinoReactors® were placed in a CO_2 rotary incubator ClinoStar® (CelVivo). Spheroids were harvested after 1 or 2 weeks in Clinostar®. Ratio of cells in apoptosis and necrosis was determined with Alexa Fluor® 647 Annexin V and 7-AAD Viability Staining Solution (Biolegend, San Diego, CA, USA), according to the manufacturer's instruction.

For electroporation of spheroids, electric pulse generator was used (Jouan GHT beta, LEROY Biotech, Saint-Orens-de-Gameville, France). Individual spheroids in 50 µl of RPMI medium were placed between two parallel electrodes with 2.4 mm-gap and electric pulses (8 pulses, duration: 100 µs, frequency: 1 Hz, 200 or 1400 V/cm) were then applied. Cytotoxicity was determined at different time points after electroporation using PrestoBlue™ Cell Viability Reagent (Thermo Fisher Scientific, Waltham, MA USA).

RESULTS

Spheroids, grown in Clinostar® for 1 week, had a smaller percentage of apoptotic/necrotic cells than spheroids, grown for 2 weeks under the same conditions (Fig. 1 and 2).

Cell survival 2 hours after electroporation was similar in all groups. After 24h, group 1400 V/cm had a significantly lower survival rate in comparison to other groups (Fig. 3).

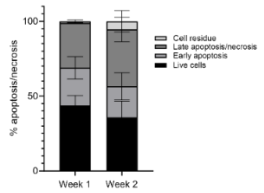

Figure 1. Apoptotic and necrotic cells in K7M2 spheroids (5000 cells/spheroids) after 1 or 2 weeks of incubation in Clinostar®.

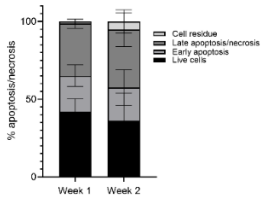

Figure 2. Apoptotic and necrotic cells in K7M2 spheroids (10 000 cells/spheroids) after 1 or 2 weeks of incubation in Clinostar®.

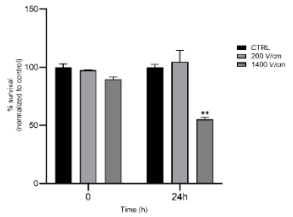

Figure 3. Cell survival after electroporation normalized to control group (CTRL: control). **p≤ 0.01, compared to every other group at timepoint 24h.

CONCLUSIONS

Spheroids, formed from 5000 cells and growing for 1 week, are a more suitable model for electrochemotherapy studies than spheroids formed from 10 000 cells, as they have a lower proportion of apoptotic and necrotic cells.

REFERENCES

[1] A. Ferrari *et al*. "Sarcomas of Soft Tissue and Bone", *Prog Exp Tumor Res*, vol. 43, pp. 128-141, 2016.

[2] G. Serša *et al*. "Preclinical Studies on Electrochemotherapy," in Handbook of Electroporation. Springer, 2017, pp. 1511-1525.

Bleomycin based electrochemotherapy with standard electrodes for advanced stage, recurring vulvar/cervix carcinomas - initial results

Marton Arpad Vas[1], Gyorgy Lazar[1], Judit Olah[2], Gabor Vass[3], Mario Vincze[4] Aurel Ottlakan[1], Erika Gabriella Kis[3];*[1]University of Szeged, Department of Surgery, 6725, Szeged, Semmelweis str. 8, HUNGARY [2]University of Szeged, Department of Oncotherapy, 6720, Szeged, Koranyi alley 12, HUNGARY [3]University of Szeged, Department of Dermatology and Allergology, 6720, Szeged, Koranyi alley 6, HUNGARY [4] University of Szeged, Department of Obstetrics and Gynecology, 6725, Szeged, Semmelweis str. 1, HUNGARY.*

INTRODUCTION

Recently bleomycin based electrochemotherapy (ECT) has been an emerging technique not only in the treatment of superficial skin tumors, but also in case of advanced, metastatic and surgically inoperable deep-seated lesions [1].

PATIENTS AND METHODS

During a 2-year period (December 2020- December 2022) 6 cases of inoperable cervix/vulva carcinomas have been treated by bleomycin based electrochemotherapy at the University of Szeged Department of Surgery. All treatments were performed under general anesthesia, with the use of standard electrodes (F-10-NL, F-15-NL, F-20-NL, F-15-NO, F-10-LG). Each procedure was started 8 minutes after intravenous bleomycin administration (15000 IU/m2) and lasted for a maximum of 40 minutes [2]. Prior to- and after treatment (1 week, 1-2-4-6 months) prospective data collection was carried out. Patient health status and QoL was assessed at each follow-up visit. Tumor response was evaluated through imaging (MRI), and gynaecological examination 2 months after ECT as per RECIST 1.1 guidelines, adverse events were evaluated and graded according to Common Terminology Criteria for Adverse Events (CTCAE) version 4.0 [3,4].

RESULTS

Five female patients (6 cases in total, 1 patient treated twice) were treated, histologically confirmed squamous cell carcinoma (n=5) and endometrial adenocarcinoma (n=1). Median age was 68,5 years, mean BMI (body mass index) 29.7, mean ASA (American Score of Anaesthesiologists) 2, mean CCI (Charlson Comorbidity Index) 5. Two tumors were located in cervical stump (after hysterectomy), 3 at the site of the vulva. Previous treatments included surgery (5 cases: 2 hysterectomies+ 3 vulvectomies), preop RTh (radiotherapy) in 3, postop RTh in 2 cases, postop CTh (chemotherapy) in 1 case. Median operative time was 30 minutes, with mean hospital stay of 3 days. Follow-up MRI at two months confirmed 1 CR (complete response), 1 PR (partial response), 2 SD (stable disease) and 1 PD (progressive disease). No major postoperative adverse events were observed, novum atrial fibrillation occurred in 1 case. Median postop pain level was 2. Previous odour and oozing from the lesions improved in each case. At 6 months follow-up 2 patients have deceased.

CONCLUSION

Our results suggest, that bleomycin based ECT is a safe and effective local anticancer treatment even in cases of advanced stage, inoperable vulvar/cervical carcinomas, mostly with palliative intent, nevertheless with improved QoL.

REFERENCES

[1] A. Simioni *et al*. "Ablation of soft tissue tumours by long needle variable electrode-geometry electrochemotherapy: final report from a single-arm, single-centre phase-2 study", *Sci Rep,* vol 10, p. 2291, 2020.

[2] J. Gehl *et al*. "Updated standard operating procedures for electrochemotherapy of cutaneous tumours and skin metastases", *Acta Oncol,* vol. 57, pp. 874-882, 2018.

[3] P.G. Casali *et al*. "ESMO Guidelines Committee and EURACAN. Soft tissue and visceral sarcomas: ESMO-EURACAN Clinical Practice Guidelines for diagnosis, treatment and follow-up", *Ann Oncol,* vol. 29, pp. 268-269, 2018.

[4] A. M. Perrone *et al*. "Quality of Life with Vulvar Carcinoma Treated with Palliative Electrochemotherapy: The ELECHTRA (ELEctroCHemoTherapy vulvaR cAncer) Study", *Cancers*, vol. 13, p. 1622, 2021.

Electrochemotherapy as a new treatment for skin cancer

Cilio A [1,2] , Campastri A [1,2] , Michinski S [3] , Lertora R [4] , Acosta AC [2] , Maglietti F [1]; *[1] Instituto de Ciencias de la Salud, Fundación Barceló-CONICET, Buenos Aires, ARGENTINA [2] Hospital de Agudos JM Ramos Mejía, Buenos Aires, ARGENTINA [3] Instituto de Física Interdsiciplinaria y Aplicada (INFINA), Facultad de Cs Exactas y Naturales, UBA-CONICET, Buenos Aires, ARGENTINA [4] Hospital de Agudos Petrona V Cordero, San Fernando, ARGENTINA.*

INTRODUCTION

Electrochemotherapy is a new treatment for skin cancer. It consists of the administration of intravenous Bleomycin in a low dose followed by the application of an electric field that induces pores in the cell membrane. This increases cytotoxicity of the drug more than 1,000 times, with very few adverse effects. The treatment is effective regardless of the histology of the tumor.

AIM

To determine the effectiveness of electrochemotherapy for skin cancer in patients who are not candidates or reject surgery.

PATIENTS AND METHODS

Patients with squamous or basal cell carcinomas who are not candidates or rejected surgery are included. Treatment is performed either with local anesthesia or a mild sedation. Intravenous bleomycin is administered at a dose of 15,000 IU/m 2, followed by the application of electroporation pulses using the OncoPore 100 (BIOTEX SRL, Argentina). The procedure is performed in an outpatient basis. A maximum of two treatment sessions are carried out and then the response was evaluated. Adverse effects and tolerance to the treatment were recorded.

RESULTS

Eight patients were enrolled, 4 with basal cell carcinoma and 4 with squamous cell carcinoma. An objective response rate of 88% was obtained (5 complete responses, 2 partial responses and 1 stable disease) (Figure 1 and 2). The adverse effects observed were edema and erythema at the application site that resolved during the first 7 days after treatment. Tolerance to treatment was excellent.

Figure 1. A female patient who had a basal cell carcinoma in the nose, left cheek and periocular. She had a complete response with one session of electrochemotherapy.

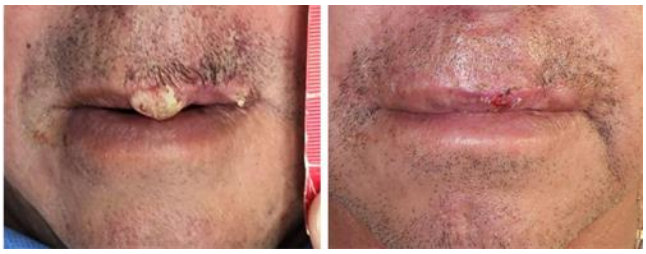

Figure 2. A male patient who had a squamous cell carcinoma in the upper lip. He had a complete response with one session of electrochemotherapy.

CONCLUSION

Electrochemotherapy is a therapeutic option with a high local response rate and few adverse effects for those patients who reject or are not candidates for surgery.

REFERENCES

[1] Y. Granot *et al*. "Mass Transfer Model for Drug Delivery in Tissue Cells with Reversible Electroporation", *Int J Heat Mass Transf*, vol. 51, pp. 5610-5616, 2008.

[2] A. Silve *et al*. "Cell Electropermeabilization and Cellular Uptake of Small Molecules: The Electrochemotherapy Concept. in *Clinical Aspects of Electroporation* (eds. Kee, S. T., Gehl, J. & Lee, E. W.) 69-82, 2011.

Use of electroporation for the treatment of bladder cancer – a scoping review

Marc Casper Meineche Andersen[1,2], Julie Gehl[2,3], Juan Luis Vásquez[1,2]; *[1] Department of Urology, Zealand University Hospital, Sygehusvej 10, DK-4000 Roskilde, DENMARK [2] Department of Clinical Medicine, Faculty of Health and Medical Sciences, University of Copenhagen, Blegdamsvej 3B, DK-2200 Copenhagen, DENMARK [3] Center for Experimental Drug and Gene Electrotransfer (C*EDGE), Department of Clinical Oncology and Palliative Care, Zealand University Hospital, Vestermarksvej 9, 2., DK-4000 Roskilde, DENMARK.*

INTRODUCTION

Bladder cancer is a common malignancy and has great impact on patients, healthcare systems and society. Today, standard care and diagnosis of bladder cancer consists of transurethral resection of bladder tumour (TURBT) and adjuvant treatment with intravesical chemotherapy or Bacillus Calmette-Guerin vaccine. In cases with muscle-invasive tumour growth,, radical cystectomy is the preferred treatment, but is associated with significant mortality and morbidity [1]. New treatment modalities must be explored.

The use of electroporation in other cancers have shown promising results, and its use in bladder cancer has yet to be investigated in humans.

This review investigates the current evidence of the use of electroporation in bladder cancer.

METHODS

This scoping review was performed in accordance with the PRISMA extension for scoping reviews [2].

A systematic literature search on the databases PubMed, Web of Science and Embase was conducted using the keywords “bladder cancer”, “transitiocellular carcinoma”, “urothelial cancer”, “electrochemotherapy”, “electro-permeabilization” and “electroporation” in June 2023.

Articles were eligible for inclusion if they 1) were original studies or case reports, 2) investigated the use of electroporation-based technology to treat bladder cancer as main part of the study, including in vitro and in vivo studies, and 3) were in English or Danish. Articles were excluded if they 1) investigated the use of electromotive drug administration and bladder cancer or 2) were abstract only. The Covidence systematic review software (Veritas Health Innovation, Melbourne, Australia) was used. Two authors performed the identification and screening of eligible articles independently.

Information regarding type of study, intervention, research questions, and outcome was extracted. For clarification purposes, a distinction will be made between laboratory use of electroporation and veterinary clinical use.

RESULTS

In total, the literature search revealed 293 abstracts. After removal of duplications, 201 abstracts were screened and 43 accepted for full text review. Finally, 29 articles were included in the review.

The included studies distributed in five in vitro studies, nine in vivo studies, nine studies reporting both in vivo and in vitro studies, two veterinary studies and three human case reports. One study investigated 3D spheroid models of bladder cancer.

All in vitro studies used bladder cancer cell lines as part of the study and application of electroporation was done in combination with either calcium, chemotherapy or gene electrotransfer. In vivo studies evaluated subcutaneous tumour growth after electroporation. Studies differed in main objective, but all delivered positive results on the use of electroporation-based treatments compared to controls.

A veterinary case series investigated the use of electrochemotherapy in three canines. Electroporation was applied by cystotomy and in combination with intravenous bleomycin and intratumoral cisplatin. Two patients showed complete remission of primary tumour within 11 and 28 days post-treatment, but both expired within 40 days after treatment. Another case series investigated irreversible electroporation delivered via a balloon catheter to treat obstructive urethral carcinoma in three canines. Results were deemed feasible and safe.

One human case report used electrochemotherapy with bleomycin and the other case report used calcium electroporation in combination with pembrolizumab. Both studies were patients bladder cancer metastases confined to the skin and showed complete response after treatment with electroporation. The final human case series was a series of different pelvis tumours and one case was recurrent bladder tumour treated with irreversible electroporation (IRE). No specific outcomes were reported but authors deemed IRE safe to use in pelvic tumours.

CONCLUSIONS

Use of electroporation-based treatments in bladder cancer primarily consist of pre-clinical evidence and show a positive effect in in vitro and in vivo studies. Veterinary studies with electroporation deemed the procedures safe and in some cases complete or partial remission of primary tumour. Human clinical use of electroporation of bladder cancer is limited to few cases all with metastases on the skin. No human patients were treated directly in the bladder, possibly due the lack a suitable electrode. However, electroporation-based treatments could be of interest in management of bladder cancer and further human studies must be conducted.

[1] A. T. Lenis *et al*. "Bladder Cancer: A Review", *JAMA*, vol. 324, p. 1980, 2020.

[2] A. C. Tricco *et al.* "PRISMA Extension for Scoping Reviews (PRISMA-ScR): Checklist and Explanation", *Ann Intern Med*, vol. 169, pp. 467-473, 2018.

RCT Investigating the Effect of Reduced Bleomycin in Electrochemotherapy Treatment on Patients with Cutaneous Malignancies (The BLESS Trial)

Anne Karen Bennedsen, MD[1], Camilla Kjær Lønkvist, MD, Ph.D.[2], Julie Gehl, Prof. Dr. med.[1];
[1]Department of Clinical Oncology and Palliative Care, Zealand University Hospital, Sygehusvej 10, 4000 Roskilde, DENMARK [2]Department of Oncology, Copenhagen University Hospital Herlev, Borgmester Ib Juuls Vej 7, 2730 Herlev, DENMARK.

INTRODUCTION

Electrochemotherapy with bleomycin is established as an effective treatment for cutaneous tumours and metastases [1,2]. It is usually well tolerated, but bleomycin may cause harm, e.g. to the lungs and skin, and the risk of toxicity rises in patients with impaired renal function [3,4].

HYPOTHESIS

Studies investigating a reduced dose of bleomycin in electrochemotherapy treatment observe a similar overall response on tumour regression as studies using a standard dose [5].

We hypothesize that electrochemotherapy with a 50% standard dose of bleomycin (7.500 IU/m2) is non-inferior to a 100% dose of bleomycin (15.000 IU/m2) and might induce less harm and make the treatment available to patients that are ineligible for a standard dose.

METHODS

We plan to perform a parallel group multicentre double-blinded randomised clinical trial with 55 patients in total. We expect that each patient will on average have two tumours, i.e., 110 tumours will be included in total. The primary endpoint is to assess overall tumour response after three months.

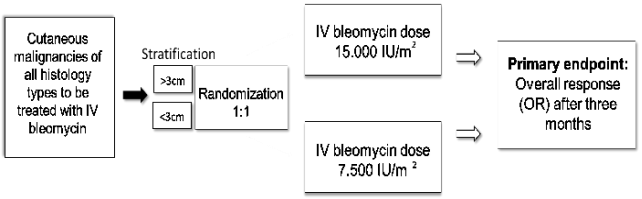

Figure 1. Study overview

Five biopsies will be collected from each patient from any tumour at the time points: 0, 2, 4, 6 and 8 minutes after bleomycin infusion, before electroporation. Two biopsies from healthy skin surrounding the tumour will also be obtained for histological analysis at the time points: 0 and 8 minutes after bleomycin infusion, before electroporation.

One blood sample will be collected before bleomycin administration, in order to evaluate kidney function (eGFR). Additionally, six blood samples will be collected after bleomycin infusion. The blood samples will be collected at the time points: 0, 5, 10, 20, 30 and 40 min after bleomycin administration. The bleomycin content in biopsies and blood samples will be analysed at the Department of Science and Environment at Roskilde University.

Qualitative interviews will be performed on 16 patients to evaluate the treatment impact on quality of life. All patients will be asked to answer the European Organisation for Research and Treatment of Cancer (EORTC) questionnaire at month 0, 3 and 12.

Adverse events and serious adverse events will be evaluated and graded according to Common Terminology Criteria for Adverse Events.

ETHICS AND DISSEMINATION

The trial will be conducted in accordance with the official version of the Declaration of Helsinki and in agreement with the ICH directions for Good Clinical Practice and the respective rules and regulations in Denmark.

EXPECTED TIMELINE

We expect the project to run for three years in total (October 2023 to October 2026). During the first three months we aim to submit the protocol to relevant authorities and complete approvals. We expect to start inclusion of patients and begin sample collection during the first quarter of 2024 and will finish inclusion after two years (February 2026). Sample analyses will be ongoing until inclusion of the last patient. Unblinding will take place when the last patient attend the three month follow up appointment. We expect to write the publication during the second quarter of 2026 and submit for publication hereafter.

REFERENCES

[1] L.M. Mir *et al*. "Standard operating procedures of the electrochemotherapy: Instructions for the use of bleomycin or cisplatin administered either systematically or locally and electric pulses delivered by the Cliniporator by means of invasive or non-invasive electrodes", *Eur J Cancer Suppl*, vol. 4, pp. 14-25, 2006.

[2] J. Gehl *et al*. "Updated standard operating procedures for electrochemotherapy of cutaneous tumours and skin metastases", *Acta Oncol*, vol. 57, pp. 874-82, 2018.

[3] Lægemiddelstyrelsen "Produktresumé for Bleomycin "Baxter", pulver til injektions- og infusionsvæske, opløsning 15.000 IE", vol. 6 , pp. 1-12, 2016.

[4] A. Groselj *et al*. "Bleomycin pharmacokinetics of bolus bleomycin dose in elderly cancer patients treated with electrochemotherapy", *Cancer Chemother Pharmacol*, vol. 77, pp. 939-947, 2016.

[5] R. Rotunno *et al*. "Electrochemotherapy of unresectable cutaneous tumours with reduced dosages of intravenous bleomycin: analysis of 57 patients from the International Network for Sharing Practices of Electrochemotherapy registry", *J Eur Acad Dermatol Venereol*, vol. 32, pp. 1147-1154, 2018.

Combined fluorescence and hyperspectral enhanced dark field microscopy – tool for analysis of intracellular distribution of silica nanoparticles

Luminita Claudia Miclea[1], Mona Mihailescu[2], Nicolae Tarba[3], Ana Maria Sandu[4], Mihaela G. Moisescu[1], Tudor Savopol[1]; *[1] Faculty of Medicine, Carol Davila University of Medicine and Pharmacy, 8 Eroii Sanitari Blvd., 050474;[2] Faculty of Applied Sciences,[3] Doctoral School of Automatic Control and Computers, [4] CAMPUS Research Center, Politehnica University, 313 Splaiul Independentei, 060042, Bucharest, ROMANIA*

INTRODUCTION

Intracellular visualisation of SBA-15 silica nanoparticles (NPs) localisation is conditioned by fluorescent labelling of the cell compartments and/or the NPs. Linking enhanced dark field microscopy (EDFM) with hyperspectral imaging (HS), would allow for unlabelled NPs to be found, counted, and tracked in correlation with their spectral signature.

Using such combined methods, we present an in vitro study on the localisation and counting of intracellular SBA-15 NPs functionalized with folate and loaded with the cytotoxic drug Irinotecan (Iri), in Caco-2 cells (human adenocarcinoma).

METHODS

After 24h from seeding, Caco-2 cells were further incubated with unlabelled NPs for 24h. The cells viability was evaluated by standard metabolic MTS assay. For EDFM the cells were labelled for cytoplasmic actin with Alexa Fluor™ 488 Phalloidin and for nuclear DNA with DAPI and *Z-stack* images were acquired. For HS microscopy, the cells were prepared similarly, but without fluorescent staining. A Cytoviva® microscopy system combining EDFM with HS, was used for images and spectra acquisitions. MATLAB-based scripts were developed for image processing and analysis of NPs distribution.

RESULTS

Three digital cellular compartments were created (nucleus, shell around the nucleus and cytoplasm), localisation and counting of NPs in each compartment was done (Fig. 1B). For visualisation purposes, 3D reconstructions of double-labelled fluorescent cells incubated with NPs are presented in Fig. 1A.

Compared to NPs without folate, the highest Iri cytotoxic effect on Caco-2 was generated by the folate-functionalized NPs (Fig. 2A) and it correlated with NPs higher intracellular concentrations, either surrounding the nucleus or in the cytoplasm (Fig. 1B).

The HS measurements showed changes in spectra peak wavelengths for NPs loaded with Iri when inside the cells after 24h incubation, when compared to NPs in suspension before the incubation (Fig. 2B); these results support the NPs capacity to deliver the cytotoxic drug.

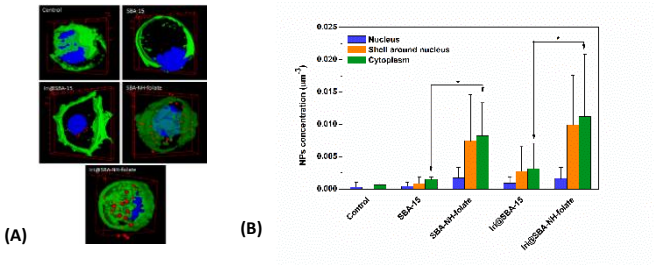

Figure 1. (A) 3D reconstructions of Caco-2 cells incubated with NPs (cytoplasm green, nuclear DNA blue and NPs red). Green zone appears discontinuous for visualisation purposes. (B) NPs count in the three digital cell compartments.

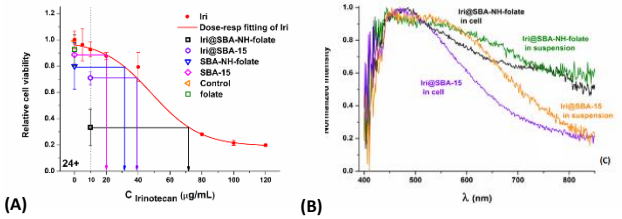

Figure 2: (A) Equivalence of NPs and Iri toxicities on Caco-2 cells, incubated for 24 h. The red line represents the dose–response fit of the Iri in solution toxicity (red dots); (B) Normalized reflectance spectra of Iri loaded NPs, functionalised or not with folate, either inside the cell (after 24h incubation) or in suspension (before incubation).

CONCLUSIONS

The NPs distribution in digitally defined cell compartments (cytoplasm, nucleus, and shell around the nucleus) and their capacity to deliver a cytotoxic were evaluated by combining the techniques of EDFM, HS and fluorescence microscopy [1]. Our results showed that the NPs conjugated with folate enter the cell more efficiently and accumulate preferentially in some compartments. The problematical issue of intracellular fate of the NPs has been addressed through a creative approach consisting in combining different microscopy techniques and serial images processing, which can be applied to various formulation of unlabelled NPs.

REFERENCES

[1] L. C. Miclea *et al.* "Evaluation of intracellular distribution of folate functionalized silica nanoparticles using fluorescence and hyperspectral enhanced dark field microscopy ", *Nanoscale*, vol. 14, pp. 12744–56, 2022.

LABORATORY SAFETY

Laboratory safety S1

Duša Hodžić
University of Ljubljana, Faculty of Electrical Engineering

BIOSAFETY

There are four biosafety levels (BSLs) for working with live organisms; each BSL consists of combinations of laboratory practices and techniques, safety equipment and laboratory facilities. Each combination is specifically appropriate for the operations performed, the suspected routes of transmission of the organisms and the laboratory function or activity.

Biosafety Level 1 represents a basic level of containment. It is suitable for work involving well-characterized agents not known to cause disease in healthy adult humans. The potential hazard to laboratory personnel and the environment is minimal.
Biosafety Level 2 is suitable for work involving agents that can cause human disease and have a moderate potential hazard to personnel and the environment. Precautions must be taken for handling and disposing of contaminated material, especially needles and sharp instruments. The laboratory must have limited access.
Biosafety Level 3 is used in laboratories where work is done with pathogens, indigenous or exotic agents which may cause serious or potentially lethal disease as a result of exposure by the inhalation route. Such microorganism can present a serious hazard to workers and a risk of spreading to the community, but there is usually effective prophylaxis or treatment available. BSL 3 requires special facilities with self-closing double doors and sealed windows, decontamination of clothing before laundering and controlled access.
Biosafety level 4 is required for work with pathogens which pose a high individual risk of aerosol-transmitted laboratory infections and life-threatening disease, for which there is no effective prophylaxis or treatment available. Such organisms present a serious hazard to workers and may present a high risk of spreading to the community. The BSL 4 facility is generally a separate building with specialized ventilation and waste management systems to prevent release of live pathogens to the environment.

GENERAL SAFETY RULES FOR WORKING IN THE LABORATORY

The following basic safety rules should be observed at all times in the laboratory:

1. Wash your hands with liquid soap and dry them with paper towels upon entering and prior to leaving the laboratory.
2. Wear laboratory coat and gloves. Tie back loose hair.
3. Do not carry your personal belongings in the laboratory; place them in specified locations – never on bench tops.
4. Do not smoke, eat, drink, apply cosmetics or insert contact lenses in a laboratory.
5. Keep doors and windows closed during the laboratory session to prevent contamination from air currents.
6. Contaminated spots on clothes or body can be sprayed with disinfectant and washed with water. Contaminated material should be put into special containers.
7. If you had any contact with hazardous chemicals while wearing your gloves, change the gloves before you touch other laboratory equipment, do not touch your face or your clothes with contaminated gloves.
8. Do not allow water or any water-based solution to come into contact with electrical cords or conductors. Make sure your hands are dry when you handle electrical equipment.
9. Report all accidents immediately to the instructor.

RULES FOR HANDLING CHEMICALS

Almost all chemicals can be harmful in some way and prolonged exposure may cause long-term effects as yet unknown. Preparation of hazardous chemicals must be conducted under the fume hood.

When handling chemicals the following rules must be strictly met:

1. **Always read labels before handling any chemical**. Learn hazard warning symbols which are displayed on the labels.
2. Take care to avoid spillage - if this occurs, neutralize any hazard and clean up immediately, including the outside of the container.
3. Some chemicals have a delayed or cumulative effect. Inform the instructor if any feeling of being unwell occurs when using chemicals.
4. Chemicals must not be disposed of by indiscriminate washing down the sink. Carefully read the appropriate material safety data sheet and follow the instructions.

CHEMICAL HAZARD SYMBOLS

Explosive

Oxidizing

Extremely/Highly flammable

(Very) Toxic

Harmful

Mutagenic, carcinogenic, causing respiratory sensitization

Corrosive

Dangerous for the environment

Pressurized gases

PIPETTING TECHNIQUE

Pipetting is one of the most frequent tasks in the laboratory and it directly affects the success and repeatability of the experiments. It is critical to follow good pipetting practice techniques.

ASEPTIC TECHNIQUE

Aseptic technique is a combination of procedures designed to reduce the probability of infection. In spite of the introduction of antibiotics, contamination with microorganisms remains a problem in tissue culture. Bacteria, mycoplasma, yeasts and fungal spores may be introduced by operator, atmosphere, work surfaces, solutions and many other sources. In order to avoid contamination aseptic technique should be used while handling cell cultures.

Correct aseptic technique provides a barrier between microorganisms in the environment and the culture within its flask or dish. Hence, all materials that will come into direct contact with the culture must be sterile and manipulations designed in such manner that exclude direct link between the culture and its nonsterile surroundings.

The elements of aseptic technique are a sterile work area, good personal hygiene, sterile reagents and media, and sterile handling.

Rules for aseptic work:

1. Start with completely clear work area and wipe the surface with 70% alcohol and a sterile gauze.
2. Spray and wipe your hands with 70% ethanol.
3. Clean the outside of the containers and other objects with 70% ethanol before placing them in the microbiological safety cabinet.
4. The work surface should be uncluttered and contain only items required for a particular procedure; it should not be used as a storage area.
5. Remove everything that is no longer required and clean with 70% alcohol before the next procedure.
6. Arrange items to have easy access to all of them without having to reach over one item to get to another.
7. Work within your range of vision, e.g., insert a pipette in the pipetting device with the tip of the pipette in your line of sight continuously and not hidden by your arm.
8. Clean up any spillage immediately with absorbent tissues and wipe with 70% alcohol.
9. Remove everything when you finish and wipe the work surface with 70% ethanol.
10. Use ultraviolet light to sterilize the air and exposed work surfaces in the microbiological safety cabinet between uses.

GMO
GMO is an abbreviation for genetically modified organism. GMO is an organism that is created when a recipient (host) organism, with the help of a vector, successfully incorporates the insert in its genetic material and can transfer it to its descendants.
Closed system is a laboratory or some other closed room for GMO work.

Recipient (host) organism = cell/organism which accepts genetic material from the original organism or the environment, replicates and expresses it and can transfer it to its descendants.
Parent organism = recipient organism before the genetic change
Original organism = organism from which the genetic material for transfer in the host is acquired
Vector = DNA tool used in genetic engineering to harbour genes of interest and transfer them to the host
Insert = genetic material that is integrated into a vector

Example: In cell and molecular biology, the GFP **(**green fluorescent protein) gene **[insert]** is frequently used as a reporter of expression. GFP is a protein that exhibits bright green fluorescence when exposed to light in the blue to ultraviolet range. It was first isolated from the jellyfish *Aequorea victoria* **[original organism]**, although many marine organisms have similar green fluorescent proteins. It is carried on plasmids **[vector]** to the target cells **[parent organism].** The cells that manage to express the protein are called **host organisms** (GMO).

When working with GMO, traceability is essential. For that it is necessary to keep a good operating and autoclave log book. Operating log is used for writing down essential GMO information, work procedure, solid and liquid waste management and potential work related accidents. Autoclave log is a record of all waste that has been autoclaved.

GMO waste can be deactivated in two different ways – thermic or chemical treatment. Deactivation prevents the GMO`s to migrate out of the closed system. Sterilized liquids can be washed down the sink, dry sterilized solid waste can be thrown in municipal waste.

In case of a GMO accident the biosafety commissioner needs to be informed and his/her directions should be followed. If a spillage occurs there has to be enough absorbent material to absorb all the liquid. Work surfaces should be decontaminated with a disinfectant.

FURTHER READING:
Freshney R. I. Culture of animal cells: a manual of basic technique.3rd ed. Wiley-Liss, Inc. New York, 1994.
http://www.biotechnology-gmo.gov.si/eng/genetically_modified_organisms/index.html

Electroporation hardware safety S2

Eva Pirc
University of Ljubljana, Faculty of Electrical Engineering

ELECTRIC SHOCK

Possible consequences of the current flow through the human body are ventricular fibrillation, cardiac asystole, respiratory arrest and burns. Voltages greater than 50 V applied across dry unbroken human skin or pulse energies above 50 J can cause ventricular fibrillation, if they produce electric currents above 30 mA in body tissues through the chest area. Frequently, the individual cannot let go of the power source due to involuntary muscle contraction. Side effect are conditioned by path of electric current, its magnitude, tissue characteristics and exposure time. The most sensitive organs to electric properties in human body are the heart and the brain. Human body is much more sensitive to mains-frequency alternating current (50/60 Hz) then to either direct current or high-frequency currents. Pain perception and muscle contraction at a given current level depend strongly on body weight and frequency. For example, 10 mA current at frequency of 50/60 Hz can result in strong muscle contraction, in a person that weights approximately 50 kg, but sensitivity decreases with the frequency increase. The amount of voltage needed to produce same effects depends on the contact resistance between the human and the power source. When dealing with high voltages we always have to keep in mind that air breakdown voltage is about 30 kV/cm, so also a non-direct contact can be dangerous.

GENERAL SAFETY PRECAUTIONS FOR WORKING WITH HIGH VOLTAGES

The following basic safety rules should be observed at all times in the laboratory:

1. Never work alone when dealing with high voltages. Consider having a co-worker with knowledge about equipment and risks.
2. Never leave electrical circuits/devices under high voltages when you are not present.
3. Before working with high voltage devices consider the potential risks. Do not have any contacts with conductive parts of device and keep distance from conductors under high voltage. Keep in mind that air breakdown can occur when dealing with voltages above 30 kV/cm.
4. Before high voltage circuit manipulation, switch OFF the power supply and discharge all high voltage capacitors (preferably through high voltage resistor).
5. Check if all high voltage capacitors are discharge using voltmeter.
6. Use only your right hand to manipulate high voltage electronic circuits, avoid simultaneous touching of two elements and make sure you are not grounded. Wear rubber bottom shoes or sneakers. Set up your work area away from possible grounds that you may accidentally contact.
7. When using electrolytic capacitors:
    b. DO NOT put excessive voltage across them,
    c. DO NOT put alternating current (AC) across them,
    d. DO NOT connect them in reverse polarity.
8. Make sure all high voltage connections, tools and instruments are adequately insulated and rated for the voltage and current used.
9. If someone comes in a contact with a high voltage, immediately shut off the power. Do not attempt to move injured person in contact with a high voltage.
10. In the event of an electrical fire do not use water but special fire extinguishers used for fires caused by electric current.
11. Do not wear any jewellery or other objects that could accidentally come in contact with the conductive parts of electrical circuit.
12. Protect your ears and eyes due to possible discharge sounds and element explosions.

NOTES

LABORATORY EXERCISES

The influence of Mg^{2+} ions on gene electrotransfer efficiency L1

Saša Haberl Meglič, Mojca Pavlin
University of Ljubljana, Faculty of Electrical Engineering

Duration of the experiment: day 1: 60 min; day 2: 60 min
Max. number of participants: 4
Location: Cell Culture Laboratory 3
Level: Basic

PREREQUISITES

Participants should be familiar with the Safety rules and Rules for sterile work in cell culture laboratory. No other specific knowledge is required for this laboratory practice.

THEORETICAL BACKGROUND

Gene electrotransfer is a non-viral method used to transfer genes into living cells by means of high-voltage electric pulses. An exposure of a cell to an adequate amplitude and duration of electric pulses leads to transient increase of cell membrane permeability for molecules which are otherwise deprived of membrane transport mechanisms. This allows various nonpermeant molecules, including DNA, to be transported across the membrane and enter the cell. Although mechanisms of the process are not yet fully elucidated, it was shown that several steps are crucial for gene electrotransfer: interaction of plasmid DNA (pDNA) with the cell membrane, translocation of pDNA across the membrane, migration of pDNA towards the nucleus, transfer of pDNA across the nuclear envelope and gene expression (Figure 1).

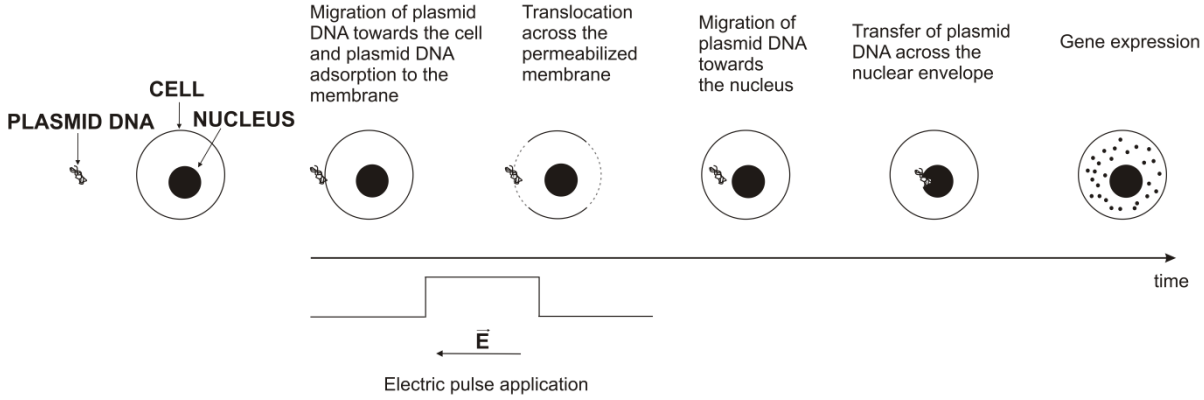

Figure 1. Steps involved in gene electrotransfer.

Many parameters have been described, which can influence the efficiency of gene electrotransfer. A few published reports have shown that the concentration of Mg^{2+} ions in electroporation medium has important impact on forming a complex between DNA and the cell membrane during application of electrical pulses. Namely, DNA is negatively charged polyelectrolyte and Mg^{2+} ions can bridge the DNA with negatively charged cell membrane. But it was shown that Mg^{2+} ions at higher concentrations may bind DNA to the cell membrane strong by enough to prevent translocation of DNA across the membrane and into the cell during electroporation consequently gene electrotransfer efficiency is decreased.

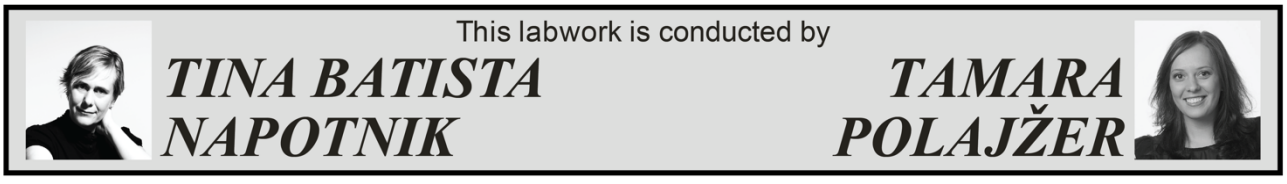

The aim of this laboratory practice is to demonstrate how different Mg^{2+} concentrations in electroporation medium affect the efficiency of gene electrotransfer and cell viability.

EXPERIMENT

We will transfect Chinese hamster ovary cells (CHO-K1) with plasmid DNA (pEGFP-N_1) that codes for GFP (green fluorescent protein) using two different electroporation media (see Protocol section). To generate electric pulses Jouan GHT 1287 electroporator (Jouan, St. Herblain, France) will be used. Pulses will be monitored on osciloscope (LeCroy 9310C).

We will determine gene electrotransfer efficiency and cell viability for both electroporation media.

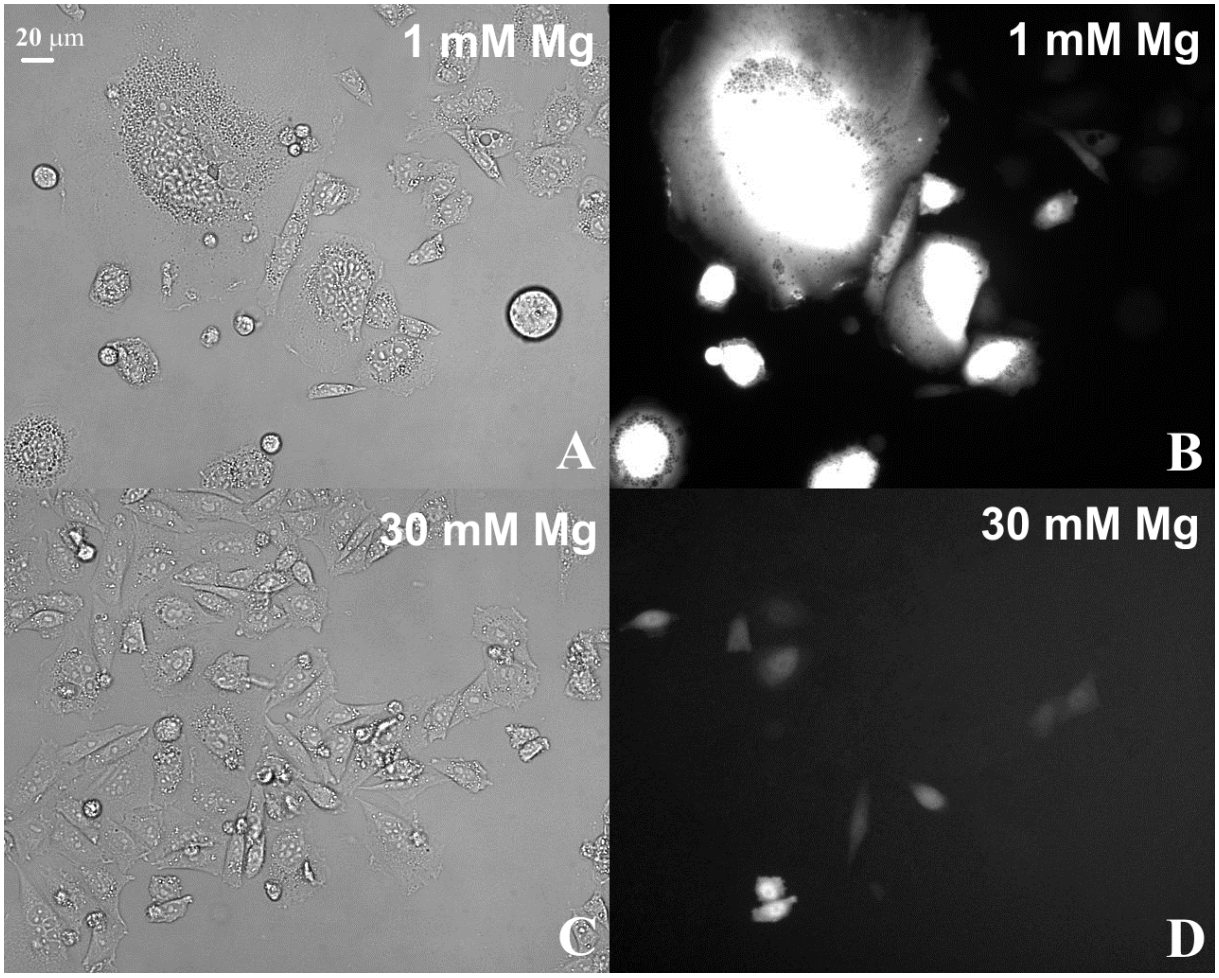

Figure 2. Gene electrotransfer of plated CHO cell 24 h after pulse application in 1 mM Mg or 30 mM Mg media. 8 x 1 ms (stainless steel wire electrodes with inter-electrode distance d = 2 mm; applied voltage U = 140 V resulting in electric field strength E = 0.7 kV/cm) pulses were applied with repetition frequency of 1 Hz to deliver pEGFP-N_1 (concentration of DNA in electroporation media was 10 μg/ml) into the cells. Phase contrast images of treated cells for (A) 1 mM Mg and (C) 30 mM Mg media and fluorescence images of treated cells for (B) 1 mM Mg and (D) 30 mM Mg media are presented. To visualize transfection 20x objective magnification was used.

Protocol 1/2 (Gene electrotransfer with different electroporation media): CHO cells will be grown in multiwells as a monolayer culture in Ham's tissue culture medium for mammalian cells with 10% fetal bovine serum (Sigma-Aldrich Chemie GmbH, Deisenhofen, Germany) at 37° C. Cells will be plated 24 h before the experiment in concentration 5 x 10^4 cells per well.

Just before the experiment remove culture media and replace it with 150 µl of electroporation media containing plasmid DNA with concentration 10 µg/ml. Use 1 mM or 30 mM electroporation media. Sucrose molarity has also been changed in order to attain the molarity of the media:

a) **1 mM Mg media** (10 mM phosphate buffer Na_2HPO_4/NaH_2PO_4, 1 mM $MgCl_2$, 250 mM sucrose; pH = 7.2)
b) **30 mM Mg media** (10 mM phosphate buffer Na_2HPO_4/NaH_2PO_4, 30 mM $MgCl_2$, 160 mM sucrose; pH = 7.2)

Incubate cells with plasmid DNA for 2-3 minutes at room temperature. Then apply a train of eight rectangular pulses with duration of 1 ms, U = 140 V resulting in electric field strength E = 0.7 kV/cm and repetition frequency 1 Hz to deliver plasmid DNA into the cells. Use stainless steel wire electrodes with inter-electrode distance d = 2 mm.
Cells in the control are not exposed to electric pulses.
Immediately after exposure of cells to electric pulses add 37.5 µl of fetal calf serum (FCS-Sigma, USA). Incubate treated cells for 5 minutes at 37ºC and then add 1 ml of culture media.

Protocol 2/2 (Determining gene electrotransfer efficiency and cell viability): After 24 h incubation at 37ºC determine the difference in gene electrotransfer efficiency and cell viability for both electroporation media by fluorescent microscopy (Leica, Wetzlar, Germany) at 20x magnification using GFP filter with excitation at 488 nm.

You will determine gene electrotransfer efficiency from the ratio between the number of green fluorescent cells (successfully transfected) and the total number of viable cells counted under the phase contrast. You will obtain cell survival from phase contrast images as the ratio between the number of viable cells in the treated sample and the number of viable cells in the control sample.

FURTHER READING:

Haberl S., Pavlin M., Miklavčič D. Effect of Mg ions on efficiency of gene electrotransfer and on cell electropermeabilization. *Bioelectrochemistry* 79:265-271, 2010.
Haberl S., Kandušer M., Flisar K., Bregar V.B., Miklavčič D., Escoffre J.M., Rols M.P., Pavlin M. Effect of different parameters used for in vitro gene electrotransfer on gene expression efficiency, cell viability and visualization of plasmid DNA at the membrane level. *J. Gene Med.* 15:169-181, 2013.
Rosazza C., Haberl Meglič S., Zumbusch A., Rols M.P., Miklavčič D. Gene electrotransfer: a mechanistic perspective. *Curr. Gene Ther.* 16:98-129, 2016.

NOTES & RESULTS

Electroporation media	Treated viable cells	Viable cells in control	Green fluorescent cells	Gene electrotransfer efficiency [%]	Viability [%]
1 mM Mg media					
30 mM Mg media					

NOTES & RESULTS

Monitoring cell membrane electroporation with ratiometric fluorescent dye Fura-2AM

L2

Gorazd Pucihar
University of Ljubljana, Faculty of Electrical Engineering

Duration of the experiments: 60 min
Max. number of participants: 4
Location: Cell Culture Laboratory 1
Level: Advanced

PREREQUISITES

Participants should be familiar with Laboratory safety (S1). The basic knowledge of handling with cells is required for this laboratory practice.

THEORETICAL BACKGROUND

Exposure of a biological cell to a sufficiently strong external electric field leads to a detectable increase of membrane permeability, a phenomenon termed electropermeabilization. Because it is assumed that an increased permeability is related to the occurrence of hydrophilic pores in the membrane, the phenomenon is often termed electroporation. Provided that the parameters of the electric field (amplitude, duration, number of pulses, frequency) are moderate, the increased permeability is reversible, and cells recover within a few minutes after the exposure. During the state of high permeability the molecules for which the membrane is otherwise impermeable (e.g. drugs, DNA) can be transported across the membrane. Electroporation is nowadays used in food processing, biotechnology, molecular biology, and different fields of medicine. It has already become an established method in oncology for electrochemotherapy of tumors, and holds great promises in gene therapy.

The efficiency of electroporation is influenced by the parameters of the electric field, cell size and geometry, and physiological characteristics of the medium surrounding the cell. Different fluorescent dyes (e.g. Propidium Iodide, Lucifer Yellow, Fura-2, Fura-3,…) can be employed to investigate the influence of these parameters on electroporation and the same dyes can be used to monitor electroporation.

The aim of this laboratory practice is to monitor electroporation with fluorescent dye and to determine the effect of cell size, shape and orientation on the efficiency of electroporation.

EXPERIMENT

We will monitor cell membrane electroporation using a fluorescent calcium sensitive indicator Fura-2AM. Calcium ions, present in the extracellular medium, do not readily cross an intact (nonporated) cell membrane and the intracellular Ca^{2+} concentration is low. Once the membrane becomes permeable due to electroporation, Ca^{2+} ions enter the cells, where they bind to the dye and change its excitation and emission spectrum (Figure 1).

This labwork is conducted by

TINA BATISTA NAPOTNIK

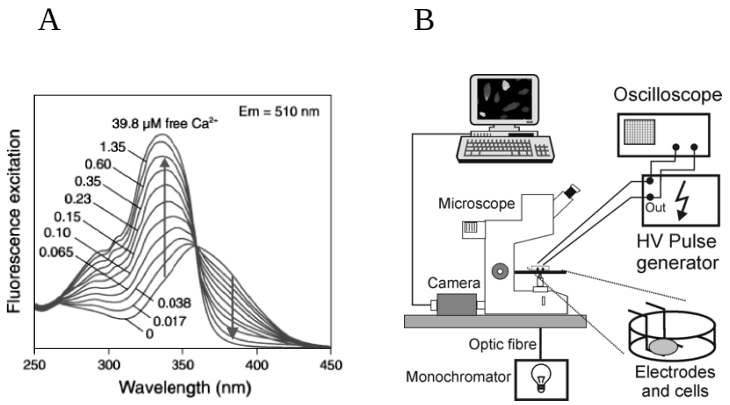

Figure 1: (A) Fluorescence excitation spectra of Fura-2 for different concentrations of Ca^{2+} (image from *http://probes.invitrogen.com/handbook/figures/0554.html*). (B) Schematic of the experiment.

Protocol: The experiments will be performed on Chinese hamster ovary cells (CHO) grown in Lab-Tek chambers (Nunc, Germany) in culture medium HAM-F12 supplemented with 10% fetal bovine serum, L-glutamine (all three from Sigma-Aldrich) and antibiotics. Plate 1.5×10^5 cells on cover glass of Lab-Tek chamber and keep them for 12-16 hours in the incubator. Before experiments, replace the culture medium with fresh medium containing 2 μM Fura-2 AM (Life Technologies). After 25-30 minutes of incubation at 37°C wash the excess dye and leave 1.5 ml of culture medium in the chamber.

Place the chamber under a fluorescence microscope (Zeiss AxioVert 200) and use ×63LD objective. Insert two parallel Pt/Ir wire electrodes with a 4 mm distance between them to the bottom of the chamber. Acquire the images using a cooled CCD camera (VisiCam 1280) and MetaFluor 7.7.5 software (Molecular Devices).

Using a ELECTRO cell B10 (BetaTech, France) device, deliver one electric pulse of 100 μs with voltages varying from 150 to 300 V. Immediately after the pulse, acquire two fluorescence images of cells at 540 nm, one after excitation with 340 nm and the other after excitation with 380 nm. Divide these two images in MetaFluor to obtain the ratio image ($R = F_{340}/F_{380}$). Wait for 5 minutes and apply pulse with a higher amplitude. After each pulse, determine which cells are being electroporated (Figure 2). Observe, which cells become electroporated at lower and which at higher pulse amplitudes.

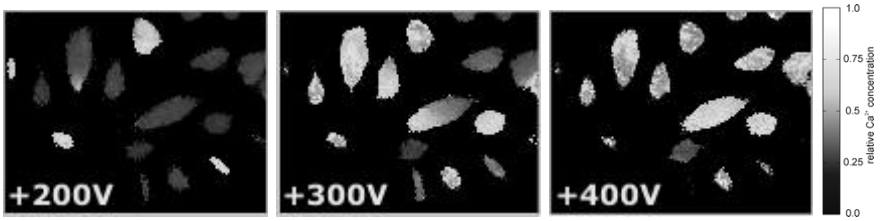

Figure 2: Cells stained with Fura-2AM and exposed to electric pulse with increasing amplitude.

FURTHER READING:

Neumann E., Kakorin S., Toensing K. Fundamentals of electroporative delivery of drugs and genes. *Bioelectrochem. Bioenerg.* 48:3-16, 1999.

Teissié J., Rols M.P. An experimental evaluation of the critical potential difference inducing cell membrane electropermeabilization. *Biophys. J.* 65:409-413, 1993.

Grynkiewicz G., Poenie M., Tsien R.Y. A new generation of Ca^{2+} indicators with greatly improved fluorescence properties. *J. Biol. Chem.* 260:3440-3450, 1985.

Teruel M.N., Meyer T. Electroporation-induced formation of individual calcium entry sites in the cell body and processes of adherent cells. *Biophys. J.* 73:1785-1796, 1997.

Valič B., Golzio M., Pavlin M., Schatz A., Faurie C., Gabriel B., Teissié J., Rols M.P., Miklavčič D. Effect of electric field induced transmembrane potential on spheroidal cells: theory and experiment. *Eur. Biophys. J.* 32:519-528, 2003.

Towhidi L., Kotnik T., Pucihar G., Firoozabadi S.M.P., Mozdarani H., Miklavčič D. Variability of the minimal transmembrane voltage resulting in detectable membrane electroporation. *Electromagn. Biol. Med.* 27:372-385, 2008.

Pucihar G., Krmelj J., Reberšek M., Batista Napotnik T., Miklavčič D. Equivalent pulse parameters for electroporation. *IEEE T. Biomed. Eng.* 58:3279-3288, 2011.

NOTES & RESULTS

Visualization of local ablation zone distribution between two needle electrodes L3

Tjaša Potočnik, Alenka Maček Lebar
University of Ljubljana, Faculty of Electrical Engineering

Duration of the experiments: 60 min
Max. number of participants: 4
Location: Cell Culture Laboratory 2 or Cell Culture Laboratory 3
Level: basic

PREREQUISITES

Participants should be familiar with Laboratory safety (S1) and Electroporation hardware safety (S2). No other specific knowledge is required for this laboratory practice.

THEORETICAL BACKGROUND

Electroporation is the method in which by applying external electric field of sufficient amplitude and duration membrane of exposed cells becomes permeabilized for molecules that otherwise cannot pass cell membrane. After reversible electroporation cell membrane reseals. With increasing amplitude of electric field the level of cell membrane permeabilization and the number of cells that are permeabilized increases. When pulses with sufficient magnitude and duration are applied, cell death is achieved and the process is defined as irreversible electroporation (IRE). IRE is an emerging ablation technique inducing apoptosis in successfully treated cells or tissues. Usually there is a sharp border between treated and untreated tissue regions because only the cells that are exposed to high enough electric field are ablated. Effective prediction of electric field can be obtained by numerical modeling, which includes the shape and position of the electrodes and parameters of electric pulses (amplitude, duration, number, frequency) used as well as electrical properties of the tissue. Using treatment planning, IRE offers benefits over other cancer therapies because it can be performed near large blood vessels, nerves, and ducts without causing damage to these structures, sparing extracellular matrix.

Electroporation can be detected by measuring increased transport of molecules across the membrane. Cell uptake of dyes, either fluorescent molecules (lucifer yellow, yo-pro-1, propidium iodide) or colour stains (such as trypan blue), is most often used for *in vitro* electroporation detection. Trypan blue can be used as an indicator of plasma membrane integrity and of cell viability. Trypan blue is normally impermeant to healthy cells. When cell membrane integrity is compromised, the dye is able to enter the cell and stains cellular structures blue, especially nuclei, making the cell appear blue. Cells that take up this dye several hours after exposure to electrical pulses are usually considered dead or dying.

The aim of this laboratory practice is to visualize local ablation zone distribution between two needle electrodes with increasing pulse amplitude using trypan blue.

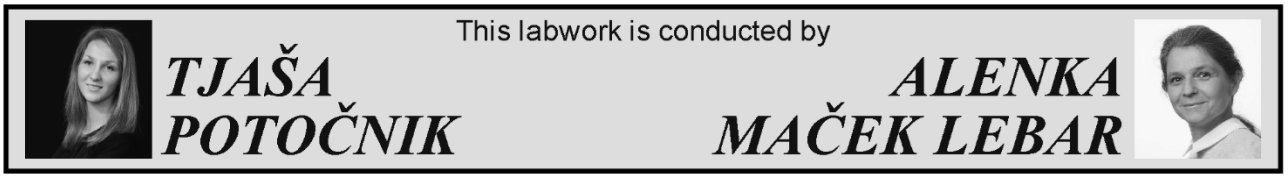

EXPERIMENT

We will visualize local ablation zone distribution between two needle electrodes using trypan blue. The effect of the pulse amplitude on the local ablation zone distribution between two needle electrodes will be determined for a train of eight 100 µs rectangular pulses delivered with the repetition frequency 1 Hz. The area of blue cells that is a consequence of efficient ablation increases with increasing pulse amplitude is presented in Figure 1.

Protocol: You will use Chinese hamster ovary cells (CHO), plated 48 h before experiment in concentration 2.5 x 10^5 cells per tissue culture dish. Cells are attached to the culture dish surface. Immediately before electric pulses are applied replace the growth medium with electroporation buffer. As electroporation buffer you will use isotonic 10 mM K_2HPO_4/KH_2PO_4 containing 1 mM $MgCl_2$ and 250 mM sucrose with pH 7.4. You will use needle electrodes 1 mm apart. For pulse delivery Gemini X2 electroporator (Hardvard apparatus BTX, USA) will be used. It can produce square and exponential pulses. During the experiment current will be monitored with an oscilloscope and a current probe. Electric field in the needle surrounding can be calculated numerically.

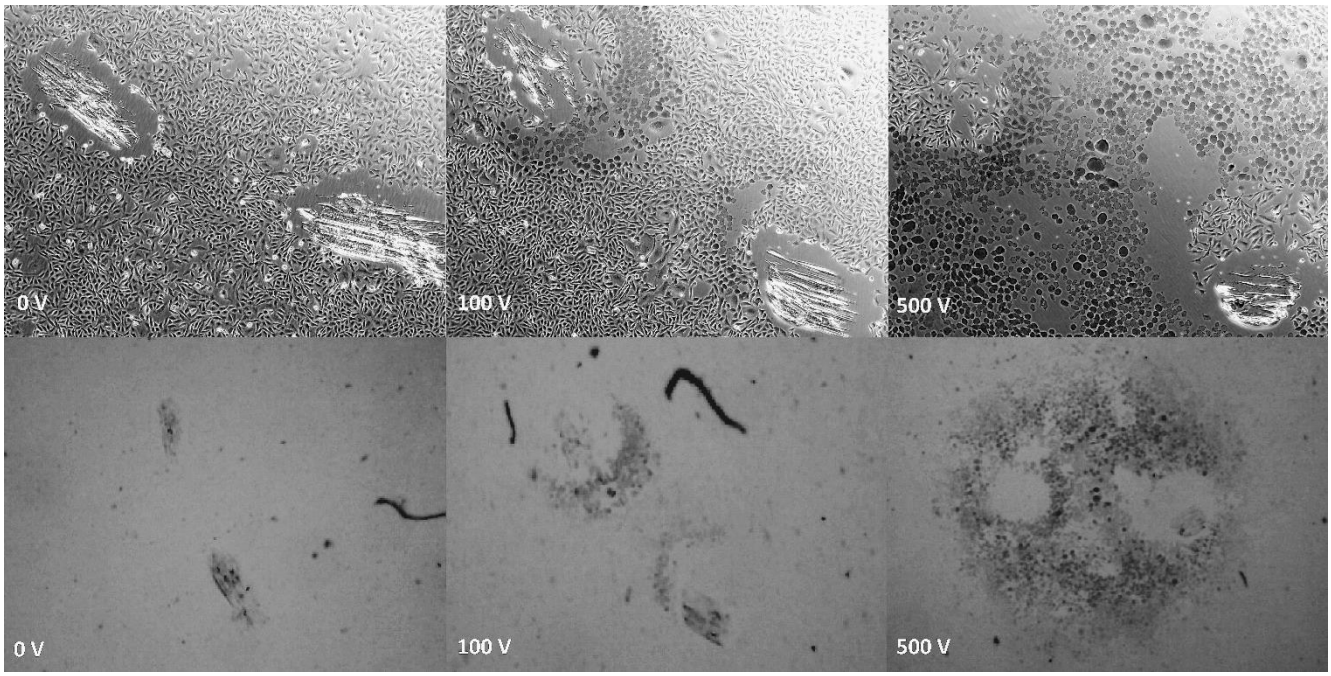

Figure 1: The sequence of the images of local ablation zone after cells were exposed to electric pulses with increasing pulse amplitude. The images were obtained by light microscopy under 10 × objective magnifications (top row) and under 5 × objective magnifications (bottom row).

Remove the tissue culture dish from the incubator and replace the growth medium with 500 µl of electroporation buffer. Carefully place needle electrodes on edge of tissue culture dish and apply electric pulses. Electric pulse parameters used are: 8 pulses, 100 µs duration and pulse repetition frequency 1 Hz, while pulse amplitude increases gradually. Increase the pulse amplitude from 0 V to 100 V, 300 V, 500 V and 700 V. After electroporation leave cells for 10 minutes at room temperature. Remove electroporation buffer and add 500 µl of trypan blue to tissue culture dish. Leave the cells for 5 minutes at room temperature then replace the trypan blue with 500 µl of fresh electroporation buffer. For visualization of local ablation zone, EVOS XL Core Imaging System (Invitrogen™) will be used.

FURTHER READING:

Batista Napotnik T., Miklavčič D. In vitro electroporation detection methods – An overview. *Bioelectrochemistry* 120:166-182, 2018.
Čemažar J., Jarm T., Miklavčič D., Maček Lebar A., Ihan A., Kopitar N.A., Serša G. Effect of electric field intensity on electropermeabilization and electrosensitivity of various tumor cell lines in vitro. *Electro and Magnetobiology* 17:263-272, 1998.
Čorović S., Pavlin M., Miklavčič D. Analytical and numerical quantification and comparison of the local electric field in the tissue for different electrode configurations. *Biomed. Eng. Online* 6:37, 2007.
Davalos R.V., Mir L.M., Rubinsky B. Tissue ablation with irreversible electroporation. *Ann. Biomed. Eng.* 33:223-31, 2005.
Dermol J., Miklavčič D. Predicting electroporation of cells in an inhomogeneous electric field based on mathematical modeling and experimental CHO-cell permeabilization to propidium iodide determination. *Bioelectrochemistry* 100:52-61, 2014.
Puc M., Kotnik T., Mir L.M., Miklavčič D. Quantitative model of small molecules uptake after in vitro cell electropermeabilization. *Bioelectrochemistry* 60:1-10, 2003.
Rols M.P. Electropermeabilization, a physical method for the delivery of therapeutic molecules into cells. *Biochim. Biophys. Acta* 1758:423-428, 2006.

NOTES & RESULTS

NOTES & RESULTS

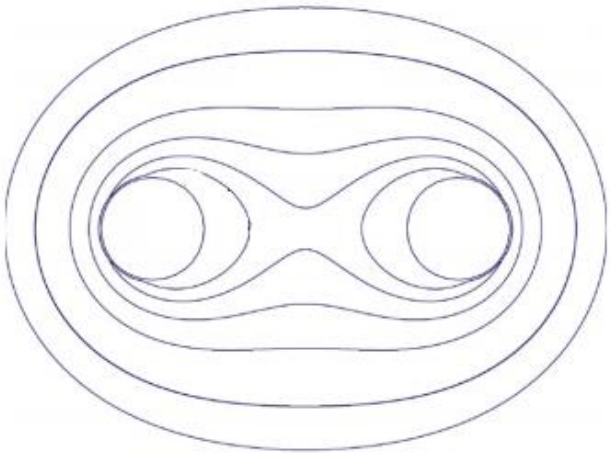

100 V

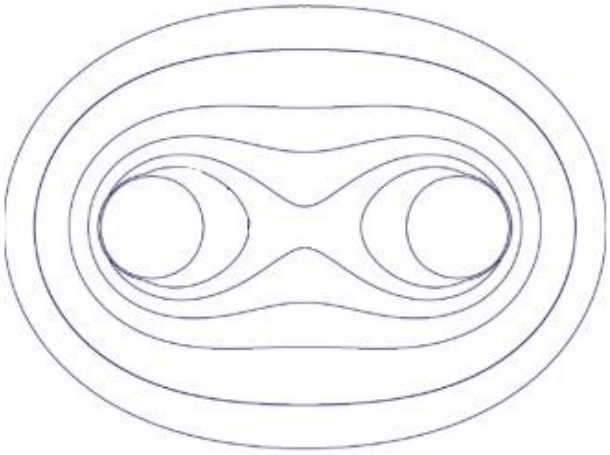

500 V

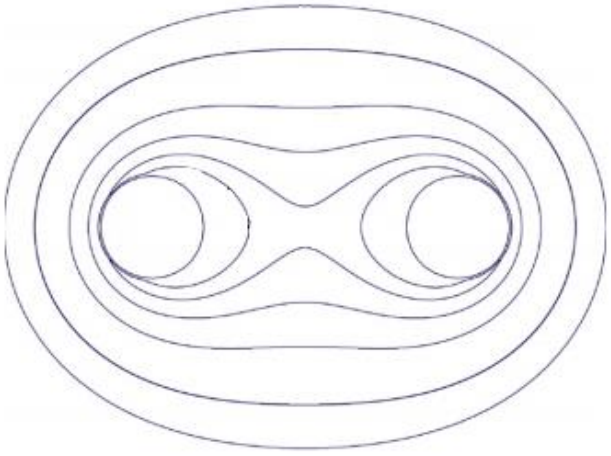

700 V

Effect of short high-frequency bipolar pulses on plasma membrane permeabilization L4

Janja Dermol-Černe, Lea Vukanović
University of Ljubljana, Faculty of Electrical Engineering

Duration of the experiments: 60 min
Max. number of participants: 4
Location: Cell Culture Laboratory 2
Level: basic

PREREQUISITES

Participants should be familiar with Laboratory safety (S1) and Electroporation Hardware Safety (S2). No other specific knowledge is required for this laboratory practice.

THEORETICAL BACKGROUND

In electrochemotherapy and irreversible electroporation as ablation technique, square 50-100 µs long monopolar pulses are usually applied at repetition frequency 1 Hz. The main drawbacks to the treatment of tissues with these monopolar pulses are discomfort and pain, the need to administer muscle relaxants and anesthesia, need for synchronization of the pulse delivery with the electrocardiogram and inhomogeneous tissue impedance. One of the possibilities to overcome these obstacles is high-frequency irreversible electroporation (HF-IRE). In HF-IRE, long monopolar pulses are replaced with bursts of a few µs long bipolar pulses, which mitigate muscle contractions, however at the expense of delivering higher energy.

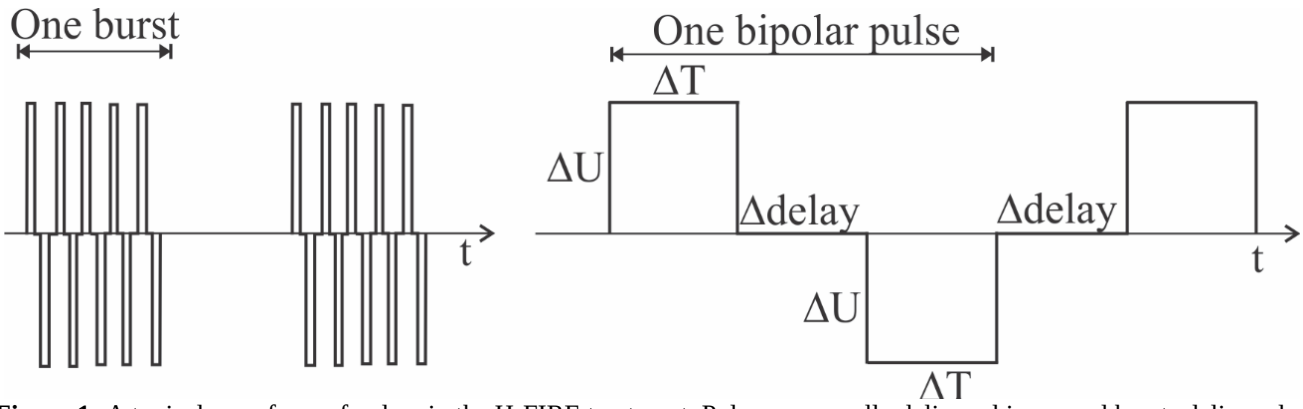

Figure 1: A typical waveform of pulses in the H-FIRE treatment. Pulses are usually delivered in several bursts delivered at repetition frequency 1 Hz. One pulse consists of a positive and a negative pulse and the delay between them.

The aim of this laboratory practice is the comparison of the effect of HF-IRE pulses and longer monopolar pulses on permeabilization of the plasma membrane as determined by spectrofluorometric measurements.

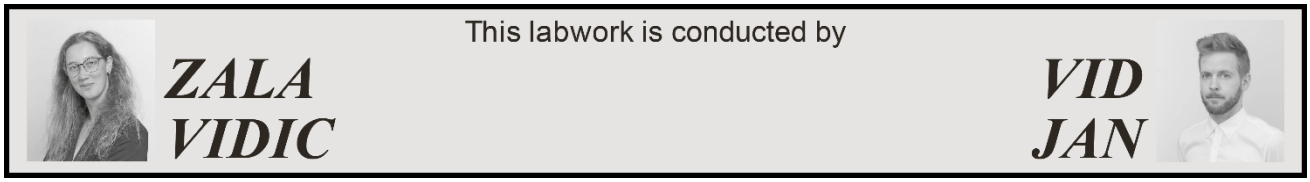

EXPERIMENT

We will detect electropermeabilization on spectrofluorometer using propidium iodide. Propidium iodide (PI) is a red-fluorescent dye. It is not permeant to live cells and is commonly used to detect dead cells in a population. After plasma membrane permeabilization, however, PI can diffuse into cells. It binds to DNA with little sequence preference. After binding, its fluorescence is increased 20- to 30-fold, with excitation maximum at 535 nm and emission maximum at 617 nm.

We will determine the effect of the pulse amplitude of HF-IRE pulses on the degree of cell membrane permeabilization. We will deliver 50 bipolar pulses consisting of 1 µs long positive 1 µs long negative pulse with 1 µs delay between them, delivered in 8 bursts at repetition frequency 1 Hz. We will compare the effect of the HF-IRE pulses on plasma membrane permeabilization with the monopolar pulses of parameters traditionally used in electrochemotherapy (8x100 µs pulses, 1 Hz repetition frequency). Thus, the duration of all pulses of HF-IRE pulses as well as of monopolar pulses is 800 µs.

We will use attached Chinese hamster ovary cells, $2.5x10^5$ cells per well plated 24 hours in advance in 24 well plate. As the electroporation buffer, we will use 10 mM K_2HPO_4/KH_2PO_4, 1 mM $MgCl_2$, 250 mM sucrose with 1.78 mS/cm, 292 mOsm/kg, and pH 7.4. We will use Pt/Ir wire electrodes with 0.8 mm diameter and 4 mm inter-electrode distance positioned at the bottom of the well. Between the electrodes, the electric field is approximately homogeneous and can be calculated as the ratio of the applied voltage and the inter-electrode distance.

For the application of pulses, we will use a laboratory prototype pulse HF-IRE pulse generator (University of Ljubljana) based on H-bridge digital amplifier with 1 kV MOSFETs (DE275-102N06A, IXYS, USA). We will monitor the delivered voltage and current by an oscilloscope, a differential probe and a current probe.

Protocol:

Remove the 24 well plate from the incubator and replace the growth medium with 300 µl per well of electroporation buffer containing 0.15 mM PI. Apply electric pulses and leave the cells for 3 minutes at room temperature to allow PI to diffuse into cells then replace the buffer with 1 ml of fresh electroporation buffer to stop PI influx. Increase the pulse amplitude of the bipolar pulses from 400 V to 1000 V. For the comparison with monopolar pulses, deliver 8x100 µs pulses with a repetition frequency of 1 Hz at 1000 V. As a negative control, apply no pulses to one well.

We will determine the fluorescence intensity spectrofluorometrically (Tecan, Infinite 200). Set the appropriate excitation and emission wavelengths for PI (535/617 nm). Plot a figure of fluorescence as a function of the electric field. Compare the fluorescence, obtained with the bipolar pulses, to the fluorescence, obtained with monopolar pulses of the same voltage.

FURTHER READING:

Sweeney D.C., Reberšek M., Dermol J., Rems L., Miklavčič D., Davalos R.V. Quantification of cell membrane permeability induced by monopolar and high-frequency bipolar bursts of electrical pulses. *Biochim. Biophys. Acta BBA - Biomembr.* 1858:2689-2698, 2016.
Arena C.B., Sano M.B., Rylander M.N., Davalos R.V. Theoretical considerations of tissue electroporation with high-frequency bipolar pulses. *IEEE Trans. Biomed. Eng.* 58:1474-1482, 2011.
Yao C. *et al.* bipolar microsecond pulses and insulated needle electrodes for reducing muscle contractions during irreversible electroporation. *IEEE Trans. Biomed. Eng.* 64:2924-2937, 2017.
Bhonsle S.P., Arena C.B., Sweeney D.C., Davalos R.V. Mitigation of impedance changes due to electroporation therapy using bursts of high-frequency bipolar pulses. *Biomed. Eng. OnLine*. 14: S3, 2015.

NOTES & RESULTS

Bipolar/Monopolar	Bipolar	Bipolar	Bipolar	Bipolar	Bipolar	Monopolar
Voltage (V)	0	400	600	800	1000	1000
Pulse duration ΔT (µs)	0	1	1	1	1	100
Raw data (a.u.)						

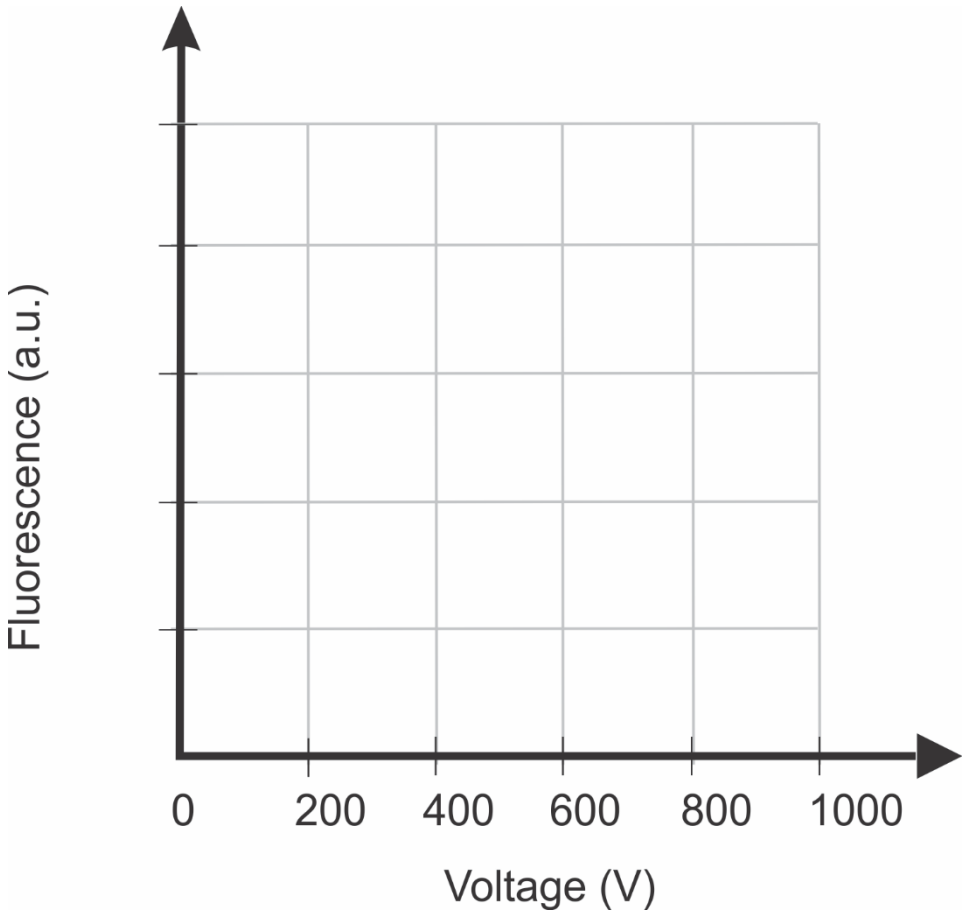

NOTES & RESULTS

Electroporation of planar lipid bilayers L5

Peter Kramar, Aljaž Velikonja, Alenka Maček Lebar
University of Ljubljana, Faculty of Electrical Engineering, Slovenia

Duration of the experiments: 120 min
Max. number of participants: 4
Location: Laboratory for skin and planar lipid bilayers
Level: Basic

PREREQUISITES

Participants should be familiar with Laboratory safety (S1). No other specific knowledge is required for this laboratory practice.

THEORETICAL BACKGROUND

A planar lipid bilayer can be considered as a small fraction of total cell membrane. As such it has often been used to investigate basic aspects of electroporation; especially because of its geometric advantage allowing chemical and electrical access to both sides of the lipid bilayer. Usually a thin bi-molecular film composed of specific phospholipids and organic solvent is formed on a small aperture separating two aqueous compartments. Electrodes immersed in these two aqueous compartments allow to measure current and voltage across the lipid bilayer (Figure 1).

Two different measurement principles of planar lipid bilayer's properties can be used: voltage or current clamp method. Planar lipid bilayer from an electrical point of view can be considered as imperfect capacitor, therefore two electrical properties, capacitance and resistance, mostly determine its behaviour.

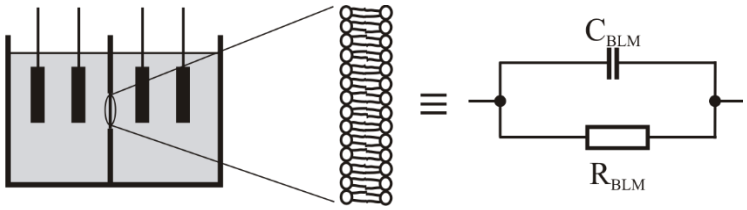

Figure 1: Equivalent circuit of a planar lipid bilayer.

The aim of this laboratory practice is to build a planar lipid bilayer by painting method (Muller - Rudin method) or/and foldig method (Montal – Mueller) and to determine capacitance and resistance of the planar lipid bilayer using LCR meter. Basic aspects of planar lipid bilayer electroporation will be given by observing formation of the pores and determining its breakdown voltage.

This labwork is conducted by

ALENKA MAČEK LEBAR

EXPERIMENT

Protocol:

Muller-Rudin method

Form a planar lipid bilayer by covering the surface of the aperture in a barrier separating two compartments of a measuring vessel with a lecithin solution (20 mg/ml of hexane). After evaporation of hexane, fill compartments with solution consisting of 0.1 mol KCl, 0.01 mol of HEPES, at pH=7.4. Connect the electrodes and apply a drop of lecithin dissolved in decane (20 mg/ml) to the aperture by the micropipette or paint it by a teflon brush. Measure capacitance and determine if the formation of planar lipid bilayer is appropriate.

Montal – Mueller method

Cover the surface of the aperture in a barrier separating two compartments of a measuring vessel with 1 µl lecithin solution (10 mg/ml of hexane and ethanol absolute in ratio 9:1). After evaporation of hexane and ethanol, add on the aperture 1,5 µl solution of pentan and hexadecane in ratio 7:3. Fill compartments with solution consisting of 0.1 mol NaCl, 0.01 mol of HEPES, at pH=7.4. On the solution surface apply 2 µl of lecithin solution in each compartment. Wait approximately 15 minutes that lipid molecules are equally spread on the solution surface. Then rise the solution surface above aperture synchronously in both compartments by pumps. Measure capacitance and determine if the formation of planar lipid bilayer is appropriate.

Measuring methods: When the planar lipid layer is formed, we apply the current or voltage to the planar lipid bilayer. In the current clamp method the current is applied to the planar lipid bilayer and we measure voltage across the bilayer. Apply a linearly increasing current and record a voltage across the bilayer. During the experiment you will obtain the time course of the voltage across the bilayer and the plot of the programmed current flowing between two current electrodes. In the voltage clamp method the voltage across the planar lipid bilayer is applied and current, which flows through planar lipid bilayer, is measured. To the planar lipid bilayer apply a linearly increasing voltage and record a flowing current. Like at the current clamp method you will obtain the time course of the flowing current and the plot of the programmed voltage across the planar lipid bilayer.

From collected data determine the breakdown voltage (U_{br}) and the lifetime (t_{br}) of planar lipid bilayer.

FURTHER READING:

Kalinowski S., Figaszewski Z., A new system for bilayer lipid membrane capacitance measurements: method, apparatus and applications, *Biochim. Biophys. Acta* 1112:57-66, 1992.

Pavlin M., Kotnik T., Miklavcic D., Kramar P., Macek-Lebar A. Electroporation of planar lipid bilayers and membranes. In Leitmanova Liu A (ed.), *Advances in Planar Lipid Bilayers and Liposomes*. 6:165-226, 2008.

Koronkiewicz S., Kalinowski S., Bryl K., Programmable chronopotentiometry as a tool for the study of electroporation and resealing of pores in bilayer lipid membranes. *Biochim. Biophys. Acta*, 1561:222-229, 2002.

Kotulska M., Natural fluctuationsof an electropore show fractional Lévy stable motion, *Biophys. J.*, 92:2412-21, 2007.

Montal M., Mueller, P. Formation of bimolecular membranes from lipid monolayers and a study of their electrical properties. *PNAS*, 69:3561-3566, 1972.

Kramar P., Miklavčič D., Maček-Lebar A. Determination of the lipid bilayer breakdown voltage by means of a linear rising signal. *Bioelectrochemistry* 70:23-27, 2007.

NOTES & RESULTS

NOTES & RESULTS

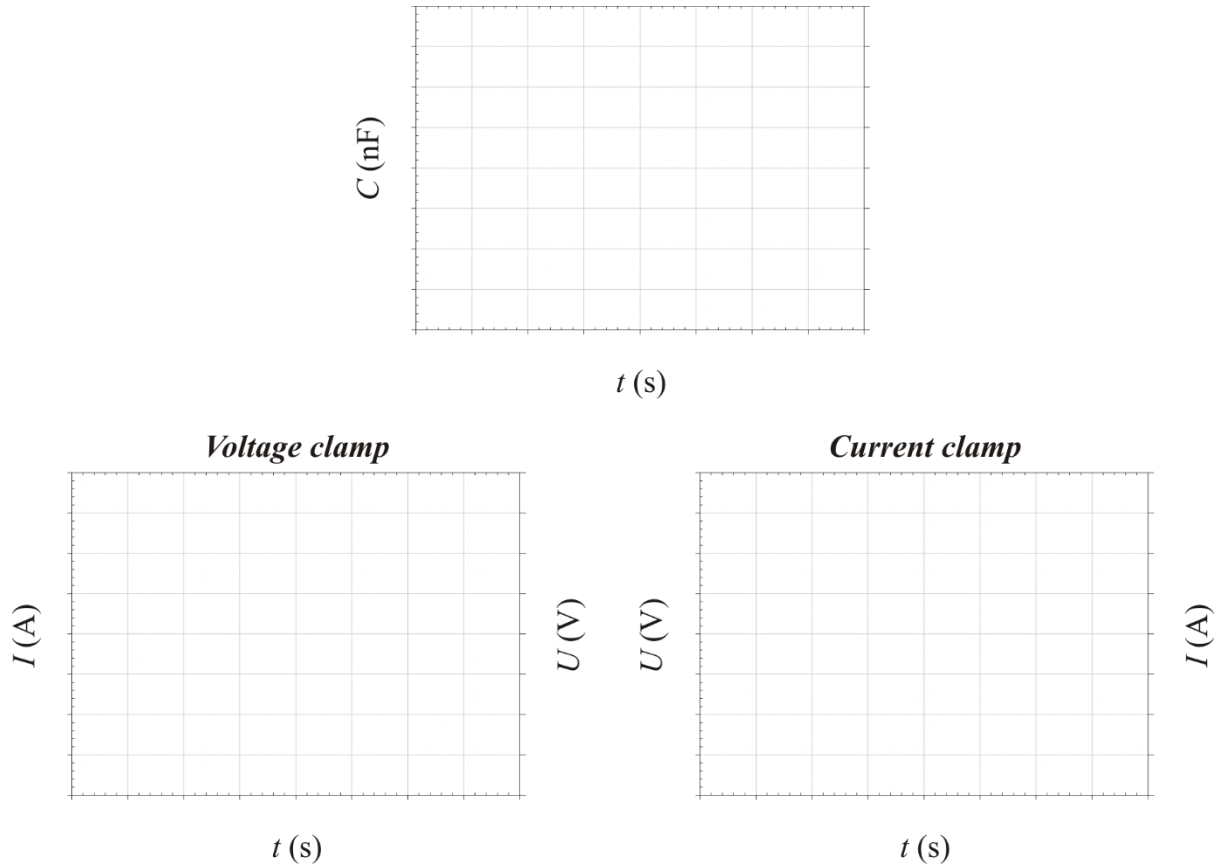

NOTES & RESULTS

Eradication of antibiotic-resistant *E. coli* by the combination of antibiotics and electroporation in a continuous mode L6

Saša Haberl Meglič, Karel Flisar
University of Ljubljana, Faculty of Electrical Engineering

Duration of the experiment: day 1: 90 min; day 2: 60 min
Max. number of participants: 4
Location: Microbiological laboratory 2
Level: Basic

PREREQUISITES

Participants should be familiar with the Safety rules and Rules for sterile work in cell culture laboratory. No other specific knowledge is required for this laboratory practice.

THEORETICAL BACKGROUND

Antibiotics have long been the mainstay in treatment of bacterial infections, but their overuse and misuse combined with inadequate infection prevention has led to increasing bacterial resistance. Therefore, the development of new approaches for efficient inactivation of drug-resistant bacteria is critical. Electroporation, a process in which electric fields are applied to bacterial cells, has shown promise as an adjunct to conventional antibiotic treatment.

The first description of the profound effect of electric pulses on the viability of a biological cell dates back to 1958. When a cell is exposed to a sufficiently high electric field, its membrane becomes permanently permeable, leading to the leakage of cellular components and thus to cell death. Electroporation has already been shown to enhance the effect of antibiotics, and various bacteria have been successfully inactivated by combining electroporation and antibiotics. In order to enable electroporation on a large scale, the development of flow-through processes has been proposed. Thus, a flow-through treatment system consists of a pulse generator that provides continuous pulse treatment, flow-through chambers with electrodes, and a fluid handling system.
Understanding how antibiotics and electroporation inactivate bacteria is critical not only for developing effective strategies to treat bacteria, but also for preventing antibiotic resistance.

The aim of this laboratory practice is to inactivate antibiotic-resistant bacteria by combining antibiotic and electroporation in a flow-through system.

EXPERIMENT

We will inactivate *Escherichia coli* K12 ER2420 cells carrying plasmid pACYC184 encoding tetracycline resistance (New England BioLabs Inc., Ipswich, Massachusetts, USA) in a continuous flow system (see Figure 1) using various tetracycline concentrations and electrical pulse parameters. A prototype square wave pulse generator will be used to generate electrical pulses. The pulses will be monitored using an oscilloscope (LeCroy 9310C). The degree of inactivation will be determined using the plate counting method.

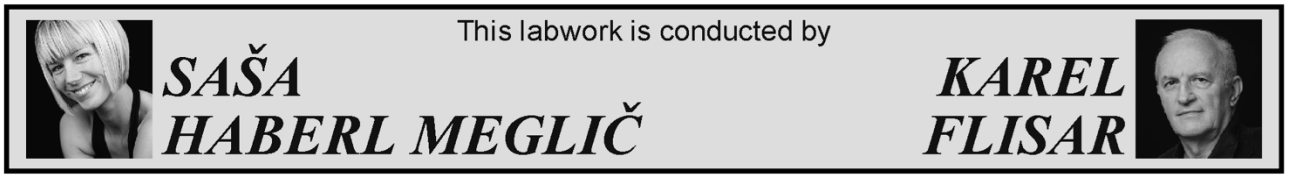

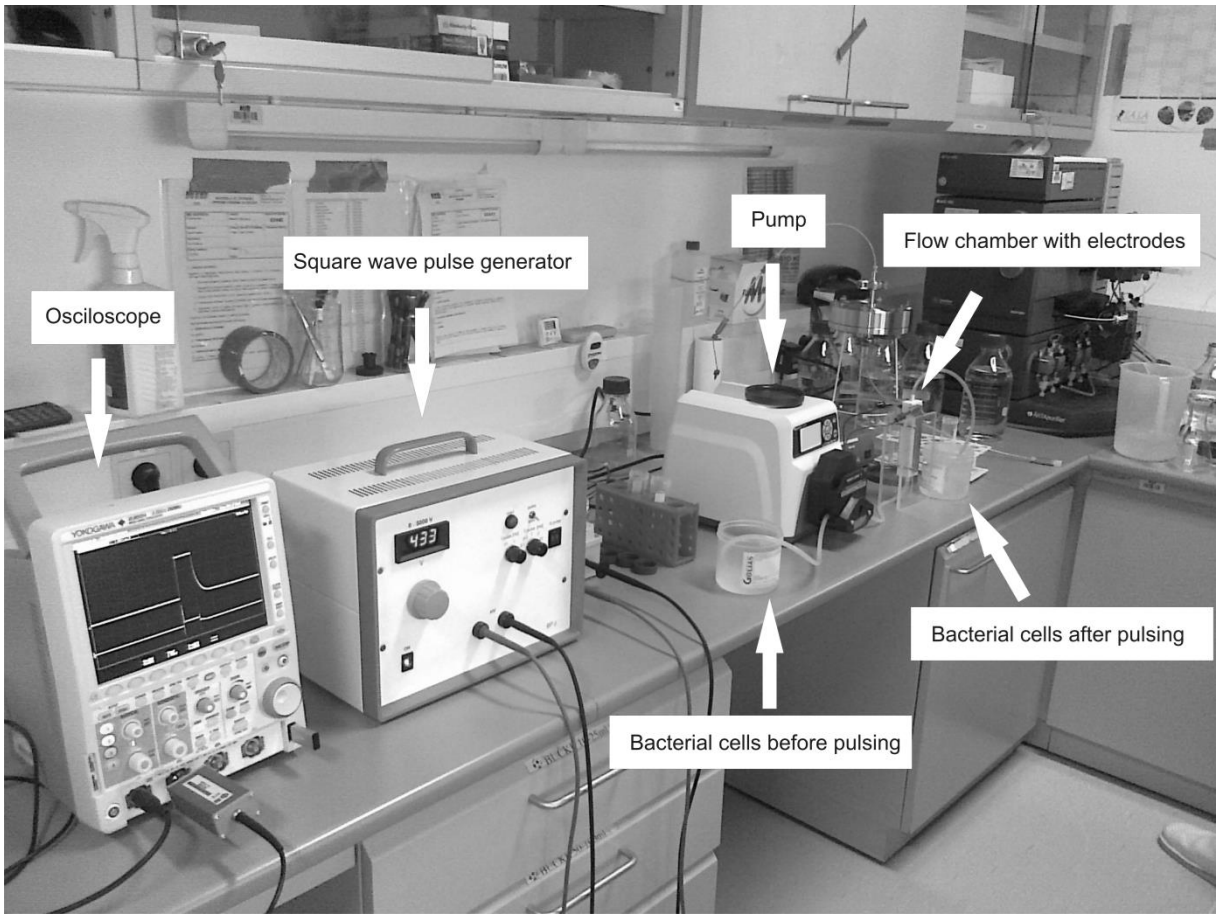

Figure 1. Continuous flow electroporation system. The circuit system includes a flow chamber with electrodes and a prototype square wave pulse generator. Voltage and current are both monitored throughout the experiment.

Protocol 1/2 (Electroporation of bacteria in a continuous flow system): On the first day of the experiment, bacterial cells will be grown for 3-4 hours (until early exponential phase) at 37°C in Luria Broth (LB) medium (Sigma-Aldrich Chemie GmbH, Deisenhofen, Germany) with shaking. *E. coli* cells will be then centrifuged (4248 g, 30 min, 4°C) and the pellet will be resuspended in 250 mM sucrose.

The exposure of cells to electrical pulses in a flow chamber in a continuous flow system depends on the geometry of the chamber and the frequency of the pulses at which the electroporator operates. The number of pulses is determined by equation 1. At this flow rate, the desired number of pulses is applied to the fluid and thus to the cells in the flow chamber. Since the volume of our cross-field chamber between the electrodes and the frequency are constant, the flow through the chamber can be determined:

$$q = \frac{f}{n} \cdot Q \tag{1}$$

where q (L/min) is the flow rate, Q (L) is the volume between the two electrodes, and n is the number of pulses received by the fluid in the chamber during the dwell time. For a frequency of 10 Hz, calculate the flow rate (q) at which all the fluid is exposed to at least one pulse. The bacterial cells will be pumped through the system at the calculated flow rate, and pulses will be applied by the prototype pulse generator.

After electroporation treatment, take a small volume of the treated sample and add 40 or 150 µg/ml of tetracycline. Collect 20 µl of the treated sample and prepare dilutions ranging from 10^{-1} to 10^{-6}. Pipette three 10-µl drops of the different dilutions onto LB agar.
To determine the number of bacterial cells in our sample, make serial dilutions of the (untreated) bacterial sample ranging from 10^{-1} to 10^{-7} (dilute 20 µl of the untreated bacterial sample in 180 µl of 0.9% NaCl). Pipette three 10-µl drops of dilutions 10^{-5}, 10^{-6} and 10^{-7} onto LB agar.

Protocol 2/2 (Determining bacterial viability): After 24 hours of incubation at 37ºC, count the colony forming units. Viability is expressed as log (N/N_0), where N is the number of colony forming units per ml in a treated sample and N_0 is the number of colony forming units per ml in an untreated sample.

Example of determining bacterial viability:
You counted 20 CFU in a control sample (dilution 10^{-7}) and 10 CFU in a treated sample (dilution 10^{-5}).

Number of bacterial cells per ml (control sample) = 20 x 10^7 (dilution factor of sample) x 100 (dilution factor of plating) = 2 x 10^{10} bacterial cells/ml

Number of bacterial cells per ml (treated sample) = 10 x 10^5 (dilution factor of sample) x 100 (dilution factor of plating) = 1 x 10^8 bacterial cells/ml

log N/N_0 = log (1 x 10^8/ 2 x 10^{10}) = ***-2.301***

FURTHER READING:

Gusbeth C., Frey W., Volkmann H., Schwartz T., Bluhm H. Pulsed electric field treatment for bacteria reduction and its impact on hospital wastewater. *Chemosphere* 75:228-233, 2009.
Pataro G., Senatore B., Donsi G., Ferrari G. Effect of electric and flow parameters on PEF treatment efficiency. *J. Food Eng.* 105:79-88, 2011.
Munoz A., Palgan I., Noci F. Cronin D.A., Morgan D.J., Whyte P., Lyng J.G. Combinations of selected non-thermal technologies and antimicrobials for microbial inactivation in a buffer system. *Food Res. Int.* 47:100-105, 2012.
Flisar K., Haberl Meglic S., Morelj J., Golob J., Miklavčič D. Testing a prototype pulse generator for a continuous flow system and its use for E. coli inactivation and microalgae lipid extraction. *Bioelectrochemistry* 100:44-51, 2014.
Novickij V., Svediene J., Paskevicius A., Markovskaja S., Lastauskiene E., Zinkeviciene A., Girkontaite I., Novickij J. Induction of different sensitization patterns of MRSA to antibiotics using electroporation. *Molecules* 7:1799, 2018.
Lovšin Ž, Klančnik A., Kotnik T. Electroporation as an efficacy potentiator for antibiotics with different target sites. *Front. Microbiol.* 12:722232, 2021.

NOTES & RESULTS

NOTES & RESULTS

Analysis of electric field orientations on gene electrotransfer – visualization at the membrane level L7

Saša Haberl Meglič, Matej Reberšek
University of Ljubljana, Faculty of Electrical Engineering

Duration of the experiment: 90 min
Max. number of participants: 4
Location: Cell Culture Laboratory 1
Level: Advanced

PREREQUISITES

Participants should be familiar with Laboratory safety (S1). The basic knowledge of handling with cells is required for this laboratory practice.

THEORETICAL BACKGROUND

Gene electrotransfer is a non-viral method used to transfer genes into living cells by means of high-voltage electric pulses. An exposure of a cell to an adequate amplitude and duration of electric pulses leads to transient increase of cell membrane permeability for molecules which are otherwise deprived of membrane transport mechanisms. This allows various nonpermeant molecules, including DNA, to be transported across the membrane and enter the cell. Although mechanisms of the process are not yet fully elucidated, it was shown that several steps are crucial for gene electrotransfer: interaction of plasmid DNA (pDNA) with the cell membrane, translocation of pDNA across the membrane, migration of pDNA towards the nucleus, transfer of pDNA across the nuclear envelope and gene expression.

Many parameters (such as electric pulse protocol) can influence the first step (interaction of DNA with the cell membrane) and by that gene electrotransfer efficiency. Therefore, different electric pulse protocols are used in order to achieve maximum gene transfection, one of them is changing the electric field orientation during the pulse delivery. Since DNA is a negatively charged molecule and it is dragged towards the cell with the electrophoretic force in the opposite direction of the electric field, changing electric field orientation increases the membrane area competent for DNA entry into the cell.

The aim of this laboratory practice is to demonstrate how different pulse polarity affects formation of DNA – membrane complex after electric pulse application.

EXPERIMENT

We will focus on the interaction of DNA with the cell membrane by using TOTO-1 dye. For the experiment, we will use Chinese hamster ovary cells (CHO-K1) and plasmid DNA (pEGFP-N_1) that codes for GFP (green fluorescent protein). To generate and deliver electric pulses a βtech electroporator (Electro cell B10, Betatech, France) and electrodes with 4 mm inter-electrode distance will be used. Pulses will be monitored on osciloscope (LeCroy 9310C).

This labwork is conducted by

TAMARA POLAJŽER

Pulse protocols (see also Figure 1):

a) SP (single polarity): the direction of electric field is the same for all pulses
b) BP (both polarities): the direction of the electric field is changed between the pulses

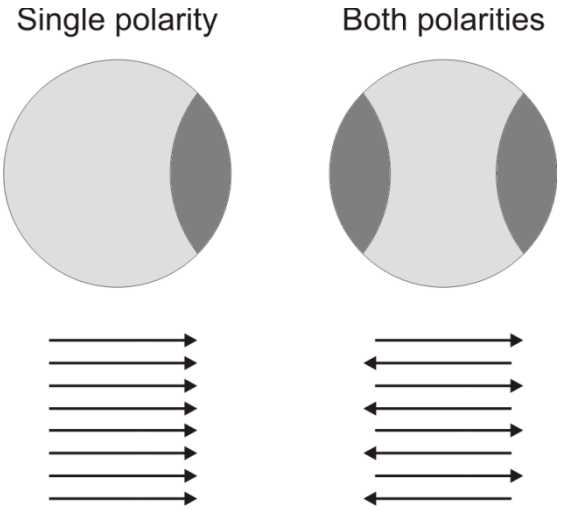

Figure 1: Two different pulse protocols will be used: single polarity (SP) and both polarities (BP).

Protocol:

Interaction of DNA with the cell membrane: CHO cells will be grown in Lab-Tek chambers as a monolayer culture in Ham's tissue culture medium for mammalian cells with 10% fetal bovine serum (Sigma-Aldrich Chemie GmbH, Deisenhofen, Germany) at 37º C. Cells will be plated 1 h before the experiment in concentration 1 x 10^5 cells per chamber.

To visualize DNA interaction with cell membrane TOTO-1 nucleic acid stain (Molecular Probes-Invitrogen, Carlsbad, California, USA) will be used. The plasmid pEGFP-N1 will be labelled on ice with 2.3 x 10^{-4} M TOTO-1 DNA intercalating dye 1 h before the experiment. Plasmid concentration will be 1 µg/µl, which yields an average base pair to dye ratio of 5.

Just before the experiment remove culture medium and rinse the cells with 1 ml of electroporation buffer (10 mM phosphate buffer K_2HPO_4/KH_2PO_4, 1 mM $MgCl_2$, 250 mM sucrose; pH = 7.4). Afterwards add 500 µl of electroporation buffer containing 5 µg of labelled plasmid DNA. Then apply a train of eight pulses with amplitude of 350 V, duration of 1 ms and repetition frequency 1 Hz using single polarity or both polarities (see Pulse protocols).

Immediately after exposure of cells to electric pulses rinse the cells three times with 1 ml of electroporation buffer. Add again 500 µl of electroporation buffer and observe the interaction of DNA with the cell membrane with fluorescent microscopy (Zeiss 200, Axiovert, Germany) using 100x oil immersion objective using TOTO filter with excitation at 514 nm.

FURTHER READING:

Faurie C., Reberšek M., Golzio M., Kandušer M., Escoffre J.M., Pavlin M., Teissie J., Miklavčič D., Rols M.P. Electro-mediated gene transfer and expression are controlled by the life-time of DNA/membrane complex formation. *J. Gene Med.* 12:117-125, 2010.

Golzio M., Teissié J., Rols M.P. Direct visualization at the single-cell level of electrically mediated gene delivery. *PNAS* 99:1292-1297, 2002.

Reberšek M., Faurie C., Kandušer M., Čorović S., Teissié J., Rols M.P., Miklavčič D. Electroporator with automatic change of electric field direction improves gene electrotransfer *in vitro*. *Biomed. Eng. Online* 6:25, 2007.

Reberšek M., Kandušer M., Miklavčič D. Pipette tip with integrated electrodes for gene electrotransfer of cells in suspension: a feasibility study in CHO cells. *Radiol. Oncol.* 45:204-208, 2011.

Video Article:

Pavlin M., Haberl S., Reberšek M., Miklavčič D., Kandušer M. Changing the direction and orientation of electric field during electric pulses application improves plasmid gene transfer in vitro. *J. Vis. Exp*. 55:1-3, 2011.

NOTES & RESULTS

NOTES & RESULTS

Comparison of flow cytometry and spectrofluorometric measurements in cell permeabilization experiments L8

Janja Dermol, Lea Vukanović
University of Ljubljana, Faculty of Electrical Engineering

Duration of the experiments: 90 min
Max. number of participants: 4
Location: Cell Culture Laboratory 2
Level: advanced

PREREQUISITES

Participants should be familiar with Laboratory safety (S1). The basic knowledge of handling with cells is required for this laboratory practice.

THEORETICAL BACKGROUND

When cells are exposed to high electric fields, otherwise non-permeant molecules can cross the cell membrane. A commonly used way of detecting cell membrane permeabilization is by using fluorescent dyes such as propidium iodide. When the cell is permeabilized, the propidium ion enters the cell, binds to nucleic acids in the cytosol and nucleus, and upon excitation starts to emit 20-times higher fluorescence than in the unbound state. Cell membrane permeabilization can be determined using different methods, e.g. fluorescent microscopy, spectrofluorometric measurements, flow cytometry, or clonogenic test after electroporation with chemotherapeutics. In this lab work, we will compare spectrofluorometric measurements and flow cytometry.

Spectrofluorometric measurements allow for the analysis of a large number of cells at different wavelengths, but the exact number of permeabilized cells cannot be extracted. Namely, as a result, we obtain the sum of the fluorescence intensities of all cells which can conceal subpopulations of differently permeabilized or even non-permeabilized cells.

Flow cytometry, on the other hand, gives information on the shape, size, internal structure, and fluorescence of each separate cell, and thus offers possibility to detect subpopulations which differ in any of the measured parameters. Cells (or any other particle) move through a laser beam and refract or scatter light in all directions. Forward scatter (FSC) is the light that is scattered in the forward direction as laser strikes the cell while side scatter (SSC) is the light that is scattered at larger angles. The magnitude of FSC is roughly proportional to the size of the particle and SSC is indicative of the granularity and the internal structural complexity. Fluorescence can be measured at different wavelengths, and the measured signal is proportional to the amount of the emitted fluorescence. After measurements, the analysis is done by gating to separate different cell subpopulations (Figure 1).

The aim of this laboratory practice is the comparison of two different methods of permeabilization detection using fluorescent dye propidium iodide.

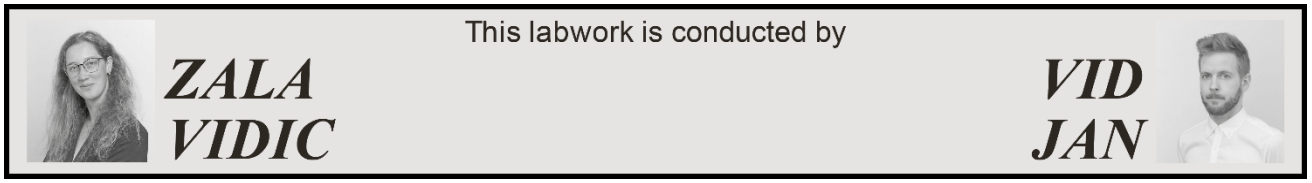

EXPERIMENT

We compare the fluorescence detected by flow cytometry (Life Technologies, Attune NxT, USA) and by the spectrofluorometer (Tecan Infinite 200, Tecan, Austria) after standard electroporation protocol (8, 100 μs pulses of different voltage applied at 1 Hz). To apply the pulses, we use the Gemini X2 electroporator (Harvard apparatus BTX, USA), and we monitor the pulses by an oscilloscope and current probe (both LeCroy, USA).

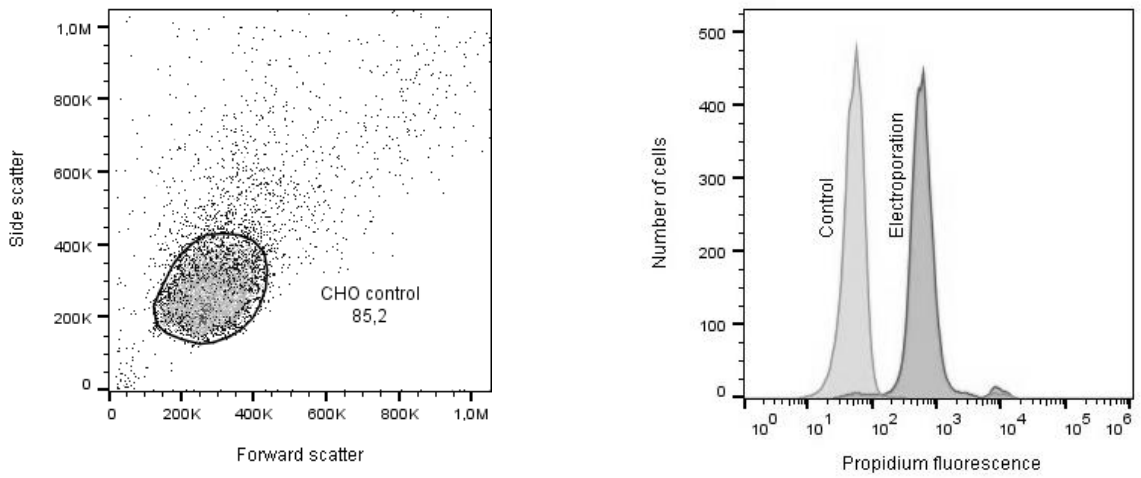

Figure 1: The analysis of the permeabilization data obtained by flow cytometry measurements in the software FlowJo (TreeStar, USA). Left: the viable cells are determined from the FSC-A and SSC-A dot diagram by gating. Right: histogram of measured fluorescence for control and pulsed cells. After electroporation, the cell fluorescence shifts for two decades which allows the discrimination between permeabilized and non-permeabilized cells. The peak at 10^4 are the dead and/or irreversibly permeabilized cells.

Protocol:

The experiments are performed on Chinese Hamster Ovary (CHO) cells. First, cells are detached by 10x trypsin-EDTA (Sigma-Aldrich, Germany), diluted 1:9 in Hank's basal salt solution (Sigma-Aldrich, Germany). Then, they are centrifuged (180g, 21°C, 5 min), the supernatant is removed and replaced with the low-conductivity KPB buffer (10 mM KH_2PO_4/K_2HPO_4, 1 mM $MgCl_2$, 250 mM sucrose) in concentration 10^7 cells/ml. 100 μl of cell suspension is dispensed in 1.5 ml microcentrifuge tubes (Isolab, Germany). Immediately before pulse application, 10 μl of 1.5 mM propidium iodide (Life Technologies, USA) is added to the tube. Then, 100 μl of cell suspension with propidium iodide is pipetted between 2 mm stainless-steel electrodes. Using Gemini X2 electroporator, 8, 100 μs pulses of different voltage at 1 Hz are applied. After the pulse application, 80 μl of cell suspension is transferred from between the electrodes to a new 1.5 ml tube. Two minutes after pulse application, the sample is centrifuged (1 min, 2000g, room temperature), the supernatant is removed and replaced by 500 μl of KPB buffer. The change of the buffer stops propidium influx in the cells and allows us to compare different parameters at the same time point. From each tube, 100 μl of the cell suspension is transferred to a 96-well plate in triplicates. 100 μl of the cell suspension is transferred to a 5 ml tube. Then, the protocol is repeated for the next sample. When all samples are prepared, we start with the measurements.

First, the fluorescence intensity is determined spectrofluorimetrically. We set the appropriate excitation (535 nm) and emission (617 nm) wavelengths. We measure at an optimal gain which prevents from signal saturation. The optimal gain is automatically determined by the software based on sensor sensitivity and the maximum signal intensity we are measuring. The average fluorescence intensity is calculated for each voltage from the triplicates. We plot the fluorescence intensity in dependence on the applied voltage.

Second, we determine the number of fluorescent cells by flow cytometry. On the control cells, we set up the optimal measuring parameters at the lowest flow rate (12.5 µl/min). When optimal parameters are determined, we measure 10,000 events for each voltage with higher flow rate (200 µl/min). By gating, living cells and the percentage of permeabilized cells are determined for each voltage. We plot the cell permeabilization in dependence on the applied voltage for both measurements (spectrofluorometric and flow cytometry) and compare the results.

FURTHER READING:

Kotnik T., Maček Lebar A., Miklavčič D., Mir, L.M. Evaluation of cell membrane electropermeabilization by means of nonpermeant cytotoxic agent. *Biotechniques* 28**:** 921-926, 2000.
Marjanovič I., Kandušer M., Miklavčič D., Keber M.M., Pavlin M. Comparison of flow cytometry, fluorescence microscopy and spectrofluorometry for analysis of gene electrotransfer efficiency. *J. Membr. Biol.* 247: 1259-1267, 2014.
Michie J., Janssens D., Cilliers J., Smit B.J., Böhm L. Assessment of electroporation by flow cytometry. *Cytometry.* 41:96-101, 2000.
Rols M.P., Teissié J. Flow cytometry quantification of electropermeabilization. *Methods Mol. Biol. Clifton NJ*. 91: 141-147, 1998.
Shapiro H.M. *Practical flow cytometry*. (Wiley-Liss, 2003).

NOTES & RESULTS

Voltage (V)	0	100	150	200	250	0 and 250
Fluorescence intensity as measured with spectrofluorometer (a.u.)						
Percentage of fluorescent cells as determined by the flow cytometry (%)						

NOTES & RESULTS

Monitoring of electric field distribution in biological tissue by means of magnetic resonance electrical impedance tomography L9

Matej Kranjc[1], Igor Serša[2]
[1]University of Ljubljana, Faculty of Electrical Engineering
[2]Institut "Jožef Stefan"

Duration of the experiment: day 1: 90 min
Max. number of participants: 4
Location: MRI Laboratory (Jožef Stefan Institute)
Level: Basic

PREREQUISITES

Participants should be familiar with Laboratory safety (S1). No other specific knowledge is required for this laboratory practice.

THEORETICAL BACKGROUND

A method capable of determining electric field distribution during the pulse delivery has a practical value as it can potentially enable monitoring of the outcome of electroporation which strongly depends on the local electric field. Measurement of electric field distribution enables detection of insufficient electric field coverage before the end of either reversible or irreversible electroporation treatment, thus enabling corrections of field coverage during the treatment and consequently increasing and assuring its effectiveness. As there are no available approaches for measurement of electric field distribution *in situ*, an indirect approach using magnetic resonance techniques was suggested. Magnetic resonance electrical impedance tomography (MREIT) enables reconstruction of electric field distribution by measurement of electric current density distribution, first, and calculation of electrical conductivity of the treated subject during application of electric pulses using MRI data as an input to numerical algorithms, second. This method enables determination of electric field distribution *in situ* also accounting for changes that occur in the tissue due to electroporation.
MREIT is a relatively new medical imaging modality based on numerical reconstruction of electrical conductivity inside a tissue by means of current density distribution measured by current density imaging (CDI) sequence. The MREIT algorithm applied for reconstruction of electrical conductivity of the tissue is based on solving Laplace's equation through iterative calculation. Electrical conductivity is updated after each iteration (k+1):

$$\sigma^{k+1} = \frac{|\mathbf{J}_{\mathrm{CDI}}|}{|\nabla u^k|}.$$

where $\mathbf{J}_{\mathrm{CDI}}$ is current density obtained by CDI and u^k is electric potential obtained as a solution of Laplace's equation. When difference between two successive conductivities falls below certain value electric field distribution can be calculated using:

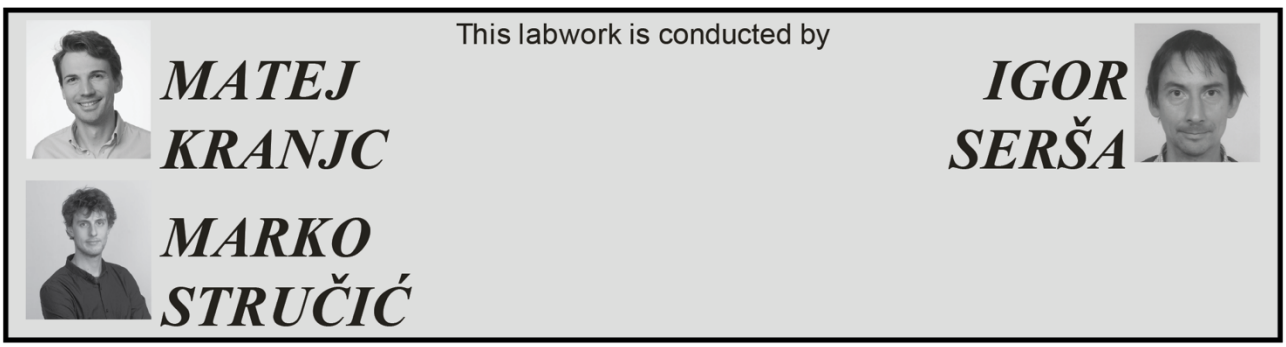

$$\mathbf{E} = \frac{\mathbf{J}_{\mathrm{CDI}}}{\sigma}.$$

The aim of this laboratory practice is to demonstrate monitoring of electric field distribution in a biological tissue using MREIT.

EXPERIMENT

We will monitor current density distribution and electric field distribution in biological tissue exposed to electric pulses by means of MREIT. We will then compare measured current density distribution and reconstructed electric field distribution with simulation results obtained by a numerical model of the tissue.

Protocol

The experiment will be performed on biological tissue (chicken liver) sliced in a disc-like sample measuring 21 mm in diameter and 2 mm in height (Fig. 1a). Electric pulses will be delivered via two cylindrically shaped electrodes inserted into the sample. After the insertion, the electrodes will be connected to an electric pulse generator connected to an MRI spectrometer. The sample will be placed in a 25 mm MR microscopy RF probe (Fig. 1b) inside a horizontal-bore superconducting MRI magnet (Fig. 1c). Electroporation treatment of the sample will be performed by applying two sequences of four high voltage electric pulses with a duration of 100 μs, a pulse repetition frequency of 5 kHz and with an amplitude of 500 V and 1000 V.

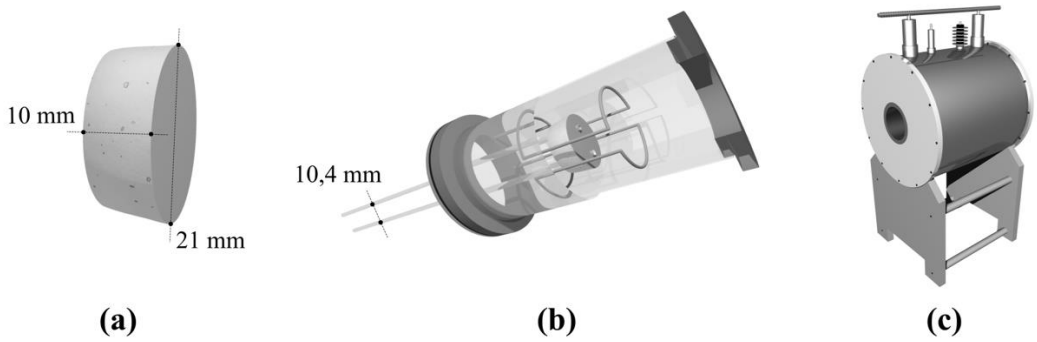

Figure 1: Biological sample (a) placed in a MR microscopy probe (b) inside a horizontal MRI magnet (c).

MR imaging will be performed on a MRI scanner consisting of a 2.35 T (100 MHz proton frequency) horizontal bore superconducting magnet (Oxford Instruments, Abingdon, United Kingdom) equipped with a Bruker micro-imaging system (Bruker, Ettlingen, Germany) for MR microscopy with a maximum imaging gradient of 300 mT/m and a Tecmag Apollo spectrometer (Tecmag, Houston TX, USA). Monitoring of electric field is enabled by CDI, which is an MRI method that enables imaging of current density distribution inside conductive sample. We will apply two-shot RARE version of the CDI sequence (Fig. 2).

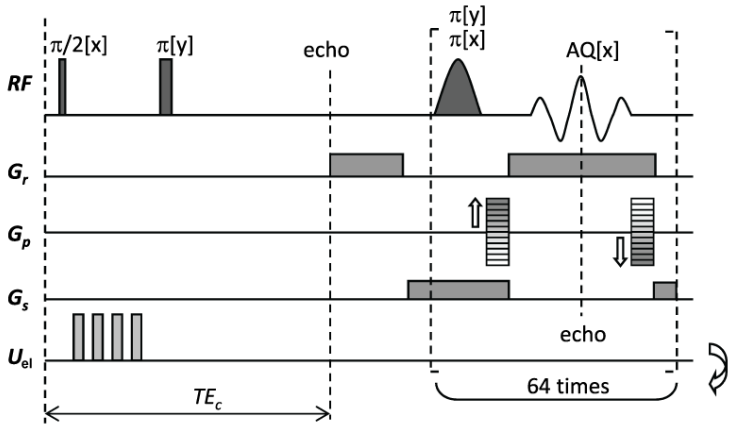

Figure 2: Two-shot RARE pulse sequence used for acquisition of current density distribution. The sequence consists of a current encoding part with a short (100 μs long) high-voltage electroporation pulse (U_{el}) delivered immediately after the nonselective 90° radiofrequency (RF) excitation pulse. In the second part of the sequence signal acquisition is performed using the single-shot RARE signal acquisition scheme that includes standard execution of readout (G_r), phase-encoding (G_p) and slice-selection (G_s) magnetic field gradients. Due to auxiliary phase encoding induced by the electric pulse, the RARE sequence is repeated twice, each time with a different phase of the refocusing pulses (0°and 90°), and the corresponding signals are co-added.

Electric field distribution in the sample will be reconstructed by iteratively solving Laplace's equation using J-substitution mathematical algorithm and finite element method with the numerical computational environment MATLAB on a desktop PC. We will compare measured current density distribution obtained by means of CDI and reconstructed electric field distribution obtained by means of MREIT in the sample with simulation results obtained by a numerical model of the sample.

FURTHER READING

Kranjc M., Bajd F., Sersa I., Miklavcic D., Magnetic resonance electrical impedance tomography for monitoring electric field distribution during tissue electroporation. *IEEE Trans. Med. Imaging* 30:1771-1778, 2011.

Kranjc M., Bajd F., Serša I., Miklavčič D., Magnetic resonance electrical impedance tomography for measuring electrical conductivity during electroporation. *Physiol. Meas.* 35:985-96, 2014.

Kranjc M., Markelc B., Bajd F., Čemažar M., Serša I., Blagus T., Miklavčič D. In situ monitoring of electric field distribution in mouse tumor during electroporation. *Radiology*. 274:115-123, 2015.

Kranjc M., Bajd F., Serša I. de Boevere M., Miklavcic D., Electric field distribution in relation to cell membrane electroporation in potato tuber tissue studied by magnetic resonance techniques. *Innov. Food Sci. Emerg. Technol.* 37:384-390, 2016.

Woo E.J., Kranjc M. Principles and use of magnetic resonance electrical impedance tomography in tissue electroporation. In *Handbook of Electroporation* (ed. Miklavcic, D.) 1–18 Springer, 2016.

Seo J.K., Woo E.J., Magnetic resonance electrical impedance tomography (MREIT). *SIAM Rev* 53:40-68, 2011.

Sersa I. Auxiliary phase encoding in multi spin-echo sequences: application to rapid current density imaging. *J. Magn. Reson.*, 190:86-94, 2008.

NOTES & RESULTS

NOTES & RESULTS

Measurements of the induced transmembrane voltage with fluorescent dye di-8-ANEPPS

L10

Gorazd Pucihar
University of Ljubljana, Faculty of Electrical Engineering

Duration of the experiments: 60 min
Max. number of participants: unlimited
Location: Online ONLY
Level: Advanced

PREREQUISITES

Participants should be familiar with Laboratory safety (S1). The basic knowledge of handling with cells is required for this laboratory practice.

THEORETICAL BACKGROUND

When a biological cell is placed into an external electric field the induced transmembrane voltage (ITV) forms on its membrane. The amplitude of the ITV is proportional to the amplitude of the applied electric field, and with a sufficiently strong field, this leads to an increase in membrane permeability - electroporation. Increased permeability is detected in the regions of the cell membrane where the ITV exceeds a sufficiently high value, in the range of 250 – 1000 mV, depending on the cell type. In order to obtain an efficient cell electroporation it is therefore important to determine the distribution of the ITV on the cell membrane. The ITV varies with the position on the cell membrane, is proportional to the electric field, and is influenced by cell geometry and physiological characteristics of the medium surrounding the cell. For simple geometric shapes the ITV can be calculated analytically (e.g. for a spherical cell, using Schwan's equation). For more complicated cell shapes experimental and numerical methods are the only feasible approach to determine the ITV.

The aim of this laboratory practice is to measure the ITV on a spherical cell by means of a fluorescent potentiometric dye di-8-ANEPPS.

EXPERIMENT

Potentiometric fluorescent dyes allow observing the variations of the ITV on the membrane and measuring its value. Di-8-ANEPPS is a fast potentiometric fluorescent dye, which becomes fluorescent when it binds to the cell membrane, with its fluorescence intensity varying proportionally to the change of the ITV. The dye reacts to the variations in the ITV by changing the intramolecular charge distribution that produce corresponding changes in the spectral profile or intensity of the dye's fluorescence.

Protocol: The experiments are performed on Chinese hamster ovary cells (CHO) grown in Lab-Tek chambers (Nunc, Germany) in culture medium HAM-F12 supplemented with 10% fetal bovine serum, L-glutamine (all three from Sigma-Aldrich) and antibiotics. When cells attach to the cover glass of a Lab-Tek chamber (usually after 2 to 3 hours to obtain attached cells of spherical shape), carefully replace the culture medium with 1 ml of SMEM medium (Spinner’s modification of the MEM, Sigma-Aldrich) containing 30 µM of di-8-ANEPPS and 0.05% of Pluronic (both Life Technologies). After staining for

This labwork is conducted by

ANJA BLAŽIČ

12 min at 4°C, wash the cells thoroughly with pure SMEM to remove the excess dye. After washing leave 1.5 ml of SMEM in the chamber. Place the chamber under a fluorescence microscope (Zeiss AxioVert 200, Germany) and use ×63 oil immersion objective. Position two parallel Pt/Ir wire electrodes, with a 4 mm distance between them, to the bottom of the chamber. Set a single 40 V, 50 ms pulse on the programmable square wave electroporator TSS20 (Intracel). This will result in a voltage-to-distance ratio of ~100 V/cm. The pulse must be synchronized with the image acquisition. Set the excitation wavelength to 490 nm and use ANEPPS filter to detect fluorescence (emission 605 nm).
Find the cells of interest. Acquire the control fluorescence image and subsequently the image with a pulse, using a cooled CCD camera (VisiCam 1280, Visitron) and MetaFluor 7.7.5 (Molecular Devices). Apply four pulses with a delay of 4 s between two consecutive pulses. For each pulse, acquire a pair of images, one immediately before (control image) and one during the pulse (pulse image) (Figures 1A and B).
Open the images in MetaMorph 7.7.5 (Molecular Devices). To *qualitatively* display the ITV on the cell membrane, convert the acquired 12-bit images to 8-bit images. For each pulse, obtain the difference image by subtracting (on a pixel-by-pixel basis) the control image from the pulse image. Add 127, so that 127, i.e. mid-gray level, corresponds to 0 V, brighter levels to negative voltages, and darker levels to positive ones (Figure 1C). Average the three difference images to increase the signal-to-noise ratio.
To *quantitatively* determine the ITV, open the acquired, unprocessed fluorescence images. Determine the region of interest at the site of the membrane and measure the fluorescence intensities along this region for the control and pulse image. Transform the values to the spreadsheet. Measure the background fluorescence in both images and subtract this value from the measured fluorescence. Calculate the relative changes in fluorescence ($\Delta F/F_C$) by subtracting the fluorescence in the control image F_C from the fluorescence in the pulse image F_P and dividing the subtracted value by the fluorescence in the control F_C; $\Delta F/F_C = (F_P - F_C) / F_C$. Average the relative changes calculated for all four acquired pairs of images. Transform the fluorescence changes to the values of the ITV (ΔF/F = -6% / 100 mV), and plot them on a graph as a function of the arc length (Figure 1D).

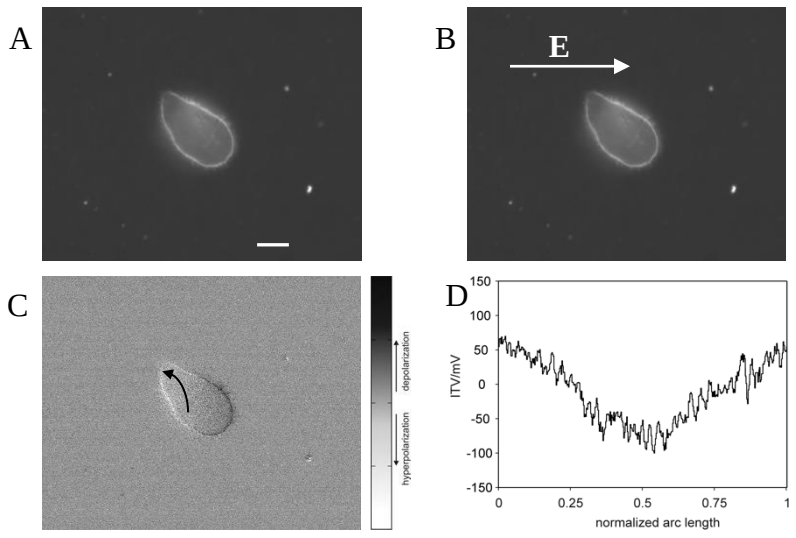

Figure 1: Measurements of the induced transmembrane voltage (ITV) on an irregularly shaped CHO cell. (A) A control fluorescence image of a cell stained with di-8-ANEPPS. Bar represents 10 μm. (B) Fluorescence image acquired during the exposure to a 35 V (~88 V/cm), 50 ms rectangular pulse. (C) Changes in fluorescence of a cell obtained by subtracting the control image A from the image with pulse B and shifting the grayscale range by 50%. The brightness of the image was automatically enhanced. (D) ITV measured along the path shown in C.

FURTHER READING:

Teissié J., Rols M.P. An experimental evaluation of the critical potential difference inducing cell membrane electropermeabilization. *Biophys. J.* 65:409-413, 1993.

Gross D., Loew L. M, Webb W. Optical imaging of cell membrane potential changes induced by applied electric fields. *Biophys. J.* 50:339-348, 1986.

Montana V., Farkas D.L., and Loew L.M. Dual-wavelength ratiometric fluorescence measurements of membrane-potential. *Biochemistry* 28:4536-4539, 1989.

Loew L.M. Voltage sensitive dyes: Measurement of membrane potentials induced by DC and AC electric fields. *Bioelectromagnetics* Suppl. 1:179-189, 1992.

Hibino M., Itoh H., Kinosita K. Time courses of cell electroporation as revealed by submicrosecond imaging of transmembrane potential. *Biophys. J.* 64:1789-1800, 1993.

Kotnik T., Bobanović F., Miklavčič D. Sensitivity of transmembrane voltage induced by applied electric fields – a theoretical analysis. *Bioelectrochem. Bioenerg.* 43:285-291, 1997.

Pucihar G., Kotnik T., Valič B., Miklavčič D. Numerical determination of transmembrane voltage induced on irregularly shaped cells. *Annals Biomed. Eng.* 34: 642-652, 2006.

Video Article:

Pucihar G., Kotnik T., Miklavčič D. Measuring the induced membrane voltage with di-8-ANEPPS (Video Article). *J. Visual Exp.* 33:1659, 2009.

NOTES & RESULTS

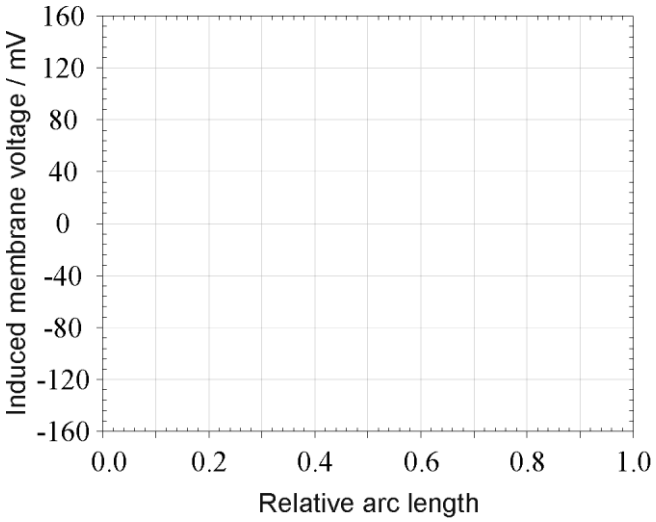

NOTES & RESULTS

Analysis of electric field orientations on gene electrotransfer efficiency L11

Saša Haberl Meglič, Matej Reberšek
University of Ljubljana, Faculty of Electrical Engineering

Duration of the experiment: 60 min
Max. number of participants: Unlimited
Location: Online ONLY
Level: Advanced

PREREQUISITES

Participants should be familiar with the Safety rules and Rules for sterile work in cell culture laboratory. The basic knowledge of handling with cells is required for this laboratory practice.

THEORETICAL BACKGROUND

Gene electrotransfer is a non-viral method used to transfer genes into living cells by means of high-voltage electric pulses. An exposure of a cell to an adequate amplitude and duration of electric pulses leads to transient increase of cell membrane permeability for molecules which are otherwise deprived of membrane transport mechanisms. This allows various nonpermeant molecules, including DNA, to be transported across the membrane and enter the cell. Although mechanisms of the process are not yet fully elucidated, it was shown that several steps are crucial for gene electrotransfer: interaction of plasmid DNA (pDNA) with the cell membrane, translocation of pDNA across the membrane, migration of pDNA towards the nucleus, transfer of pDNA across the nuclear envelope and gene expression.

Many parameters (such as electric pulse protocol) can influence the first step (interaction of DNA with the cell membrane) and by that gene electrotransfer efficiency. Therefore different electric pulse protocols are used in order to achieve maximum gene transfection, one of them is changing the electric field orientation during the pulse delivery. Since DNA is a negatively charged molecule and it is dragged towards the cell with the electrophoretic force in the opposite direction of the electric field, changing electric field orientation increases the membrane area competent for DNA entry into the cell.

The aim of this laboratory practice is to demonstrate how different pulse polarity affects the efficiency of gene electrotransfer and cell viability.

EXPERIMENT

For the experiment we will use Chinese hamster ovary cells (CHO-K1) and plasmid DNA (pEGFP-N_1) that codes for GFP (green fluorescent protein). To generate and deliver electric pulses a high-voltage prototype generator and electrodes with four cylindrical rods, which were developed at a Laboratory of Biocybernetics will be used. Pulses will be monitored on osciloscope (LeCroy 9310C).

This labwork is conducted by

TJAŠA POTOČNIK

Pulse protocols (see also Figure 1):

a) SP (single polarity): the direction of electric field is the same for all pulses
b) OBP (orthogonal both polarities): the direction of the electric field is changed between the pulses

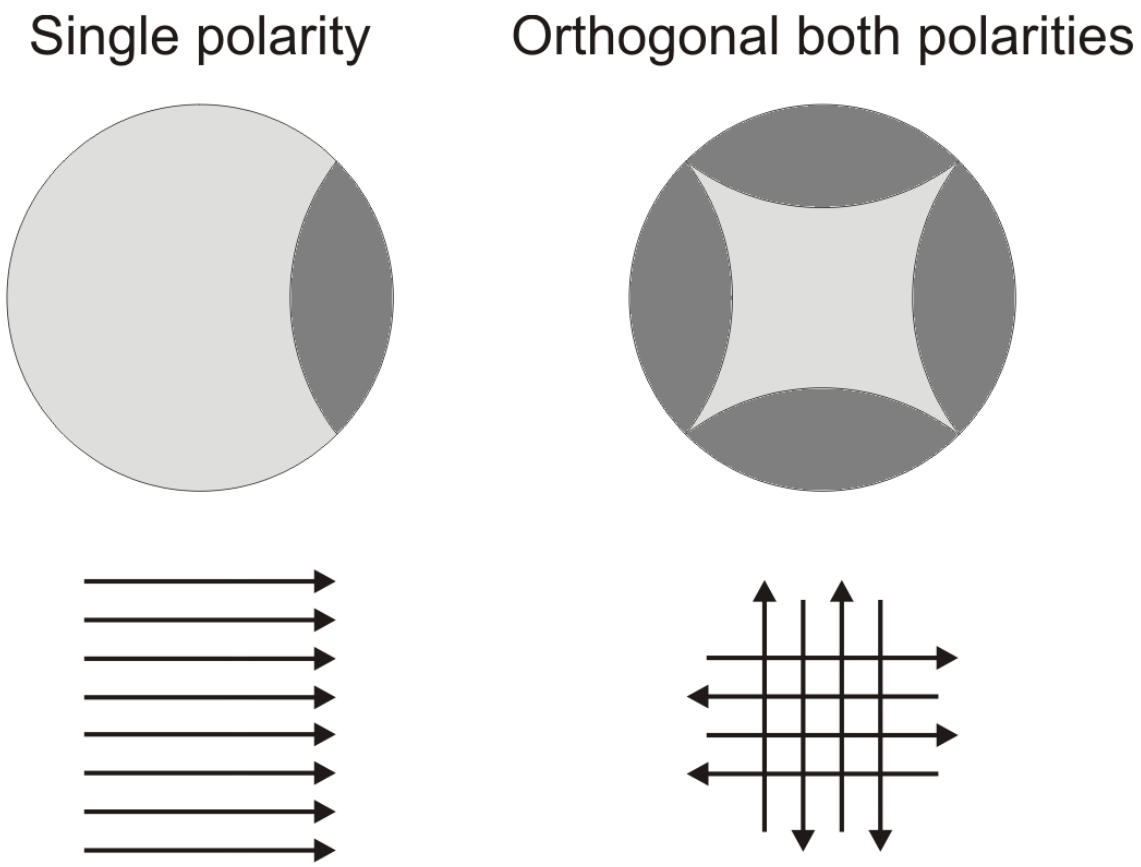

Figure 1: Two different pulse protocols will be used: single polarity (SP) and orthogonal both polarities (OBP)

Protocol 1/2 (Gene electrotransfer with different pulse parameters): CHO cells will be grown in multiwells as a monolayer culture in Ham's tissue culture medium for mammalian cells with 10% fetal bovine serum at 37º C. Cells will be plated 24h before the experiment in concentration 5 x 10^5 cells per well.
Just before the experiment remove culture medium and replace it with 150 µl of electroporation buffer containing plasmid DNA with concentration 10 µg/ml. Incubate cells with plasmid for 2-3 minutes at room temperature. Then apply a train of eight pulses with amplitude of 225 V, duration of 1 ms and repetition frequency 1 Hz using single polarity and orthogonal both polarities (see Pulse protocols) to deliver plasmid DNA into the cells.
Cells in the control are not exposed to electric pulses.
Immediately after exposure of cells to electric pulses add 37 µl of fetal calf serum (FCS-Sigma, USA). Incubate treated cells for 5 minutes at 37º C and then add 1 ml of culture medium.

Protocol 2/2 (Determining gene electrotransfer efficiency and cell viability): After 24 h incubation at 37º C determine the difference in gene electrotransfer efficiency and cell viability for both pulse protocols by fluorescent microscopy (Leica, Wetzlar, Germany) at 20x magnification using GFP filter with excitation at 488 nm.

You will determine gene electrotransfer efficiency from the ratio between the number of green fluorescent cells (successfully transfected) and the total number of cells counted under the phase contrast. You will obtain cell survival from phase contrast images as the ratio between the number of viable cells in the treated sample and the number of viable cells in the control sample.

FURTHER READING:

Faurie C., Reberšek M., Golzio M., Kandušer M., Escoffre J.M., Pavlin M., Teissie J., Miklavčič D., Rols M.P. Electro-mediated gene transfer and expression are controlled by the life-time of DNA/membrane complex formation. *J. Gene Med*. 12:117-125, 2010.
Golzio M., Teissié J., Rols M.P. Direct visualization at the single-cell level of electrically mediated gene delivery. *PNAS* 99:1292-1297, 2002.
Pavlin M., Haberl S., Reberšek M., Miklavčič D., Kandušer M. Changing the direction and orientation of electric field during electric pulses application improves plasmid gene transfer in vitro. *J. Vis. Exp*. 55:1-3, 2011.
Reberšek M., Faurie C., Kandušer M., Čorović S., Teissié J., Rols M.P., Miklavčič D. Electroporator with automatic change of electric field direction improves gene electrotransfer *in vitro*. *Biomed. Eng. Online* 6:25, 2007.
Reberšek M., Kandušer M., Miklavčič D. Pipette tip with integrated electrodes for gene electrotransfer of cells in suspension: a feasibility study in CHO cells. *Radiol. Oncol*. 45:204-208, 2011.

NOTES & RESULTS

Pulse parameters	Gene electrotransfer efficiency [%]	Cell viability [%]
Single polarity		
Orthogonal both polarities		

Monitoring cell membrane depolarization due to electroporation using fluorescent plasma membrane potential indicator

L12

Anja Blažič, Lea Rems
University of Ljubljana, Faculty of Electrical Engineering

Duration of the experiments: 90 min
Max. number of participants: 4
Location: Cell Culture Laboratory 3
Level: Advanced

PREREQUISITES

Participants should be familiar with Laboratory safety (S1). The basic knowledge of handling with cells is required for this laboratory practice.

BACKGROUND

All cells maintain an electric potential difference across their plasma membranes, which results from the differences in membrane permeabilities for potassium, sodium, calcium, and chloride ions. This potential difference is called the resting transmembrane voltage or resting potential and is maintained by a system of ion channels and pumps. By convention the resting transmembrane voltage is negative, meaning that the cell interior is electrically more negative compared to its exterior. The value of the resting transmembrane voltage changes dynamically with the cell cycle and has an important biological function by controlling the activity of various membrane proteins. When cells are electroporated, their transmembrane voltage changes and the membrane remains depolarized for several minutes after pulse exposure. As membrane depolarization acts as a biological signal, factors that influence prolonged depolarization upon electroporation can have an important influence on the biological outcome of electroporation.

The aim of this laboratory practice is to monitor the time course of transmembrane voltage changes after exposure to conventional electroporation pulses, and to determine the influence of pulse amplitude and ambient temperature on the extent and longevity of membrane depolarization.

EXPERIMENT

We will monitor the time course of membrane potential changes using the plasma membrane potential indicator (PMPI) of the FLIPR Membrane Potential Assays Kit (Molecular Devices). PMPI consists of a two-part system which includes a fluorescent anionic voltage-sensor and a quencher. When the interior of the cell has a relatively negative charge the anion dye remains on the extracellular side, where the quencher prevents fluorescence excitation. During depolarization the voltage sensor translocates to the intracellular side, which increases the fluorescence intensity inside the cells. This translocation is reversible, which makes it possible to monitor membrane depolarization and repolarization as the cells recover and return to their baseline level. The fluorescence intensity is linearly proportional to the change in the membrane potential difference, making this method comparable to patch-clamp measurements upon dye calibration.

This labwork is conducted by

ANJA BLAŽIČ

Protocol: U87-MG human glioblastoma cells will be plated in Nunc Lab-Tek II chambered coverglass three to four days before the experiments. On the day of the experiments, the cells will be stained for 30 min at 37°C with the Component A of the FLIPR Membrane Potential Assay Red (Molecular Devices, #R7291), diluted in Live Cell Imaging Solution (Invitrogen, #A14291DJ). Afterwards, the cells will be placed on the microscope stage. The cells will be exposed to a single 100 μs pulse of selected amplitude, delivered by βtech B10 pulse generator through a pair of Pt-Ir wire electrodes. Time lapse images of the cells will be acquired before and after pulse application. We will compare the response of the cells at room temperature and at 37°C, to observe how cell recovery depends on the temperature. The cells will be imaged on inverted microscope Leica DMi8 with LED8 illumination source controlled by the LasX software (all Leica Microsystems). The membrane potential dye will be excited with green LED (555/28 nm) and its florescence will be passed through DFT51010 filter and detected with the Leica DFC9000 Gt camera.

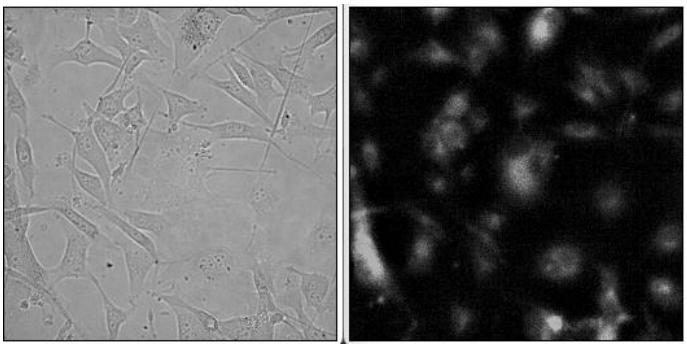

Figure 1: Brightfield image (*left*) and fluorescence (*right*) of U87-MG cells stained with FLIPR membrane potential assay.

FURTHER READING:

Wegner L.H., Frey W., Silve A. Electroporation of DC-3F cells is a dual process. *Biophys. J.* 108:1660-71, 2015.
Baxter D.F., Kirk M., Garcia A.F., Raimondi A., Holmqvist M.H., Flint K.K., Bojanic D., Distefano P.S., Curtis R., Xie Y. A novel membrane potential-sensitive fluorescent dye improves cell-based assays for ion channels. *J. Biomol. Screening* 7:79-85, 2002.
Klapperstück T., Glanz D., Hanitsch S., Klapperstück M., Markwardt F., Wohlrab J. Calibration procedures for the quantitative determination of membrane potential in human cells using anionic dyes. *Cytometry Part A* 83A:612-26, 2013.
Burke R.C., Bardet S.M., Carr L., Romanenko S., Arnaud-Cormos D., Leveque P., O'Connor R.P. Nanosecond pulsed electric fields depolarize transmembrane potential via voltage-gated K^+, Ca^{2+} and TRPM8 channels in U87 glioblastoma cells. *Biochim. Biophys. Acta (BBA) - Biomembranes* 1859:2040-50, 2017.
Dermol-Černe J., Miklavčič D., Reberšek M., Mekuč P., Bardet S.M., Burke R., Arnaud-Cormos D., Leveque P., O'Connor R.P. Plasma membrane depolarization and permeabilization due to electric pulses in cell lines of different excitability. *Bioelectrochemistry* 122:103-14, 2018.
Blackiston D.J., McLaughlin K.A., Levin M. Bioelectric controls of cell proliferation: ion channels, membrane voltage and the cell cycle. *Cell Cycle* 8(21):3527-36, 2009.
Vodovnik L., Miklavčič D., Serša G. Modified cell proliferation due to electrical currents. *Med. Biol. Eng. Comput.* 30:CE21-8, 1992.

NOTES & RESULS

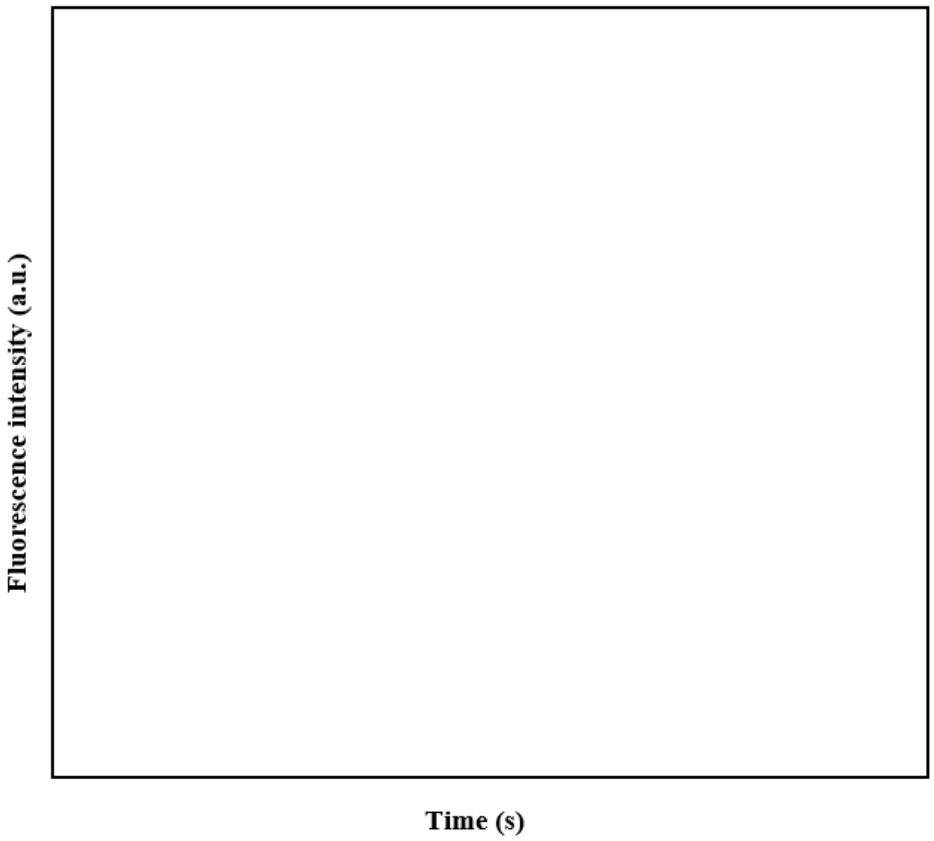

Impedance and texture analysis techniques for detecting and characterising electroporation in plant tissues L13

Samo Mahnič-Kalamiza, Rok Šmerc
University of Ljubljana, Faculty of Electrical Engineering

Duration of the experiments: 120 min
Max. number of participants: 4
Location: Tissue Laboratory
Level: Basic

PREREQUISITES

Participants should be familiar with Laboratory safety (S1). No prior knowledge of laboratory work is required. Basic skills of handling electronic instruments such as an oscilloscope and impedance analyser are an advantage, but not prerequisite.

THEORETICAL BACKGROUND

The application of PEF treatment in food processing is gaining momentum and seeing intensive research and development. New electroporation-based treatments are continuously put to the test and are optimized both at the laboratory and industrial scale processes. PEF treatment offers increasing benefits in terms of low energy requirements and minimization of food quality deterioration. For successful treatment, an appropriate choice of methods assessing changes due to electroporation occurring in biological matrices of alimentary interest is crucial. Despite a considerable body of literature in the field, detailed information regarding the detection and quantification of the effects of electroporation in complex and highly inhomogeneous multicellular systems, such as real food systems (e.g., plant tissues), is still limited. Moreover, due to the unique characteristics and properties of the biological tissue processed, a case-by-case PEF treatment optimization protocol is often required.

In food-related PEF applications, measurements of the dielectric properties of the tissue are often used for the determination of the degree of cell membrane disruption by electroporation. Electrical impedance spectroscopy (EIS) has been suggested as a reliable method to estimate the extent of tissue damage due to PEF treatment. EIS relies on the theory that, from an electrical point of view, an individual cell can be represented as an insulating membrane exhibiting relatively high resistance to electric current and considerable capacitance, and intra- and extra-cellular media (electrolytes) that behave as a resistive (ohmic) load up to hundreds of MHz. As electroporation affects the permeability (i.e., conductivity) of the cell membrane, multifrequency impedance measurements can be used to assess the degree of membrane permeabilization due to PEF treatment.

Another possibility of assessing changes in electroporated plant tissues is offered by texture analysis (texture in the sense of the response of a material to mechanical forces). Plant tissues in structures such as roots, fruits, and tubers, often exhibit considerable turgidity (high turgor pressure) when fresh and not dehydrated. Disrupting the selectively permeable membrane of the cells by electroporation can result in release of the intracellular water that is filtered out through the extracellular matrix. From the analysis of tissue's response to external force at the exact moment of electroporation and within minutes after, it is possible to evaluate the extent to which the electroporated plant tissue has been affected by the

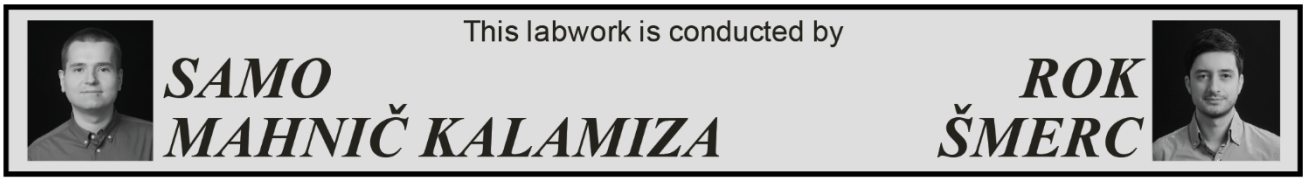

treatment. Texture analysis offers an alternative method to evaluating the degree of cell membrane disruption in treatment protocol optimisation where impedance measurements are either unavailable or impractical.

The aim of this laboratory practice is to detect (and quantify) electroporation effects in plant tissues of disparate origin, structure, and water content & solute composition, by employing electrical impedance measurements and texture analysis (i.e., tissue's response to mechanic forces). Students will learn of the importance of plant tissue composition and structure, and how these properties impact detection and quantification of electroporation effects in fresh plant matrices.

EXPERIMENT

We will perform concurrent sample deformation analysis (at constant loading force) and impedance measurements (pre- and post-pulse delivery) on two plant tissues: an apple fruit sample, and a potato tuber sample. To vary the treatment efficacy, and thus the extent of changes in tissue caused by electroporation, we will perform a voltage escalation study at three different voltages (and thus three different voltage-to-distance ratios), and repeat every experiment twice to ensure we have a stable set of data to work with (we would opt for a higher number of repetitions in a non-learning environment, the limit to two is due to time constraints). Altogether, we will perform 12 sets of impedance and texture measurements. In addition to recording the impedance and piston displacement, we will also be monitoring the pulse voltage and current with an oscilloscope (Teledyne LeCroy HDO6104A-MS).

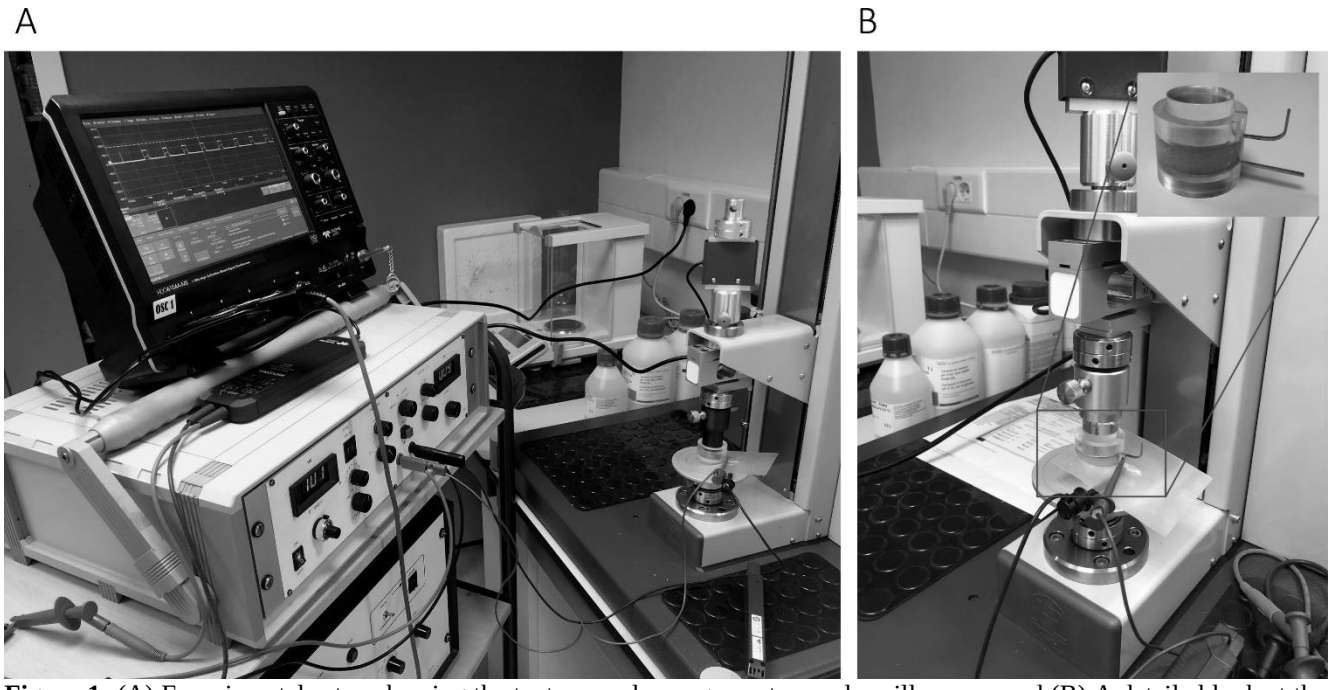

Figure 1: (A) Experimental setup showing the texture analyser, generator, and oscilloscope; and (B) A detailed look at the treatment chamber as set up under the texture analyser piston and of the treatment chamber setup on its own.

Protocol:

We will prepare six samples of apple fruit (cultivar depending on availability) cut into 6 mm thick cylinders of 25 mm in diameter. We will also prepare six samples of a potato tuber (cultivar depending on availability) cut into cylinders of identical dimensions as for the apple fruit.

Samples will be placed into a cylindrical treatment chamber with plate electrodes at the top and bottom of the sample (see Figure 1), the entire setup will then be placed under the piston of a texture analyser

(Hegewald & Peschke Inspect solo 1 kN-M) and subjected to a constant force of 5 N and 10 N for apple fruit and potato tuber, respectively. Electrodes will be connected both to a pulse generator (prototype device), as well as an impedance analyser (in short – an LCR meter, Keysight E4980A), and a switching circuit that will switch between the pulse generator and the impedance analyser to protect the LCR instrument from high-voltage pulses (prototype device).
The force will be applied for a total of 2 minutes. After 30 seconds under load, you will measure the pre-pulse impedance, and then immediately deliver 8 pulses of 100 us at 1 Hz repetition frequency, then immediately measure the post-pulse impedance. The loading of the sample will then continue for another minute or so (until 2 minutes total loading time is reached).
Deformation curves obtained from the texture analyser and impedance measurements will then be imported into MATLAB using scripts prepared in advance for further analysis, during which you will:

- Calculate the ratio of post- to pre-pulse electrical impedance of the sample at 5 kHz frequency and plot it versus the applied voltage.
- Calculate the total deformation of the sample from the moment of pulse delivery and up to the end of the constant force application and plot this deformation versus the applied voltage.

We will then compare the two functions/plots for both plant tissues and we will discuss the interpretation. The lab work concludes with a printout of graphs that you will paste into your workbooks (under NOTES & RESULTS to the right).

FURTHER READING:

Lebovka N., Vorobiev E. Techniques to detect electroporation in food tissues. In *Handbook of Electroporation* (ed. Miklavcic, D.) Springer, 2017.
Angersbach. A., Heinz V., Knorr, D. Electrophysiological model of intact and processed plant tissues: Cell disintegration criteria. *Biotechnol. Prog.* 15/4:753-762, 1999.
Grimi N., Lebovka N., Vorobiev E., Vaxelaire J. Compressing behavior and texture evaluation for potatoes pretreated by pulsed electric field. *J. Texture Stud.* 40, 208-224, 2009.
Mahnič-Kalamiza S., Vorobiev E. Dual-porosity model of liquid extraction by pressing from biological tissue modified by electroporation. *J. Food Eng.* 137:76-87, 2014.

NOTES & RESULS

Modelling, visualising, and tracking pH front formation during pulse delivery to agarose-based tissue phantoms L14

Samo Mahnič-Kalamiza, Rok Šmerc
University of Ljubljana, Faculty of Electrical Engineering

Duration of the experiments: 120 min
Max. number of participants: 4
Location: Tissue Laboratory
Level: Basic

PREREQUISITES

Participants should be familiar with Laboratory safety (S1). No prior knowledge of laboratory work is required. Possession of basic skills of handling chemical/biological laboratory equipment (pipette, analytical scale) is an advantage, but not prerequisite.

THEORETICAL BACKGROUND

In electroporation applications we inevitably encounter chemical phenomena associated with the direct supply of electrical energy to living organisms by means of metallic electrodes. As these are inserted into an electrolyte solution, such as is tissue, a special region (layer) forms at the interface between the electrode and the tissue, where dynamic electrochemical processes occur to enable flow of an electric current. The products of these processes can be both beneficial or highly harmful to tissue (and electrodes). Assuming monopolar pulse delivery, an acidic pH front forms at the anode and a basic at the cathode, propagating away from the electrodes during, but also after pulse delivery.

While gene electrotransfer (GET) holds great potential for therapeutic applications, it is important to consider the potential effects of pH changes induced by this method in target tissues. Change of pH levels during GET can lead to tissue damage and cell death, reducing the effectiveness of the treatment by potentially damaging portions of the tissue where transfection would otherwise be successful. The presence of hydroxyl ions increases the damage and is even more fatal for the cells, as their interaction with lipids leads to disruption and breakdown of the cell membrane structure. It is thus important to carefully optimize the electroporation parameters to minimize pH-induced damage and maintain tissue viability during GET, where often longer (several milliseconds) pulses are used as part of the treatment protocol.

There has been intense development of alternative tissue ablation therapies recently, either using high-voltage pulses such as in irreversible electroporation (IRE) or pulsed field ablation (PFA), or (side)products of electrochemical reactions in what is called electrochemical therapy (EChT), or a combination of both, called electrolytic electroporation (E^2). These therapies exploit not only the effects of high field strengths, but also the altered acid-base properties of the tissue (change of pH), to successfully remove pathologically altered tissue. It is thus of importance for treatment design and success that these electro-chemical processes altering pH in tissue are well understood and, if appropriate, exploited to our advantage.

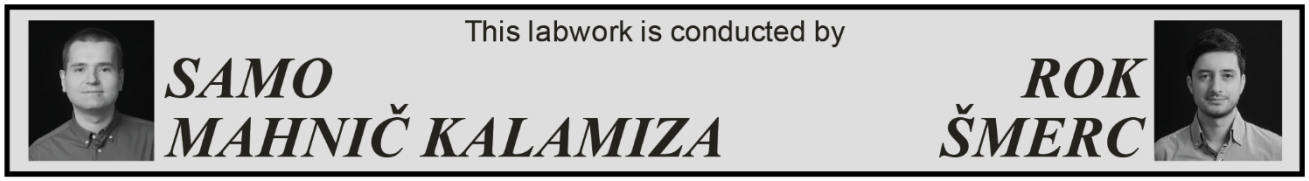

One effective approach to detect and visualize pH changes during the delivery of electrical pulses to model tissues or tissue phantoms involves the use of pH-sensitive dyes or indicators.

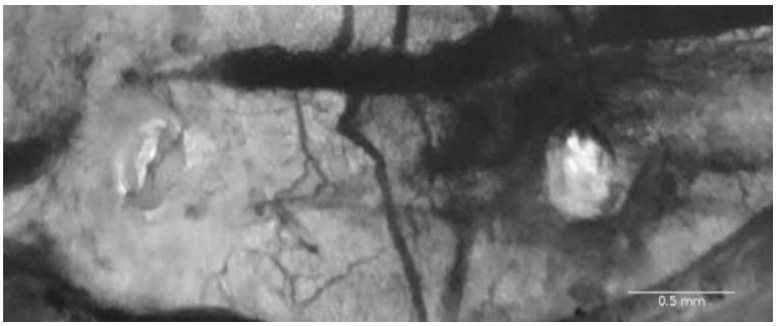

Figure 1: pH changes in the skin due to pulse delivery, surrounding the two needle electrodes (anode-left, cathode-right). Dorsal skin flap of a mouse, observed through a window chamber, in vivo. From Marino et al., 2017.

These dyes exhibit a colour change in response to variations in pH values, allowing for real-time monitoring of pH dynamics within the tissue or tissue phantoms. By incorporating these pH-sensitive dyes into the model tissue, which can be prepared using materials such as collagen or agarose, we can observe and analyse the electrochemical reactions and subsequent pH changes that occur at the interface between the metal electrodes and the tissue. This enables a direct visualization of the impact of electrical pulse delivery on the pH environment, providing valuable insights into the underlying processes and helping to optimize the therapeutic applications of electroporation. The pH-sensitive dyes act as visual indicators, offering a convenient and non-invasive means to assess the local pH changes induced by the electrical pulses, thus enhancing our understanding of the intricate electrochemical interactions between metal electrodes and biological tissues.

The aim of this laboratory practice is to showcase how we can use numerical modelling techniques using advanced finite-element software models (COMSOL Multiphysics) to study complex electrochemical phenomena occurring at the electrode-electrolytic solution interface, and their propagation by electromigration and diffusion in a phantom tissue model. The laboratory exercise will demonstrate, through practical work, how such models can subsequently be validated using practical and comparatively simple lab experiments. The students will learn just how much electrochemistry is "going on" during a typical electroporation application.

EXPERIMENT

We will first review simulation results demonstrating pH front evolution and advancement in a typical needle-electrode delivery of pulses using a typical GET protocol to i.) an unbuffered medium, and ii.) a buffered medium of comparable buffering capabilities to those of tissue. We will then move to the wet lab portion of the lab work, where we will deliver pulses to agarose phantoms using the same pulse protocol as previously demonstrated through simulation results at various voltages (field strengths). Additionally, we will deliver pulses to the phantoms using an additional protocol employing short, biphasic pulses, to study if these do indeed result in significantly less change in pH as per theory.

We will prepare the agarose phantoms with either unbuffered or buffered saline to demonstrate the natural buffering capabilities of tissue. The two pulse protocols will be chosen to demonstrate the difference between monophasic and biphasic delivery of pulses. The experimental system for observing pH changes consists of a high-speed digital camera with a macro lens, a camera stand with lighting panel, an electroporation pulse generator, and a suitable laptop for capturing the camera's video signal.

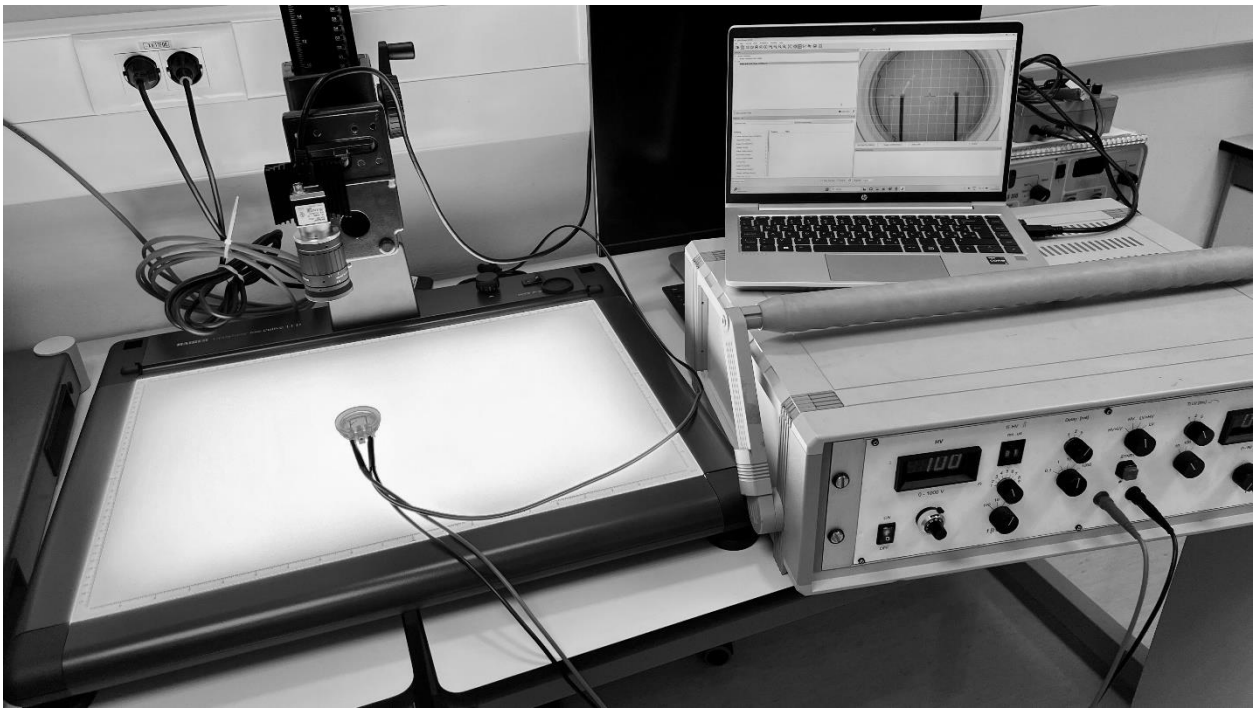

Figure 2: Experimental setup showing the camera rig and the agarose sample under treatment in a mini petri dish with a custom made cover/electrode holding guide, pulse generator, and laptop computer for controlling the camera and recording video data.

Protocol:

Following the demonstration of numerical simulation results (a slide presentation), we will move to the wet lab where we will begin by mixing an indicator solution using purified water, methyl red, bromothymol blue, and phenolphthalein disodium salt in the following quantities: 150 mL water, 0.012 g methyl red, 0.060 g bromothymol blue, and 0.050 g phenolphthalein disodium salt. We will then prepare a 0.60 % agarose solution using two different ready-made solutions; the first will be a representation of an unbuffered medium and will consist of 0.9 % saline, the second will be prepared by taking 1 molar phosphate-buffered saline that will act as an example of a buffered medium. Note that PBS consists of saline, potassium chloride, dibasic sodium hydrogen phosphate, and monobasic potassium hydrogen phosphate and has a pH of 7.4. Both solutions need to be diluted in a solution-to-purified water ratio of 5-to-1, since we would like our agarose phantoms to model *in vivo* tissue conductivity of skeletal muscle of about 0.25 S/m[1].

Having prepared the buffered and unbuffered agarose solution, the two solutions should be quickly heated using a microwave almost to the point of boiling, after which (but before pouring into petri dishes) the solutions have to be supplemented with the indicator solution in the ratio of 9-to-1 (medium-to-indicator). Following the addition of the indicator solution and agitation, agarose can be measured out into small petri dishes with a pipette (3 mL per dish) and await hardening (about 10-15 minutes should suffice).

Once hardened, you will deliver to the agarose phantoms either a typical gene electrotransfer (GET) protocol (4 x 5 ms delivered at 1 s^{-1}), or a typical short, biphasic (HFIRE) protocol (5 µs positive/negative phase, 5 µs interphase delay, 500 µs interpulse delay, 200 pulses per train, train repetition frequency 1 s^{-1}, 10 trains in total) using the pulse generator and a pair of needle electrodes. Note the total "on time" of the two protocols is the same – 20 ms. Different amplitudes of the pulses can be used to study the

[1] Skeletal muscle conductivity exhibits a wide range of values that can fall anywhere between 0.04 and 0.8 S/m. We chose 0.25 S/m for the model and experiment as a rough midpoint off that interval (Miklavčič et al. 2006).

effects of lower/higher pulse current (the phantom conductivity is constant) – try experimenting with a few voltages!

You will record the videos of the experiments using the fast camera and subsequently analyse the pH front spatial progression and colour changes (in qualitative terms) by comparing the observed front appearance and migration (at a single chosen voltage, to save time):

- with model results seen earlier during the theoretical introductory part of the lab work for the GET protocol considering the buffered and unbuffered medium, and
- for the two different protocols, i.e., the monophasic GET and biphasic HFIRE as experimentally recorded in the buffered and unbuffered medium.

FURTHER READING:

Cindrič H., Kos B., Miklavčič D. Irreversible electroporation as a novel method for soft tissue ablation: review and challenges in clinical practice. *Zdrav. Vestn.* 90:38-53, 2021.

Kim K.H., An J., Park Y.J., Park J.H., Kim H.B., Yi J.H., Kim H.S. Tissue ablation using irreversible electrolytic electroporation with reduced voltage. *Electronics* 12:2916, 2023.

Li Y., Wu M., Zhao D., Wei Z., Zhong W., Wang X., Liang Z., Li Z. Electroporation on microchips: the harmful effects of pH changes and scaling down. *Sci. Rep.* 5:17817, 2015.

Marino M., Olaiz N., Signori E., Maglietti F., Suárez C., Michinski S., Marshall G. pH fronts and tissue natural buffer interaction in gene electrotransfer protocols. *Electrochimica Acta* 255:463-471, 2017.

Miklavčič D., Pavšelj N., Hart F.X. Electric properties of tissues, in: Akay, M. (Ed.), Wiley Encyclopedia of Biomedical Engineering. John Wiley & Sons, New York, NY, 3578-3589, 2006.

Nilsson E., Berendson J., Fontes E. Development of a dosage method for electrochemical treatment of tumours: a simplified mathematical model. *Bioelectrochem. Bioenerget.* 47:11-18, 1998.

Nilsson E., Fontes E. Mathematical modelling of physicochemical reactions and transport processes occurring around a platinum cathode during the electrochemical treatment of tumours. *Bioelectrochemistry* 53:213-224, 2001.

Perkons N.R., Stein E.J., Nwaezeapu C., Wildenberg J.C., Saleh K., Itkin-Ofer R., Ackerman D., Soulen M.C., Hunt S.J., Nadolski G.J., Gade T.P. Electrolytic ablation enables cancer cell targeting through pH modulation. *Commun. Biol.* 1:48, 2018.

Phillips M., Krishnan H., Raju N., Rubinsky B. Tissue ablation by a synergistic combination of electroporation and electrolysis delivered by a single pulse. *Ann. Biomed. Eng.* 44:3144-3154, 2016.

Potočnik T., Maček Lebar A., Kos B., Reberšek M., Pirc E., Serša G., Miklavčič D. Effect of experimental electrical and biological parameters on gene transfer by electroporation: A systematic review and meta-analysis. *Pharmaceutics* 14:2700, 2022.

Rubinsky L., Guenther E., Mikus P., Stehling M., Rubinsky B. Electrolytic effects during tissue ablation by electroporation. *Technol. Cancer Res. Treat.* 15:95-103, 2016.

Sugrue A., Vaidya V., Witt C., DeSimone C.V., Yasin O., Maor E., Killu A.M., Kapa S., McLeod C.J., Miklavčič D., Asirvatham S.J. Irreversible electroporation for catheter-based cardiac ablation: a systematic review of the preclinical experience. *J. Interv. Card. Electrophysiol.* 55:251-265, 2019.

NOTES & RESULTS

Simultaneous measurement of sarcomere shortening and calcium transients in primary rat cardiomyocytes exposed to electroporation electrical pulses

L15

Vid Jan, Marko Stručić
University of Ljubljana, Faculty of Electrical Engineering

Duration of the experiments: 90 min
Max. number of participants: 4
Location: Cell Culture Laboratory 1
Level: Advanced

PREREQUISITES

Participants should be familiar with Laboratory safety (S1). Basic knowledge of handling with cells is required for this laboratory practice.

THEORETICAL BACKGROUND

Despite a long history of using electric pulses on the cardiac tissue for defibrillation and pacing, effects of high-voltage (supraphysiological) electric pulses at the level of a single cardiomyocyte (or even neurons and excitable cells in general, for that matter), remain relatively unexplored. It is known that during electroporation, cell membrane is damaged and cell homeostasis disrupted. Voltage-gated channels can also get affected, although the consensus on the mechanisms and the consequences is not yet reached. Interestingly, in a recent molecular dynamics study, the voltage sensor area of the voltage-gated channels was shown to be permanently damaged under the influence of high electric fields.
During electroporation, Ca^{2+} enters the cell in an uncontrolled way through the permeabilized membrane. Thus, the precise calcium balance, needed for normal cardiomyocyte function is disrupted. This can lead to undesired and unpredictable side-effects. For example, excitation-contraction coupling (pairing cardiomyocyte depolarization with mechanical contraction) depends largely on Ca^{2+} signalling and disturbances of Ca^{2+} homeostasis can severely impact muscle physiology and give rise to various myopathies and cardiac disorders. Under physiological conditions, cardiomyocytes can efficiently remove the excess intracellular Ca^{2+}, which enters during the action potential plateau phase to prepare for the next cycle. However, with electroporation, the uptake of Ca^{2+} can be much higher than in normal working conditions; moreover, the cell membrane is damaged and does not reseal for minutes after the treatment. Furthermore, ATP, necessary for membrane resealing and operation of pumps, following electroporation leaks out of the cell.
The efficiency of electroporation is influenced by the parameters of the electric field, cell size, geometry, and position, and physiological characteristics of the medium surrounding the cell. Different fluorescent dyes (e.g. Rhod-2, Fluo-4, Fura-2, Fura-3,…) can be employed to investigate the influence of these parameters on electroporation and the same dyes can be used to monitor electroporation.

The aim of this laboratory practice is to monitor the effects of monophasic single electric pulse on Ca^{2+} homeostasis, contractility and recovery of adult rat ventricular cardiomyocytes.

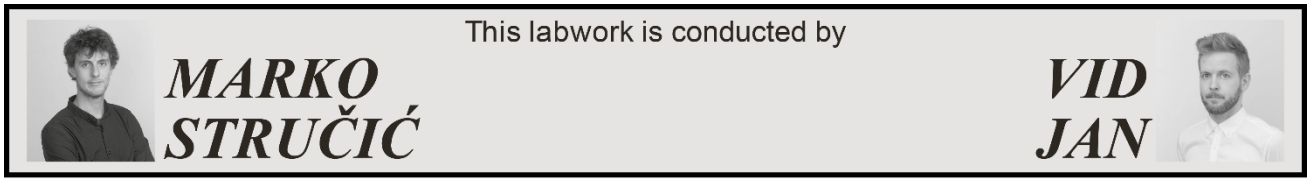

EXPERIMENT

We will simultaneously monitor sarcomere shortenings, i.e., contraction and Ca^{2+} transients of rat cardiomyocytes with IonOptix-upgraded Zeiss Axiovert microscope which applies Fast Fourier Transform to measure sarcomere length while at the same time measuring signal from fluorescent Ca^{2+} sensitive indicator Rhod-2AM. As cardiomyocytes are paced, Ca^{2+} concentrations inside the cells change, due to its importance in action potentials, while supraphysiological electric pulses cause changes in Ca^{2+} concentrations due to perturbations in membrane permeability (due to electroporation). Once Ca^{2+} enters the sarcoplasm of cardiomyocytes, they bind to the dye and change its fluorescence intensity more than 100-fold (Figure 1).

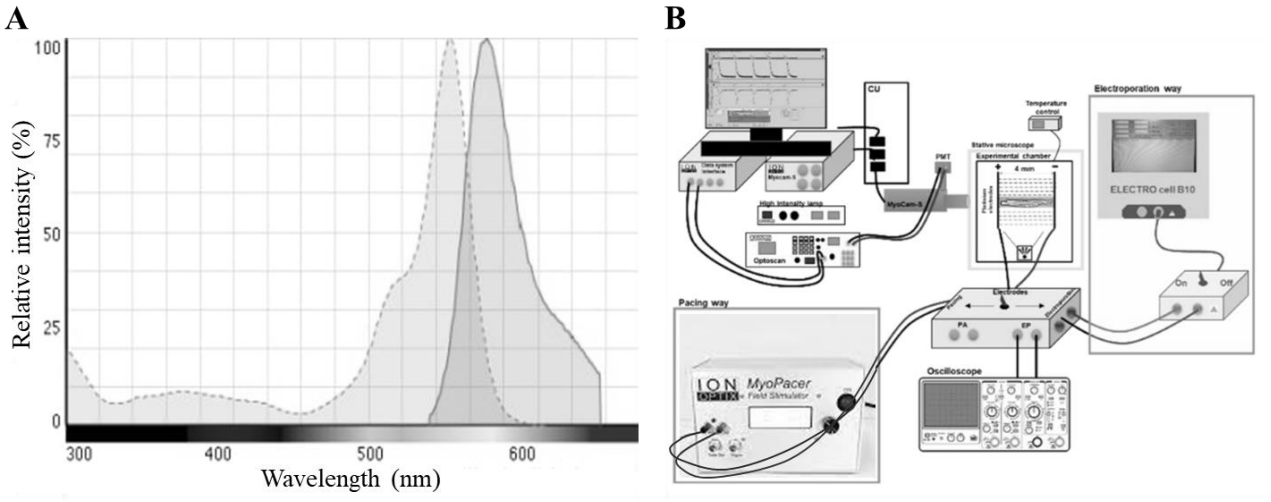

Figure 1: (A) Fluorescence excitation (blue) and emission (red) spectra of Rhod-2 for different concentrations of Ca^{2+} (image from *https://www.thermofisher.com/order/fluorescence-spectraviewer?SID=srch-svtool&UID=14220ca#!/*). (B) Schematic of the experimental setup (adapted from Chaigne, S. et al., 2022).

Protocol: The experiments will be performed on adult rat ventricular cardiomyocytes, isolated from Wistar rats, weighing 250-350 grams. Briefly, on the morning of the experiments adult Wistar rat will be euthanized by anaesthetic isoflurane overdose. After the onset of asphyxia heart will quickly be excised, submerged briefly in cold EGTA solution and then perfused on Langendorff set-up. It will be first perfused with EGTA solution for approximately 5 minutes and then with enzyme solution until the heart will be sufficiently digested. Atria will be removed, while ventricles will be cut in smaller pieces and triturated with a Pasteur pipette for 3 minutes. Cell suspension will then be filtered through a 200 µm nylon mesh filter and resuspended in $CaCl_2$ buffers of increasing Ca^{2+} concentrations until we reach final concentration of 1 mM. Isolated cardiomyocytes will then be pelleted, supernatant will be removed, and the pellet will be resuspended in 199 medium, supplemented with Earle's salts, L-glutamine, 25 mM HEPES, 2.2 g/L $NaHCO_3$, FBS (5 % v/v) and PenStrep. After 60 min of incubation in 199 medium, cardiomyocytes will be washed twice with Tyrode solution (134 mM NaCl, 5 mM KCl, 12 mM HEPES, 1.2 mM $MgSO_4$, 1.2 mM NaH_2PO_4, 11 mM Glucose, 1 M $CaCl_2$, and 5 mM Sodium Pyruvate), after which they will be ready for our measurements. Before measurements, cardiomyocytes will be incubated in Tyrode buffer with 2 µM Rhod-2AM for 20 min at 37 °C (Thermo Fisher Scientific). After the incubation time, cardiomyocytes will be washed with fresh Tyrode to remove excess dye and then seeded on 25 mm square coverslips for imaging.

Insert laminin-coated glass coverslips into IonOptix stimulation chamber on fluorescence microscope (Zeiss Axiovert 200) and use 40xLD objective. Wait 5 min and then start the perfusion of Tyrode buffer at 37 °C. IonOptix MyoCam-S3™ Fast CMOS camera will be used to capture sarcomere shortening while IonOptix photomultiplier tube with be used to capture signals for Rhod-2AM. Measurements will be recorded and processed using IonOptix IonWizard software.

Using a IonOptix MyoPacer Field Stimulator pace cardiomyocytes on the coverslip with bipolar pulses at 1 Hz and 4 ms. IonOptix stimulation chamber is equipped with 2 platinum electrodes (4 mm spacing) and our setup also includes a switch box to alternate between pulses from the IonOptix MyoPacer Field Stimulator for physiological pacing and ELECTRO cell B10 (BetaTech, France) for monopolar supraphysiological pulses. Using a framing adapter, frame a cardiomyocyte that is perpendicular to the electric field (90±10°) and contracts. Measure basal changes in sarcomere length and Ca^{2+} transients (capture at least 10 contractions). Afterwards use ELECTRO cell B10 device and deliver one electric pulse of 100 µs with voltages either 80 or 140 V (200 and 350 V/cm, respectively) while measuring sarcomere length and Ca^{2+} transients. 1 min after 80 or 140 V supraphysiological pulse delivery start pacing the cell again and record sarcomere length and Ca^{2+} transients for the last time (10 contractions). Capture all measurements for 3 cardiomyocytes on one coverslip for 80 V and one coverslip for 140 V. Compare values for sarcomere shortening and Ca^{2+} transients for both 80 V and 140 V (as shown in Figure 2).

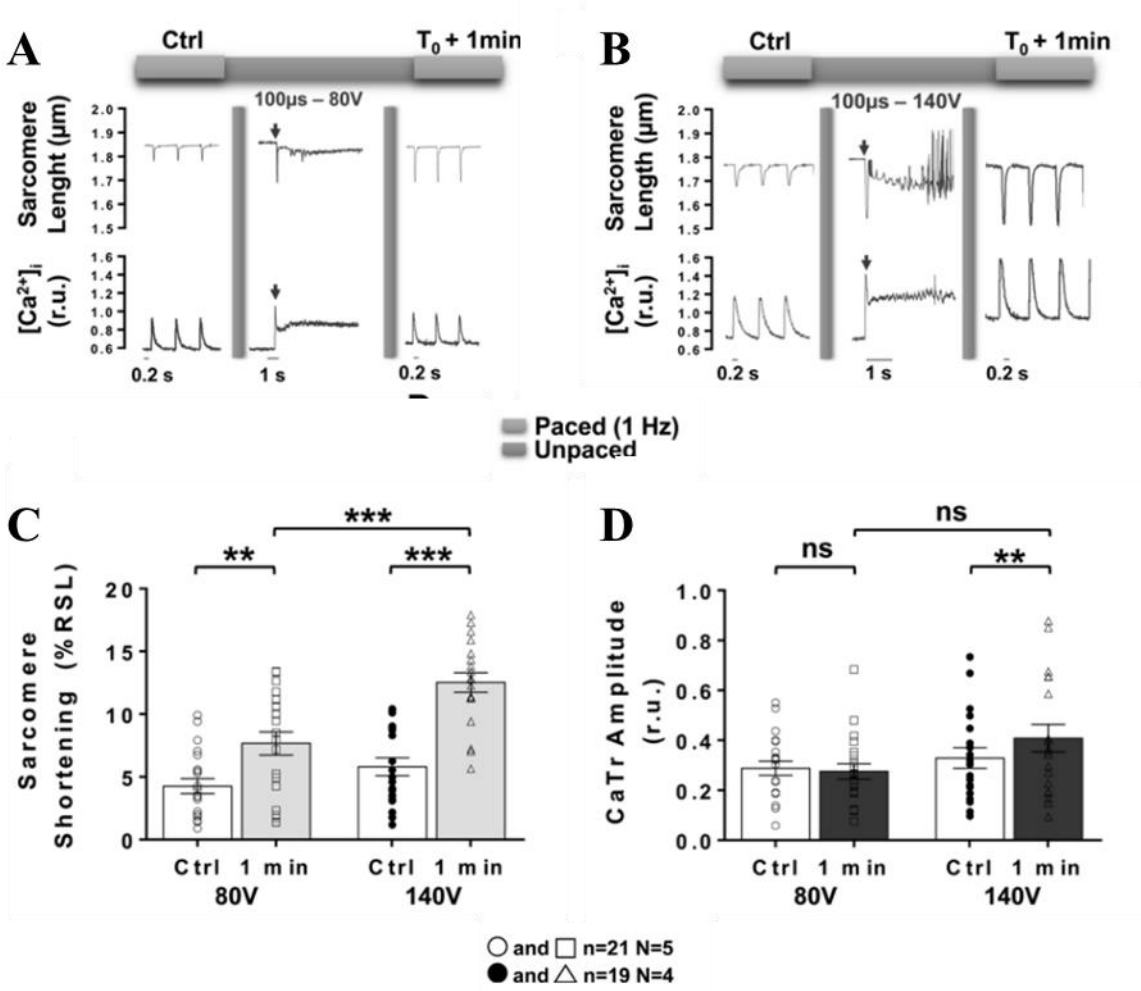

Figure 2: (A-D) Examples of measurements for the effects of 80 and 140 V pulsed electric fields on rat ventricular cardiomyocyte shortening and intracellular Ca^{2+} ($[Ca^{2+}]i$) at 1 minute after application. Representative sarcomere lengths and $[Ca^{2+}]i$ traces obtained from an isolated left ventricular myocytes during baseline (control [Ctrl]) 1 Hz pacing and 1 minute after (T0+1 minute) a 100 µs electric pulse (EP) delivered at (A) low- (80 V) and (B) intermediate-voltage (140 V). (C) Sarcomere shortening, expressed as a percentage of the resting sarcomere length (%RSL) was increased 1 minute after EP with a low- and an intermediate-voltage pulses. (D) Ca^{2+} transient (CaTr) amplitudes expressed in 340:380 ratio units (r.u.), were increased 1 minute after EP with an intermediate but not with a low-voltage pulse. Data are represented as mean±SE of the mean with individual values for each cell. N indicates number of animals; n, number of cells; and ns, not significant. Paired t test: ns, **P<0.01, ***P<0.001. (image from Chaigne, S. et al., 2022).

FURTHER READING:

Rems L., Kasimova M.A., Testa I. Delemotte L. pulsed electric fields can create pores in the voltage sensors of voltage-gated ion channels. *Biophys. J.* 119:190-205, 2020.
Chaigne S., Sigg D.C., Stewart M.T., Hocini M., Batista Napotnik T., Miklavčič D., Bernus O., Benoist D. Reversible and irreversible effects of electroporation on contractility and calcium homeostasis in isolated cardiac ventricular myocytes. *Circ. Arrhythm. Electrophysiol.* 15: e011131, 2022.
Polajzer T., Jarm T. Miklavčič D. Analysis of damage-associated molecular pattern molecules due to electroporation of cells in vitro. *Radiol. Oncol.* 54:317-328, 2020.
Tung L., Tovar O., Neunlist M., Jain S.K., O'Neill R J. Effects of strong electrical shock on cardiac muscle tissuea. *Ann. N. Y. Acad. Sci.* 720:160-175, 1994.
Batista Napotnik T., Miklavčič, D. In vitro electroporation detection methods – An overview. *Bioelectrochemistry* 120:166-182, 2018.
Pucihar G., Kotnik T., Miklavčič D. Measuring the induced membrane voltage with Di-8-ANEPPS. *J. Vis. Exp.* 1659, 2009.
Louch W.E., Sheehan K.A., Wolska B.M. Methods in cardiomyocyte isolation, culture, and gene transfer. *J. Mol. Cell. Cardiol.* 51:288-298, 2011.
Cao L., Manders E., Helmes M. Automatic detection of adult cardiomyocyte for high throughput measurements of calcium and contractility. *PLOS ONE* 16:e0256713, 2021.
Nippert F., Schreckenberg R., Schlüter K.D. Isolation and cultivation of adult rat cardiomyocytes. *J. Vis. Exp.* 56634, 2017.

NOTES & RESULTS

COMPUTER MODELING

Treatment planning for electrochemotherapy and irreversible electroporation: optimization of voltage and electrode position

C1

Anže Županič[1], Bor Kos[2]
[1]National Institute of Biology Ljubljana, Department of Biotechnology and Systems Biology
[2]University of Ljubljana, Faculty of Electrical Engineering

Duration of the experiments: 60 min
Max. number of participants: 6
Location: Laboratory of Biocybernetics
Level: Basic

PREREQUISITES

No specific knowledge is required for this laboratory exercise.

THEORETICAL BACKGROUND

Electrochemotherapy (ECT) is an efficient local treatment of cutaneous and subcutaneous tumors, which combines the delivery of nonpermeant, cytotoxic chemotherapeutics (e.g. bleomycin, cisplatin) and short high-voltage electric pulses. The pulses induce electric fields inside the tissue, thereby increasing cell membrane permeability in tissue (electropermeabilization) to otherwise nonpermeant chemotherapeutics. ECT requires the electric field inside the tumor to be higher than the threshold value needed for reversible electroporation (E_{rev}) while irreversible electroporation (E_{irrev}) in nearby critical structures should be limited. For IRE, the electric field in the entire tumor volume needs to be above the irreversible electroporation threshold. It is not necessary that the whole tumor is electropermeabilized by one pulse or pulse sequence - sometimes a combination of several pulse sequences or a combination of different electrodes is required.

The aim of this laboratory practice is to learn how to use optimization techniques to achieve suitable electric field distribution for electrochemotherapy experimental planning and treatment planning.

EXPERIMENT

A finite element based numerical modeling program package COMSOL Multiphysics version 5.4 (COMSOL AB, Stockholm, Sweden) will be used to optimize voltage between the electrodes and position of the electrodes on a simple 3D model of a spherical subcutaneous tumor and surrounding tissue (Figure 1a). Electrode positions and the applied voltage should be chosen, so that the following objectives are fulfilled:

- For electrochemotherapy: the tumor is permeabilized ($E_{tumor} > E_{rev} = 400\ V/cm$),
- For irreversible electroporation: the tumor is permeabilized above the irreversible threshold ($E_{tumor} > E_{irrev} = 600\ V/cm$),
- the damage to healthy tissue is kept to a minimum.

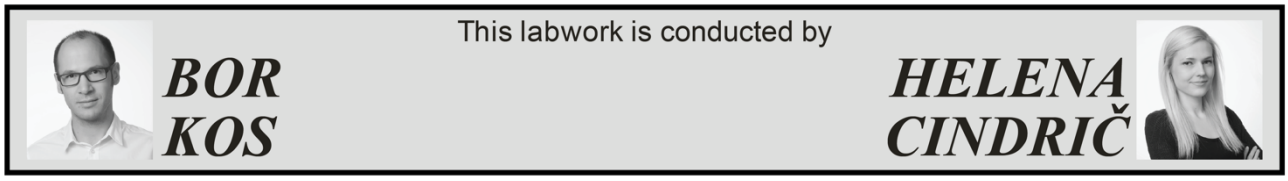

We will calculate the electric field distribution in the model after each change of the electrode placement or voltage. The final goal of this exercise is to achieve 100 % $E_{tumor} > E_{rev}$ (or 100 % $E_{tumor} > E_{irr}$ when planning for IRE) and minimize E_{irr} in healthy tissue.

Protocol: Build the 3-d model by following the lecturer's instructions and take into account your tissue-specific electric properties. Solve the model and evaluate the initial solution. In case, the initial solution is inappropriate (see e.g., Figure 1b), try to improve on the solution by changing electrode positions and voltage between the electrodes. Calculate the electric field distribution in the model after changing the electrode positions or voltage and then determine the coverage of tumor tissue with $E_{tumor} > (E_{rev}$ or $E_{irrev})$ and determine damage to healthy tissue due to irreversible electroporation. Repeat the process, until the quality of your solution reaches the set goals. Compare the results with others, who have used different tissue properties. Use a parametric study to find the lowest voltage which achieves the objective for the selected electrode geometry.

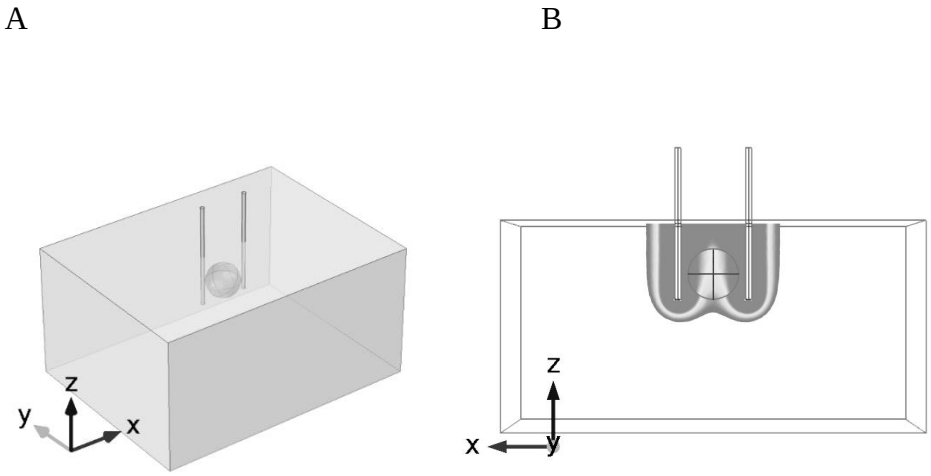

Figure 1: (A) Simple 3D model of tumor and needle electrodes in healthy tissue; (B) electric field over reversible threshold inside the healthy tissue and the tumor.

FURTHER READING:

Miklavčič D., Čorović S., Pucihar G, Pavšelj N. Importance of tumor coverage by sufficiently high local electric field for effective electrochemotherapy. *EJC Supplemen.ts* 4:45-51, 2006.

Čorović S., Županič A., Miklavčič D. Numerical modeling and optimization of electric field distribution in subcutaneous tumor treated with electrochemotherapy using needle electrodes. *IEEE Trans. Plasma Sci.,* 36:1665-1672, 2008.

Županič A., Čorović S., Miklavčič D. Optimization of electrode position and electric pulse amplitude in electrochemotherapy. *Radiol. Oncol.* 42:93-101, 2008.

Edd J.F., Davalos R.V. Mathematical modeling of irreversible electroporation for treatment planning, *Technol. Cancer Res. Treat.* 6:275-286, 2007.

Kos B., Županič A., Kotnik T, Snoj M, Serša G, Miklavčič D. Robustness of treatment planning for electrochemotherapy of deep-seated tumors. *J. Memb. Biol.* 236:147-153, 2010.

Cukjati D., Batiuskaite D., Andre F., Miklavčič D., Mir L. Real time electroporation control for accurate and safe in vivo non-viral gene therapy. *Bioelectrochemistry* 70:501-507, 2007.

NOTES & RESULTS

NOTES & RESULTS

Numerical modeling of thermal effects during irreversible electroporation treatments

C2

Paulo A. Garcia[1], Bor Kos[2]
[1]Virginia Tech – Wake Forest University
[2]University of Ljubljana, Faculty of Electrical Engineering

Duration of the experiment: 90 min
Max. number of participants: 6
Location: Laboratory of Biocybernetics
Level: Advanced

PREREQUISITES

Basic to advanced knowledge of finite element modeling.

THEORETICAL BACKGROUND

Irreversible electroporation (IRE) is a new, safe, and effective minimally invasive ablation modality with the potential to treat many currently unresectable and/or untreatable tumors. The non-thermal mode of cell death in IRE is unique in that it does not rely on thermal changes from Joule heating to kill tumor cells thus allowing for successful treatment even in close proximity to critical structures and without being affected by the heat sink effect. Accurate modeling of the electrical and thermal responses in tissue is important to achieve complete coverage of the tumor and ensure that the thermal changes during a procedure do not generate thermal damage, especially in critical structures (e.g. bile ducts, nerves and sensitive blood vessels).

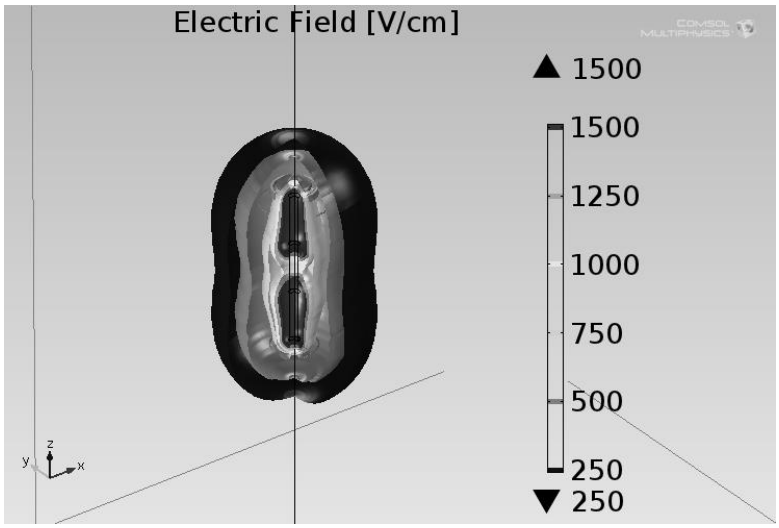

Figure 2: Electric Field distribution resulting from a bipolar electrode with an applied voltage of 1250 V.

The temperature distribution (T) within the tissue will be obtained by transiently solving a modified heat conduction equation with the inclusion of the Joule heating source term $Q = \sigma|\nabla\varphi|^2$

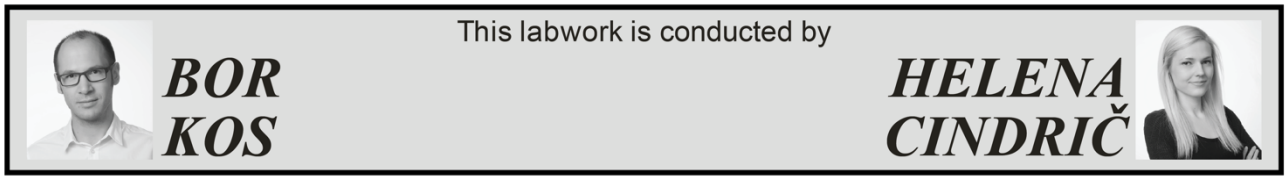

$$\rho C \frac{\partial T}{\partial t} = \nabla \cdot (k \nabla T) + Q \qquad (1)$$

where σ is the electrical conductivity, φ the electric potential, k is the thermal conductivity, C is the specific heat capacity, and ρ is the density of the tissue. At each time step, the current density and electric field distribution are determined and updated in the Joule heating term to capture the electrical conductivity changes in liver tissue from electroporation and temperature.

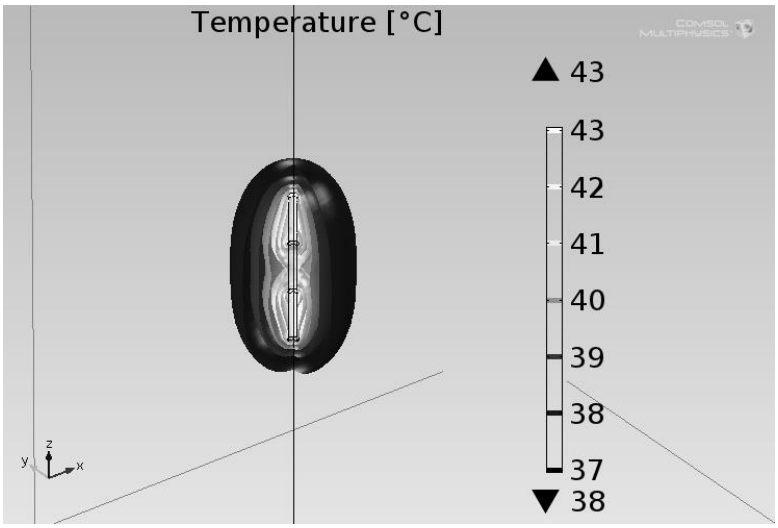

Figure 3: Temperature distribution after a ninety 100-µs pulse IRE treatment in liver tissue at 1 pulse per second.

Thermal damage is a process that depends on temperature and time. If the exposure is long, damage can occur at temperatures as low as 42°C, while 50°C is generally chosen as the target temperature for instantaneous damage. The damage can be calculated based on the temperatures to assess whether a particular set of pulse parameters and electrode configuration will induce thermal damage in superposition with IRE. The thermal damage will be quantified using the Arrhenius rate equation given by:

$$\Omega(t) = \int_{t=0}^{t=\tau} \zeta \cdot e^{\frac{-E_a}{R \cdot T(t)}} dt \qquad (2)$$

where R is the universal gas constant, 8.314 J/(mol·K); ζ is the pre-exponential factor, 7.39×10^{39} s^{-1}, a measure of the effective collision frequency between reacting molecules in bimolecular reactions; E_a the activation energy barrier that molecules overcome to transform from their "native state" to the "damaged state", 2.577×10^5 J/mol for liver tissue. It is important to note that the pre-exponential factor and activation energy are tissue specific parameters that describe different modes of thermal damage such as microvascular blood flow stasis, cell death, and protein coagulation. In terms of finite element modeling of thermal damage, an integral value $\Omega(t) = 1$ corresponds to a 63% probability of cell death and an integral value $\Omega(t) = 4.6$ corresponds to 99% probability of cell death due to thermal effects. In order to convert the damage integral to a probability of cell death, $P(\%)$, we will use:

$$P(\%) = 100 \cdot \left(1 - e^{-\Omega(t)}\right)$$

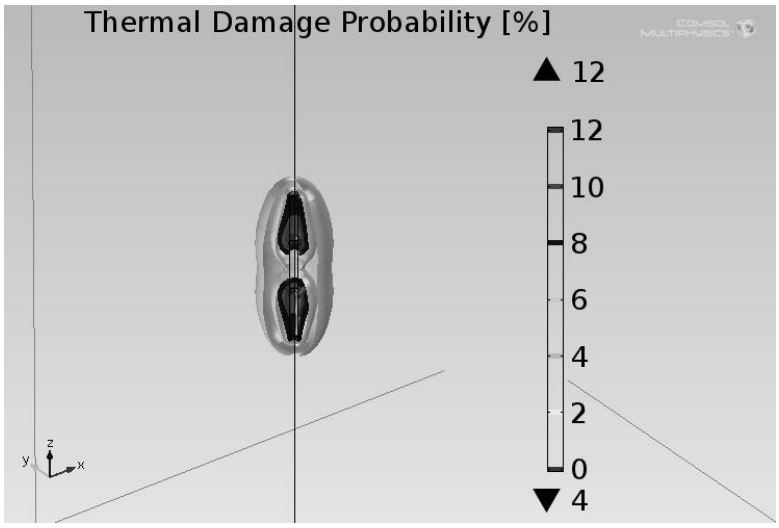

Figure 4: Thermal damage probability of cell death due to excessive thermal effects as a result of Joule heating.

The aim of this laboratory practice is to get familiar with the numerical simulation tools needed for capturing the electrical and thermal responses during a ninety 100-µs pulse IRE. We will accomplish this by coupling the Laplace, Heat Conduction, and Arrhenius equations using COMSOL Multiphysics 5.4 (Comsol AB, Stockholm, Sweden) to determine the IRE zones of ablation and evaluate if the increase in temperature due to Joule heating due to the pulses generates any potential thermal damage.

EXPERIMENT

In this exercise we will compare the effect of a static, σ_0, and dynamic, $\sigma(E)$, electrical conductivity functions in the resulting electrical and thermal effects during an entire IRE protocol in liver tissue. Initially we will determine the volume of tissue affected by IRE from the electric field distributions. We will then evaluate the temperature increase in liver tissue as a result of the Joule heating and determine if there was a probability of cell death due to thermal damage with the given IRE protocols employed. This exercise will provide the participants with accurate predictions of all treatment associated effects which is a necessity toward the development and implementation of optimized treatment protocols.

Specifically:
1) Simulate the electric field distribution using a static conductivity and 1000 V, 1500 V, and 2000 V.
2) Simulate the electric field distribution using a dynamic conductivity and 1000 V and 1500 V.
3) Include the Heat Conduction Equation by coupling with the Laplace Equation via Joule Heating.
4) Explore the resulting temperature distributions as a function of pulse number and frequency.
5) Incorporate the Arrhenius equation to assess potential thermal damage from the Joule Heating.
6) Investigate the effect of pulse frequency (1 Hz, 10 Hz, and 100 Hz) for ninety 100-µs pulses.

FURTHER READING:

Davalos RV, Rubinsky B, Mir LM. Theoretical analysis of the thermal effects during in vivo tissue electroporation. *Bioelectrochemistry* 61(1-2): 99-107, 2003

Chang, IA and Nguyen, UD., Thermal modeling of lesion growth with radiofrequency ablation devices. *Biomed Eng Online*, 3(1): 27, 2004

Davalos, R.V. and B. Rubinsky, Temperature considerations during irreversible electroporation. *International Journal of Heat and Mass Transfer*, 51(23-24): 5617-5622, 2008

Pavšelj N and Miklavčič D, Numerical modeling in electroporation-based biomedical applications. *Radiology and Oncology*, 42(3): 159-168, 2008

Lacković I, Magjarević R, Miklavčič D. Three-dimensional finite-element analysis of joule heating in electrochemotherapy and in vivo gene electrotransfer. *IEEE T. Diel. El. Insul.* 15: 1338-1347, 2009

Garcia, PA, et al., A Parametric Study Delineating Irreversible Electroporation from Thermal Damage Based on a Minimally Invasive Intracranial Procedure. *Biomed Eng Online*, 10(1): 34, 2010

Pavšelj N, Miklavčič D. Resistive heating and electropermeabilization of skin tissue during in vivo electroporation: A coupled nonlinear finite element model. *International Journal of Heat and Mass Transfer* 54: 2294-2302, 2011

NOTES & RESULTS

Molecular dynamics simulations of membrane electroporation C3

Mounir Tarek
CNRS- Université de Lorrains, Nancy France
Europeen Laboratory EBAM

Duration of the experiments: 90 min
Max. number of participants: 18
Location: Computer room (P18-A2)
Level: Basic

PREREQUISITES

No specific knowledge is required for this laboratory practice.

THEORETICAL BACKGROUND

The application of high electric fields to cells or tissues permeabilizes the cell membrane and is thought to produce aqueous-filled pores in the lipid bilayer. Electroporation is witnessed when the lipid membrane is subject to transmembrane voltages (TMV) of the order of few hundred millivolts, which results from the application of electrical pulses on a microsecond to millisecond time scale

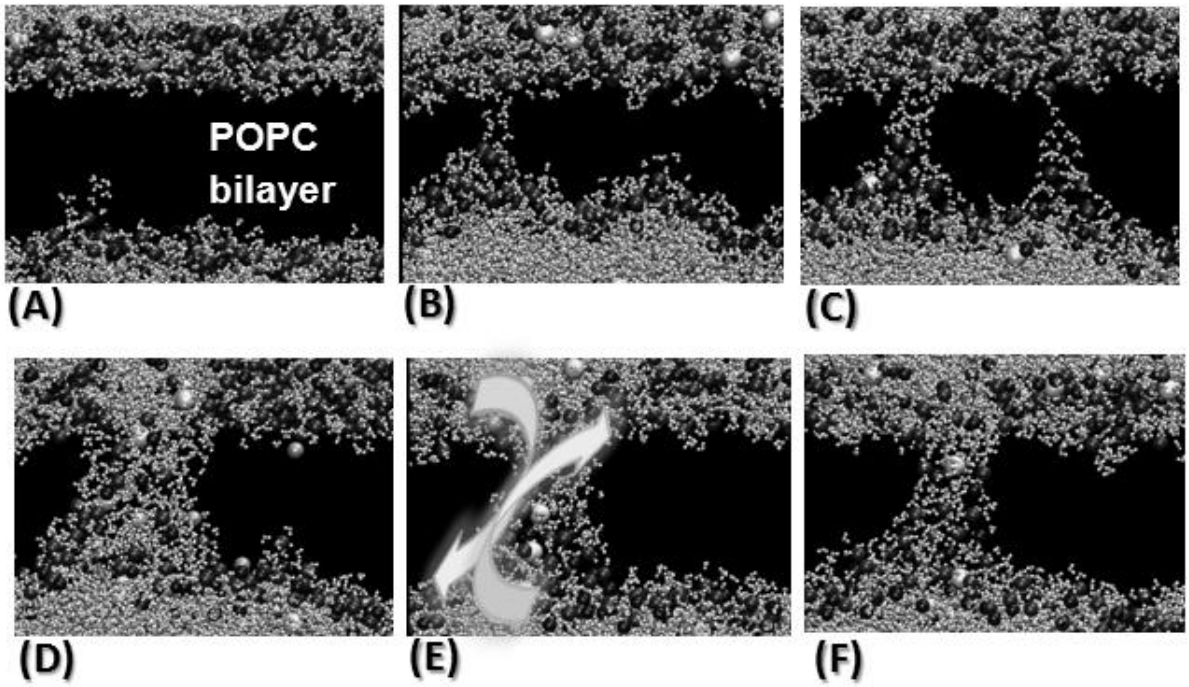

Figure 1: Configurations from the MD simulation for a large POPC subject to a transverse electric field (A) Bilayer at equilibrium. (B-C) Formation of water wires at the initial stage of the electroporation process (D-F) Formation at a later stage of large water pores that conduct ions across the membrane and that are stabilized by lipid head-group (yellow cyan). (Delemotte and Tarek. *J. Membr. Biol.* 2012).

This labwork is conducted by

MOUNIR TAREK

which are sufficient to produce a transient trans-membrane potential and an electrical field across the membrane of the order of ~ 10^8 V/m. This process is believed to involve (1) charging of the membrane due to ion flow, (2) rearrangement of the molecular structure of the membrane, (3) formation of pores, which perforate the membrane and are filled by water molecules (so-called aqueous, or hydrophilic, pores), (4) an increase in ionic and molecular transport through these pores, and, under appropriate conditions, membrane integrity recovery when the external field stress is removed.

Molecular Dynamics (**MD**) simulations belong to a set of computational methods in which the dynamical behaviour of an ensemble of atoms or molecules, interacting via approximations of physical pair potentials, is determined from the resolution of the equation of motions. MD simulations enable ones to investigate the molecular processes affecting the atomic level organization of membranes when these are submitted to voltage gradient of magnitude similar to those applied during electropulsation. The aim of this practical exercise is to characterize from MD simulations trajectories the electrostatic properties of membranes subject to a transmembrane potential (0 to 2 V).

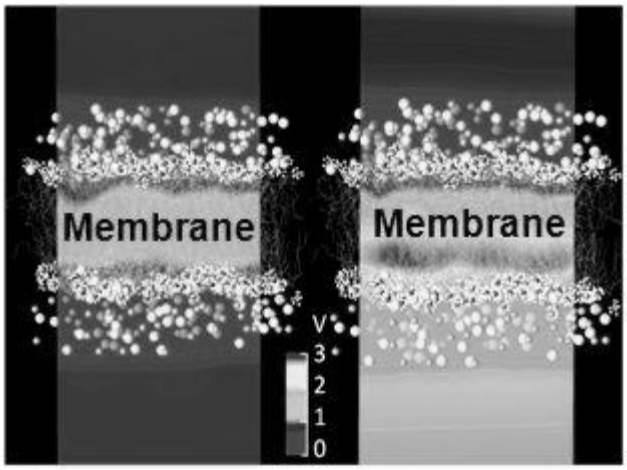

Figure 2: Electrostatic potential maps generated from the MD simulations of a POPC lipid bilayer (acyl chains, green; head groups, white) surrounded by electrolyte baths at 1 M NaCl (Na+ yellow, Cl- green, water not shown) terminated by an air/water interface. Left: net charge imbalance Q = 0 e (TMV=0 mV). Right: Q = 6 e (TMV=2 V).

The aim of this laboratory practice is to get familiar with the tools for molecular dynamics, possibilities to set on models and graphical presentation of atomistic models.

EXPERIMENT

Due to the limited time and large resources needed to generate MD trajectories of membranes, the latter will be provided to the students. The simulations concern pure planar phospholipid bilayers (membrane constituents) and water described at the atomic level. A set of long trajectories spanning few nanoseconds generated with or without a transmembrane voltage induced by unbalanced ionic concentrations in the extracellular and intracellular will be provided. The students will (1) determine the distribution of potential and electric field in model membrane bilayers (2) measure the membrane capacitance, (3) visualize at the molecular level the formation of membrane pores under the influence of a transmembrane voltage, and measure the intrinsic conductance of such pores.

FURTHER READING:

Tarek M. Membrane electroporation: A molecular dynamics study *Biophys. J.* 88:4045-4053, 2005.
Dehez F., Tarek M., Chipot C. Energetics of ion transport in a peptide nanotube *J. Phys. Chem. B* 111:10633-10635, 2007.
Andrey A.G., Jamshed A., Vattulainen I. Defect-mediated trafficking across cell membranes: insights from in silico modeling, *Chem. Rev.* 110:6077-6103, 2010.
Delemotte L., Tarek, M. Molecular dynamics simulations of membrane electroporation. *J. Membr. Biol.* 245/9:531-543, 2012.
Polak A., Tarek M., Tomšič M., Valant J., Poklar Ulrih N., Jamnik A., Kramar P., Miklavčič D. Electroporation of archaeal lipid membranes using MD simulations. *Bioelectrochemistry* 100:18-26, 2014.

NOTES & RESULTS

HARDWARE
DEVELOPMENT AND MEASUREMENT

Measurement of electroporation pulses with oscilloscope, and voltage and current probes

H1

Matej Reberšek
University of Ljubljana, Faculty of Electrical Engineering

Duration of the experiment: 60 min
Max. number of participants: 10
Location: Laboratory of Biocybernetics
Level: Basic

PREREQUISITES

No specific knowledge is required for this laboratory exercise.

THEORETICAL BACKGROUND

Electroporation is initiated by the delivery of electrical pulses to biological cells. Electrical pulses may vary in pulse parameters such as pulse shape, amplitude, duration and polarity. We may deliver different number of pulses, use combination of different pulses or vary pulse repetition rates. We also may deliver pulses in bursts or in different directions relative to the cell. The process of the electroporation is strongly dependent on the pulse parameters of the delivered electrical pulses. In order to control the process of the electroporation and to exactly specify the experimental method, and thus enable the reproduction of experiments under the same conditions, we should exactly determine and describe these electrical parameters. When reporting electroporation methods we should: 1) describe exactly how the electric pulses were measured; 2) provide time-domain waveforms of the electric pulse at the electrodes; and 3) calculate or otherwise determine to what electric field the cells were exposed to.

The aim of this laboratory practice is to learn how to use standard measurement equipment to measure or monitor the delivery of electroporation pulses. During the laboratory practice we will also learn what are the electrical parameters of electroporation pulses, what should we report in our studies concerning the measurement and what are some possible complications during the pulse delivery or measurement.

EXPERIMENT

Oscilloscope, and voltage and current probes will be used to monitor the delivery of the electroporation pulses to the load. We will first learn how to set the three main controls (vertical, horizontal and trigger) for adequate data acquisition. We will learn how to use measuring tool to automatically measure the pulse parameters, how to use sequencing to measure several pulses with low pulse repetition rate and how to set acquire to measure bursts of pulses.

This labwork is conducted by

MATEJ REBERŠEK

We will monitor the delivery of microsecond and nanosecond pulses to the load. Learn how to detect disconnection and improper impedance matching of the load, and how a point of measuring and improper wiring may affect the measuring and the delivery of the pulse.

Eight different commercial available electroporators: BTX (GEMINI X^2), IGEA (Cliniporator Vitae, GeneDrive), Invitrogen (Neon), Intracel (TSS20), Leroy(Beta-tech B10), Pulse Biosciences (CellFX), Societe Jouan (JOUAN) will be presented during the exercise and available for demonstrations at the end of the exercise. Additionally, also custom made prototype electroporaotrs designed and developed in our laboratory will be on display.

FURTHER READING:

Batista Napotnik T., Reberšek M., Vernier P.T., Mali B., Miklavčič D. Effects of high voltage nanosecond electric pulses on eukaryotic cells (in vitro): A systematic review. *Bioelectrochemistry* 110:1-12, 2016.
Reberšek M., Miklavčič D., Bertacchini C., Sack M. Cell membrane electroporation –Part 3: The equipment. *IEEE Electr. Insul. M.* 30:8-18, 2014.
Silve A., Vézinet R., Mir L.M. Nanosecond-duration electric pulse delivery *in vitro* and *in vivo*: experimental considerations. *IEEE Trans. Instrum. Meas.* 61:1945-1954, 2012.
Kenaan M., El Amari S., Silve A., Merla C., Mir L.M., Couderc V., Arnaud-Cormos D., Leveque P. Characterization of a 50-Ω exposure setup for high-voltage nanosecond pulsed electric field bioexperiments. *IEEE T. Biomed. Eng*. 58:207-214, 2011.
Reberšek M., Miklavčič D. Concepts of electroporation pulse generation and overview of electric pulse generators for cell and tissue electroporation. In *Advanced Electroporation Techniques in Biology and Medicine, CRC Press*, 17:341-352, 2010.
Silve A., Villemejane J., Joubert V., Ivorra A., Mir L.M. Nanosecond pulsed electric field delivery to biological samples: difficulties and potential solutions. In *Advanced Electroporation Techniques in Biology and Medicine, CRC Press*, 18: 353-368, 2010.

NOTES & RESULTS

Development of pulsed power generators for electroporation H2

Matej Reberšek, Eva Pirc
University of Ljubljana, Faculty of Electrical Engineering

Duration of the experiment: 60 min
Max. number of participants: 4
Location: Laboratory for Physiological Measurements
Level: Advanced (Electrical Engineer)

PREREQUISITES

Basic to advanced knowledge of electrical engineering.

THEORETICAL BACKGROUND

Electroporation is initiated by the delivery of electrical pulses to biological cells. To generate electrical pulses for electroporation applications a pulsed power generator is required. Pulsed power generators operate in two phases: a charge and a discharge phase. During the charge phase, energy is accumulated over a long period of time in an energy storage element such as capacitor. In the discharge phase, stored energy is quickly released into the load. Several different concepts are used to generate electroporation pulses. The most common method of generating micro- and millisecond electroporation pulses is a square wave pulse generator, in which an on/off switch is used to connect and disconnect capacitor to the load. To generate nanosecond square wave electroporation pulses pulse forming networks or lines are used because high-voltage power switches cannot turn off in nanoseconds.

The aim of this laboratory practice is to learn how to develop milli-, micro- and nanosecond square wave pulse generators. During the laboratory practice we will learn how to choose or calculate the values of the electrical components for a given load and pulse duration.

EXPERIMENT

We will design and assemble two pulse generators: a square wave pulse generator and a Blumlein generator. The square wave pulse generator will enable generation of up to 1 kV micro- and millisecond electroporation pulses. And the Blumlein generator will enable generation of up to 1 kV nanosecond pulses. The output signals of the generators will be measured by oscilloscope, and voltage and current probes.

Square wave pulse generator: We will assemble this generator (Figure 1) by using: a high voltage power supply (V), high voltage capacitor (C), MOSFET switch (S), MOSFET driver (MD) and function generator (FG).

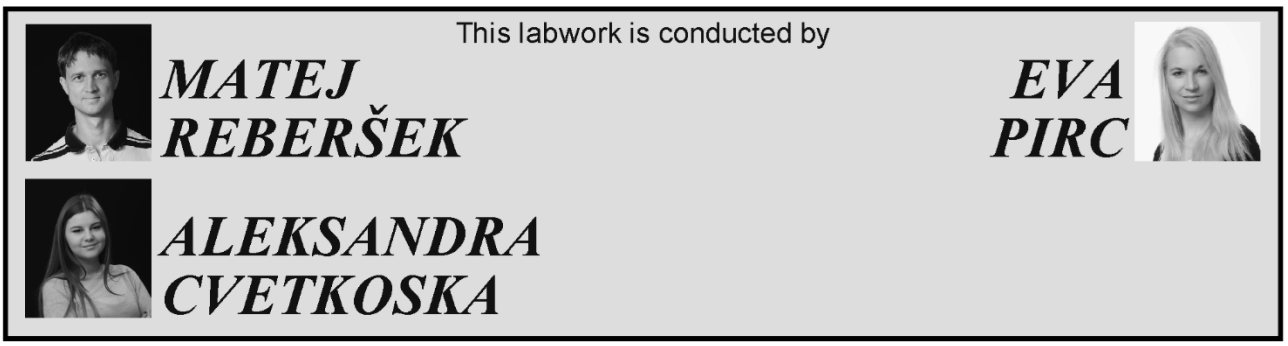

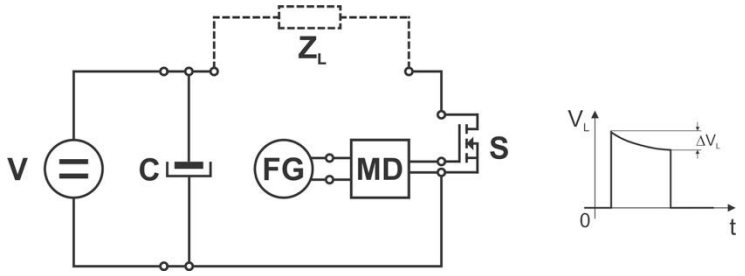

Figure 1. Schematics of the square wave pulse generator and its typical output waveform on load (Z_L).

To power the generator, we will use high voltage DC power supply MCP 350-1250 (FUG, Germany). To store enough energy in the capacitor for the pulse generation, we will calculate its minimal capacitance (equation 1). MOSFET switch will be chosen from the datasheets considering the pulse maximal output voltage and current, and rise, fall and turn off delay time. We will use 4422 (Microchip, USA) MOSFET driver circuit to drive the MOSFET switch and a function generator (HP, USA) to generate a control signal.

$$i_C = C\frac{dV_C}{dt};\ \ i_L = \frac{V_L}{Z_L} \xrightarrow{i_C=i_L;\ V=V_C=V_L;\ dV=\Delta V;\ dt=N\cdot t_P} C = \frac{N\cdot t_P}{\frac{\Delta V}{V}Z_L} \quad (1)$$

We will assemble the square wave pulse generator in four steps, by gradually increasing the requirements for pulse parameters and load (Table 1). We will vary pulse number (N), pulse duration (t_P), relative voltage drop ($\Delta V/V$) and resistance of the load (Z_L). In the first step, we will assemble the generator for one short (10 µs) fully square (1%) pulse on high resistive (1 kΩ) load. In the second step, we will lower the resistance of the load and observe the operation of MOSFET switch and output pulse waveform. In the third step, we will improve the pulse waveform. And in the final step, we will improve the pulse waveform for prolonged pulse duration and number of pulses.

Table 1. Parameters of the pulses that will be generated and resistance of the loads that will be used in specific assembly step.

Step	N	t_P [µs]	$\Delta V/V$ [%]	Z_L [Ω]	C [µF]	S
1	1	10	1	1000		
2	1	10		50	1	
3	1	10	1	50		
4	8	100	5	50		

Blumlein generator: We will assemble this generator (Figure 2) by using: a high voltage power supply (V), resistor (R), transmission lines (T_1 and T_2), radiofrequency MOSFET switch (S), MOSFET driver (MD) and function generator (FG).

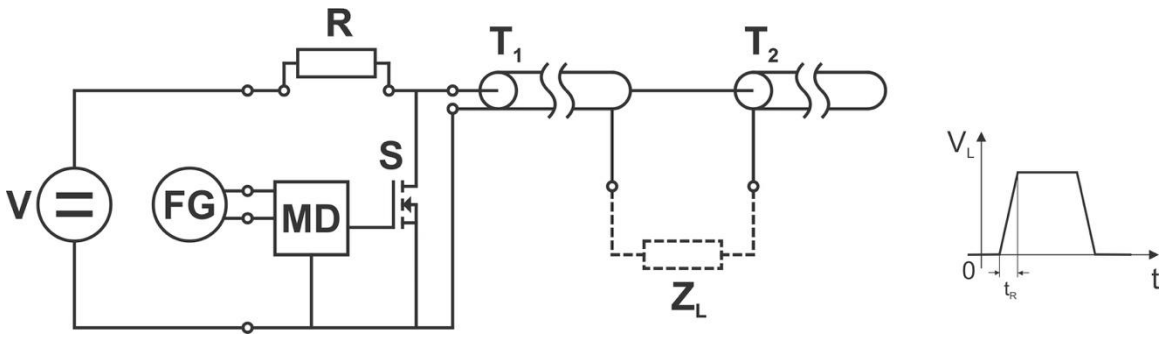

Figure 2. Schematics of the Blumlein generator and its typical output waveform on load (Z_L).

To power the generator, we will use high voltage DC power supply MCP 350-1250 (FUG, Germany). High-voltage and high-impedance resistor will be used to charge the transmission lines. The length of the transmission lines will be calculated (Equation 2) by propagation velocity (v_P) of the signal in transmission line. High-voltage, high- frequency and high-current MOSFET switch (IXYS, USA) will be used to quickly discharge the transmission lines. We will use 4422 (Microchip, USA) MOSFET driver circuit to drive the MOSFET switch and a function generator (HP, USA) to generate control signal.

$$v_P = \frac{1}{\sqrt{\varepsilon \cdot \mu}} \overset{\mu_r=1}{\Longrightarrow} \frac{c}{\sqrt{\varepsilon_r}} \overset{polyethylene}{\Longrightarrow} \frac{3 \cdot 10^8 \frac{m}{s}}{\sqrt{2.25}} = 0.2 \frac{m}{ns}; \quad l = \frac{v_P \cdot t_P}{2} \tag{2}$$

The Blumlein generator will be assembled to generate 1 kV, 20 ns square wave pulses on 100 Ω load.

FURTHER READING:

Reberšek M., Miklavčič D., Bertacchini C., Sack M. Cell membrane electroporation –Part 3: The equipment. *IEEE Electr. Insul. M.* 30:8-18, 2014.
Reberšek M., Miklavčič D. Advantages and disadvantages of different concepts of electroporation pulse generation. *Automatika (Zagreb)*, 52:12-19, 2011.
Reberšek M., Miklavčič D. Concepts of electroporation pulse generation and overview of electric pulse generators for cell and tissue electroporation. In *Advanced Electroporation Techniques in Biology and Medicine*, *CRC Press*, 17:341-352, 2010.
Kolb J.F. Generation of ultrashort pulse. In *Advanced Electroporation Techniques in Biology and Medicine*, *CRC Press*, 17:341-352, 2010.
Smith P.W. Transient electronics: pulsed circuit technology. *Wiley*, 2002.

NOTES & RESULTS

E-LEARNING

Electroporation of cells and tissues - interactive e-learning course E1

Selma Čorović, Samo Mahnič-Kalamiza
University of Ljubljana, Faculty of electrical engineering

Duration of the experiment: app. 90 min
Max. number of participants: 18
Location: Computer room (P9-B0)
Level: Basic

PREREQUISITES

No specific knowledge is required for this laboratory practice.

The aim of this laboratory practice is to provide the participants with basic knowledge on local electric field distribution in cells and tissues exposed to high voltage electric pulses (i.e. electroporation pulses) by means of interactive e-learning course content. The e-learning content is based on the available knowledge from the scientific literature.

PROTOCOL OF THE E-LEARNING COURSE

The participants will be gathered in a computer-computer classroom providing each participant with a computer. A short test will be given to establish the baseline knowledge before the e-learning course.
Within the first part of the e-learning course we will bring together the educational material on basic mechanisms underlying electroporation process on the levels of cell membrane, cell and tissues as a composite of cells (Figure 1).

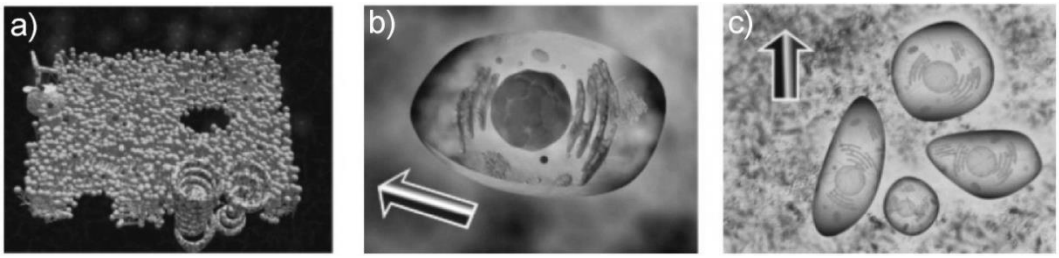

Figure 1: Introduction of small molecules (blue molecules) through a cell membrane (a) into an electroporated cell (b) and into the successfully electroporated cells within an exposed tissue (c) (Čorović et al., 2009).

Within the second part of the course we will provide basic knowledge on important parameters of local electric field needed for efficient cells and tissue electroporation, such as: electrode geometry (needle or plate electrodes as illustrated in Figure 2, electrode position with respect to the target tissue and its surrounding the tissues (Figure 3), the contact surface between the electrode and the tissue, the voltage applied to the electrodes and electroporation threshold values. This part of the e-learning course content will be provided by an interactive module we developed in order to visualize the local electric field distribution in 2D and 3D dimensional tissue models.

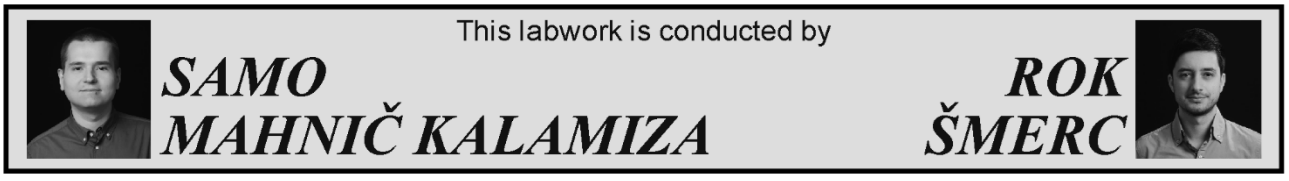

The objective of this module is to provide:
- local electric field visualization in cutaneous (protruding tumors) and subcutaneous tumors (tumors more deeply seeded in the tissue);
- guideline on how to overcome a highly resistive skin tissue in order to permeabilize more conductive underlying tissues and
- visualization and calculation of successfully electroporated volume of the target tissue and its surrounding tissue (i.e. the treated tissue volume exposed to the electric field between reversible and irreversible electroporation threshold value $E_{rev} \leq E < E_{irrev}$) with respect to the selected parameters such as: number and position of electrodes, applied voltage on the electrodes.

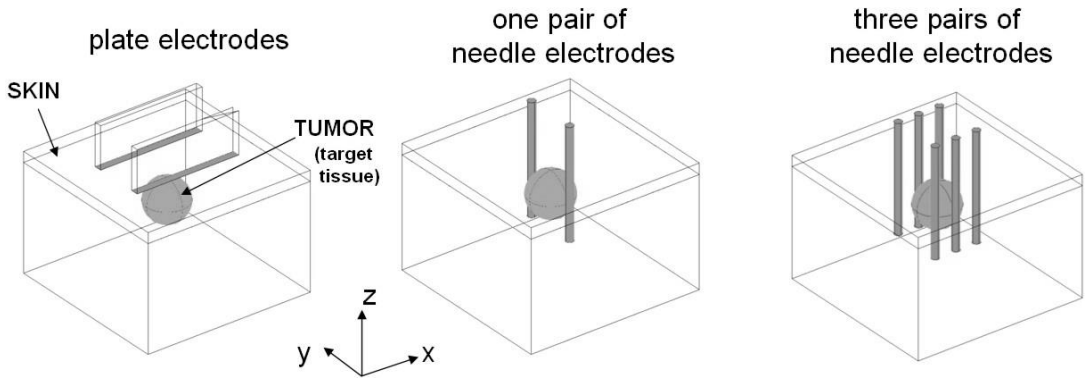

Figure 2: Plate electrodes vs. needle electrodes with respect to the target tissue (e.g. tumor tissue).

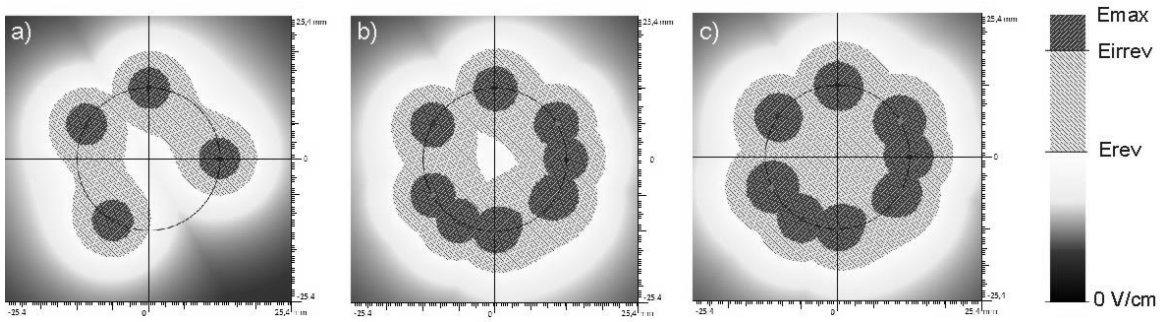

Figure 3: Electric field distribution within the tumor (inside the circle) and within its surrounding tissue (outside the circle) obtained with three different selection of parameters (number and position of electrodes and voltage applied): (a) 4 electrodes, (b) 8 electrodes and (c) 8 electrodes with increased voltage on electrodes so that the entire volume of tumor is exposed to the $E_{rev} \leq E < E_{irrev}$.

After the e-learning course the pedagogical efficiency of presented educational content and the e-learning application usability will be evaluated.

FURTHER READING:

Čorović S., Pavlin M., Miklavčič D. Analytical and numerical quantification and comparison of the local electric field in the tissue for different electrode configurations. *Biomed. Eng. Online* 6:37, 2007.
Serša G., Miklavcic D. Electrochemotherapy of tumours (Video Article). *J. Visual Exp.* 22:1038, 2008.
Čorović S., Županič A., Miklavčič D. Numerical modeling and optimization of electric field distribution in subcutaneous tumor treated with electrochemotherapy using needle electrodes. *IEEE T. Plasma Sci.* 36:1665-1672, 2008.
Čorović S., Bešter J., Miklavčič D. An e-learning application on electrochemotherapy. *Biomed. Eng. Online* 8:26, 2009.
Čorović S., Županič A., Kranjc S., Al Sakere B., Leroy-Willig A., Mir L.M., Miklavčič D. The influence of skeletal muscle anisotropy on electroporation: in vivo study and numerical modeling. *Med. Biol. Eng. Comput.* 48:637-648, 2010.
Edhemovic I., Gadzijev E.M., Brecelj E., Miklavčič D., Kos B., Županič A., Mali B., Jarm T., Pavliha D., Marcan M., Gasljevič G., Gorjup V., Mušič M., Pečnik Vavpotič T., Čemazar M., Snoj M., Serša G. Electrochemotherapy: A new technological approach in treatment of metastases in the liver. *Technol Cancer Res Treat* 10:475-485, 2011.
Bergues Pupo A.E., Reyes J.B., Bergues Cabrales L.E., Bergues Cabrales J.M. Analitical and numerical quantification of the potential and electric field in the tumor tissue for different conic sections. *Biomed. Eng. Online* 10:85, 2011.
Neal R.E. II, Garcia P.A., Robertson J.L., Davalos R.V. Experimental characterization and numerical modeling of tissue electrical conductivity during pulsed electric fields for irreversible electroporation treatment planning. *IEEE T. Biomed. Eng.* 59:1077-1085, 2012.
Čorović S., Mir L.M., Miklavčič D. In vivo muscle electroporation threshold determination: realistic numerical models and in vivo experiments. *J. Memb. Biol.* 245:509-520, 2012.
Essone Mezeme M., Pucihar G., Pavlin M., Brosseau C., Miklavčič D. A numerical analysis of multicellular environment for modeling tissue electroporation. *Appl. Phys. Lett.* 100:143701, 2012.
Mahnič-Kalamiza S., Kotnik T., Miklavčič D. Educational application for visualization and analysis of electric field strength in multiple electrode electroporation. *BMC Med. Educ.* 12:102, 2012.
Čorović S., Lacković I., Šuštarič P., Šuštar T., Rodič T., Miklavčič D. Modeling of electric field distribution in tissues during electroporation. *Biomed. Eng. Online* 12:16, 2013.

NOTES & RESULTS

NOTES & RESULTS

Faculty members

Damijan Miklavčič
University of Ljubljana, Faculty of Electrical Engineering,
Tržaška 25, SI-1000 Ljubljana, Slovenia
E-mail: damijan.miklavcic@fe.uni-lj.si

Lluis M. Mir
Université Paris-Saclay, CNRS, Institut Gustave Roussy, Metabolic and systemic aspects of oncogenesis (METSY),
114 rue Edouard Vaillant, F-94805 Villejuif Cédex, France
E-mail: luis.mir@cnrs.fr

Marie-Pierre Rols
Institute of Pharmacology and Structural Biology, CNRS - University of Toulouse III,
IPBS UMR 5089, 205, route de Narbonne, 31077 Toulouse, France
E-mail: rols@ipbs.fr

Gregor Serša
Institute of Oncology,
Zaloška 2, SI-1000 Ljubljana, Slovenia
E-mail: gsersa@onko-i.si

Mounir Tarek
Theoretical Physics and Chemistry Laboratory, Université de Lorraine,
CNRS, LPCT, F-54000 Nancy
E-mail: mounir.tarek@univ-lorraine.fr

P. Thomas Vernier
Frank Reidy Research Center for Bioelectrics, Old Dominion University,
4211 Monarch Way, Norfolk, VA 23508, USA
E-mail: pvernier@odu.edu

Julie Gehl
University of Copenhagen, Department of Clinical Medicine,
Blegdamsvej 3, 2200 København N Denmark
E-mail: kgeh@regionsjaelland.dk

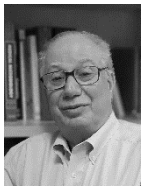

Richard Heller
Department of Medical Engineering, College of Engineering and Morsani College of Medicine
University of South Florida
12901 Bruce B. Downs Blvd., MDC 111, Tampa, FL 33612
E-mail: rheller@usf.edu